MASSACHUSETTS INSTITUTE OF TECHNOLOGY

THE ENERGY LABORATORY

ADVANCED WET-DRY COOLING TOWER CONCEPT PERFORMANCE PREDICTION

by
Troxell Snyder
Jeffrey Bentley
Martin Giebler
Leon R. Glicksman
Warren M. Rohsenow
Department of Mechanical Engineering, M.I.T.

Energy Laboratory
Report No. MIT-EL 77-002 Volume I January 1977
Heat Transfer Laboratory Report No. 83307-99

Advanced Wet-dry Cooling Tower Concept

by

Troxell Snyder
Jeffrey Bentley
Martin Giebler
Leon R. Glicksman
Warren M. Rohsenow

Energy Laboratory

In Association With

Heat Transfer Laboratory
Department of Mechanical Engineering

Massachusetts Institute of Technology

Sponsored by:

Reactor Research and Development Division
Energy Research and Development Administration

January 31, 1977

ENERGY LABORATORY REPORT NO. MIT-EL 77-002

HEAT TRANSFER LABORATORY REPORTS NO. 83307-99

ACKNOWLEDGEMENTS

The Reactor Research and Development Division of the Energy Research and Development Administration sponsored this study under ERDA Contract E(11-1)-2500.

Special thanks are due to Mr. William F. Savage. His active interest and suggestions were a great benefit to the program.

ABSTRACT

The purpose of this years' work has been to test and analyze the new dry cooling tower surface previously developed. The model heat transfer test apparatus built last year has been instrumented for temperature, humidity and flow measurement and performance has been measured under a variety of operating conditions.

Tower Tests showed approximately 40-50% of the total energy transfer as taking place due to evaporation. This can be compared to approximately 80 to 85% for a conventional wet cooling tower. Comparison of the model tower test results with those of a computer simulation has demonstrated the validity of that simulation and its use as a design tool. Computer predictions have been made for a full-size tower system operating at several locations.

Experience with this counterflow model tower has suggested that several design problems may be avoided by blowing the cooling air horizontally through the packing section. This crossflow concept was built from the previous counterflow apparatus and included the design and fabrication of new packing plates.

Instrumentation and testing of the counterflow model produced data with an average experimental error of 10%. These results were compared to the predictions of a computer model written for the crossflow configuration. In 14 test runs the predicted total heat transfer differed from the measured total heat transfer by no more than 8% with most runs coming well within 5%. With the computer analogy's validity established, it may now be used to help predict the performance of fullscale wet-dry towers.

TABLE OF CONTENTS - VOLUME I

LIST OF FIGURES - VOLUME I

LIST OF TABLES

Principle Symbols

Symbol	Description
A	area
C	heat capacity
cp	heat capacity
D_h	hydraulic diameter
h	height
h	specific enthalpy
$h_{dry\ surface}$	dry surface heat transfer coefficient
h_o h_D	wet surface mass transfer coefficient
h_{fg_T}	latent heat to vaporization of water at T
h_{fg}^o	latent heat to vaporization of water at T_o
H	Total enthalpy
ITD	$(T_{\ell_{in}} - T_{a_{in}})$
k	thermal conductivity
$\dot{M}$, $\dot{m}$	mass flow rate
Nu	Nusselt Number
P	pressure
Pr	Prandtl Number
Q	heat transfer rate
Q_{design}	design heat transfer rate for performance models of Chapter 4, 20,000 BTU/min/tower
Re	Reynolds Number
R H	relative humidity
t	plate thickness

Symbol	Description
T	temperature
T_o	reference temperature
V	velocity
Z	length of fin
W.C.	water consumption
$W.C._{wet}$	water consumption of wet tower
$W.C._{basis}$	fixed rate of water consumption used for comparison 0.82 lb_m/1000 BTU rejected
W	specific humidity of air-water vapor mixture

Greek

η_f	fin efficiency
ρ	density

Subscripts

a	air
in	inlet
ℓ	liquid (water)
mix	mixture(air-water vapor)
out	outlet
v	water vapor

CHAPTER I

INTRODUCTION

1.1 History of Project

Early in 1975, work was started at M.I.T. to develop a single heat transfer surface which would give low evaporation rates at costs competitive with equal wet tower capacity. The wet-dry concept is the result of this work. In this design, water is distributed onto a packing plate fabricated (see Figure 1-1) to keep the hot water in discrete channels over which cooling air is blown. These channels serve to restrict the free surface area of the water, thus reducing evaporation and water loss. The packing plates are made of conductive material which acts as a fin heated at the base by the channeled water and cooled by forced convection [1]. By conceding a small amount of evaporation the fabrication costs for the wet-dry surface have been reduced far below those of a completely closed or dry heat exchanger.

To demonstrate this concept a model test tower was built during 1975. In addition, a computer program was written based on analytic studies of evaporative cooling. Tests of the partially instrumented tower indicated high heat transfer rates while the initial results of the computer analogy indicated a substantial reduction in evaporation rate. This year's work has led to more quantitative results and predictions.

1.2 Progress This Year

Work this year has included the instrumentation and testing of the model cooling tower referred to above. Comparison (Chapter 3) of these test results with the computer program predictions has shown the program to accurately predict the heat transfer performance of the V-trough packing section under the available range of operating conditions.

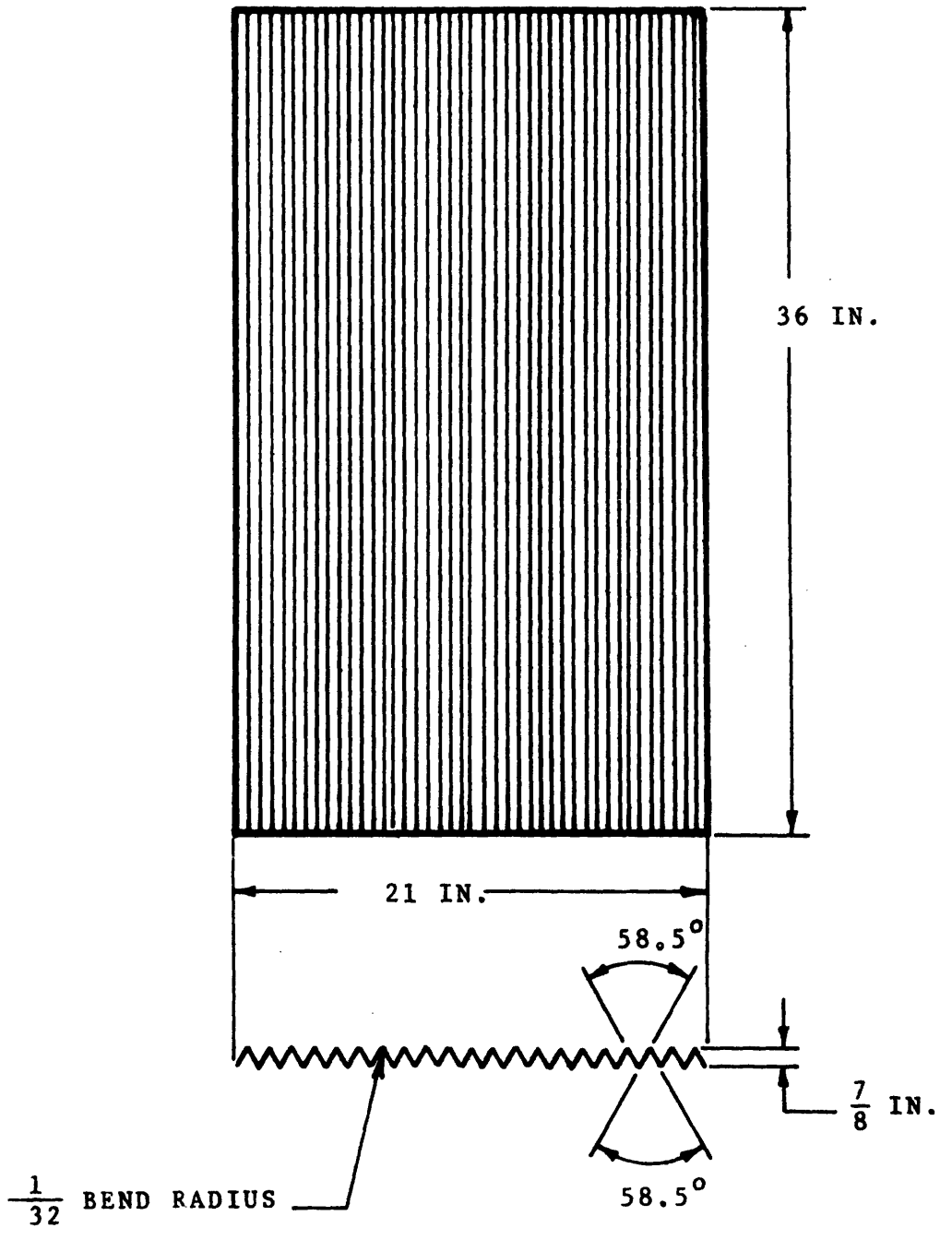

FIGURE 1-1 V-TROUGH PACKING PLATE

Using the computer analogy as a design tool several types of cooling tower systems were sized and compared under a wide range of inlet conditions. These comparisons are reveiwed in Chapter 4 and include comparisons for several sites around the United States.

During the course of the experimental evaluation several design drawbacks were found to the present air-water counterflow design. A proposed solution to these shortcomings was to alter the air flow to blow horizontally across the packing section. The advantages of this crossflow design are described in Chapter 5 as well as a discussion of the appearance of a full size cross= flow tower.

Chapter 6 contains a simplified estimation of the costs of a full size set-dry towers system based on cost estimation procedures described in the WASH-1360 report [16]. Volume 2 of the report describes the adaptation of the counterflow model tower to a crossflow configuration. This new design required a new type of packing plate as well as complete re-instrumentation of the former model tower.

The final project conclusions, along with recommendations for future work can also be found in Volume 2. Technical and special interest subjects are included as appendices at the end of each part.

CHAPTER 2

EXPERIMENTAL APPARATUS AND DESCRIPTION OF INSTRUMENTATION MODEL

2.1 Model Tower

The model tower tested for this report is essentially the same as described in Reference [1], and instrumented as described in the following sections.

As a brief review, the model tower (Figure 2-1) is an induced-draft counterflow design with a plan area of four square feet (0.37 m^2). The heat transfer packing section holds the packing plates. Hot water is distributed at the top of the packing section and collected in troughs at the bottom. Ambient air from the laboratory enters from the bottom of the packing section and exits at the top.

There are 14 V-trough packing plates each (Figure 2-2) with 21 troughs making up a total heat transfer area of 280 ft^2 (26 m^2) [1]. Air flow was fixed by fan size and was approximately 350 ft^3/min/plan foot square area (1.8 m^3/s/plan m^2 area). Inlet water flow rate could be varied from 2.7 to 6.0 gpm/plan ft^2 (1.8 to 4.1 l/s/plan m^2) with temperatures as high as 150 F(66 C). [1].

Instrumentation of the model included installation of 55 thermocouples measuring air and water temperature at the inlet and exhaust of the packing section. Calibrated rotometers measured water flow rate and a pitot tube was used to check airflow rate. Changes in moisture content of the air were measured by an optical dewpoint hygrometer (Section 2.3).

Error analysis (Section 2.5) has predicted a maximum error between the air and water energy balance of about 15%. The highest error observed in the nine test runs was 24% with the average error approximately 13% (See section 3.3).

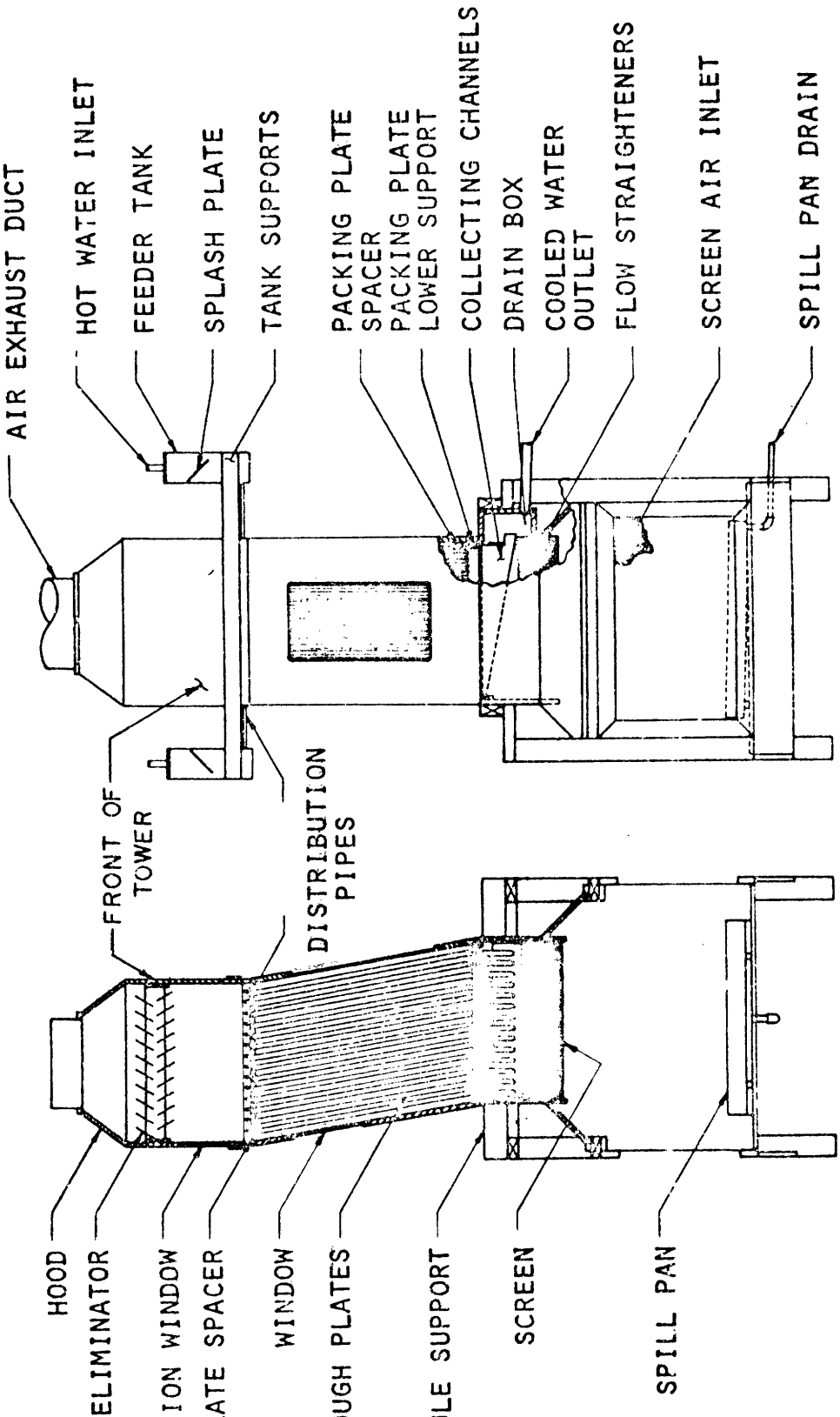

FIGURE 2.1 HEAT TRANSFER TEST APPARATUS ASSEMBLY

2.2 Temperature Measurement

The principal goals of the tower instrumentation were to fully describe the performance of the tower and to check the validity of the computer program. To accomplish this it was necessary to determine the inlet and outlet conditions of both the air and water. The specific measurements required included the temperature change experienced by the water and air streams, the amount of water transferred to the air and the air and water flow reates. It was decided that an accuracy of at least $\pm$ 10% be required for the temperature differences measured, and the water evaporation rate. This would result in possible errors in the energy balance of less than 10%.

Copper constantan thermocouples were chosen for the temperature measurement. Preliminary computer runs predicted a water temperature drop of less than 4°F for some typical laboratory operating conditions. In order to maintain the accuracy required for this change, the two water temperature measurements would have to be repeatable to about .2°F. However, thermocouple wire manufacturers do not guarantee this accuracy for all lengths of wire. Therefore, before installation a calibration check was made of the fifty-four thermocouples after assembly with switches and other hardware (See Appendix A). A single ice bath junction was used between the switches and the readout device. The calibration method was to use one thermocouple as a standard and to compare each of the others to it, when placed in the same constant temperature bath. A steam bath was first used in an attempt to maintain a constant temperature. However, it was found that a calibration to better than .5°F was difficult using this method. A stirred silicon oil bath was then obtained which was

thermostatically controlled. The two thermocouples being tested were placed in a narrow glass tube with oil covering the junctions. The temperature of the bath inside the tube was held constant to ± .1°F at about 176°F. However, these fluctuations were slow enough so that the output of the thermocouples could be measured and compared to ± .05°F. It was found that while the thermocouples produce a steady voltage for a short time, their calibration will change by about ± .1°F over a period of several hours. In addition, the thermocouples were in general with ± .1°F of each other. Therefore, the thermocouples were found to have a repeatability of ± .1°F not only with time, but also with respect to each other. Accuracy of the system was of lesser importance than repeatability, but comparison with an NBS claibrated thermometer readable to ± .5°F showed that the thermocouple millivolt outputs could be converted to temperatures by use of standard conversion tables. Also, testing at a lower temperature (104°F) indicated that the error tends to decrease as the temperature decreases.

During both calibration tests and tower runs, a digital voltmeter was used to measure the thermocouple output. This meter had a resolution of ± 1 microvolt which corresponds to about ± .05°F. An accurate potentiometer was used to check the calibration of the voltmeter. Since the meter had high input impedance (10 MΩ) compared to the wire resistance (50Ω) the effect of the small current flow on the thermocouple voltage is much smaller than 1 microvolt snesitivity of the meter. Potentiometers were not used for the runs, because a device of the accuracy required is often bulky and sensitive to vibration. The digital meter also made it possible to read all fifty-four thermocouples in a shorter time.

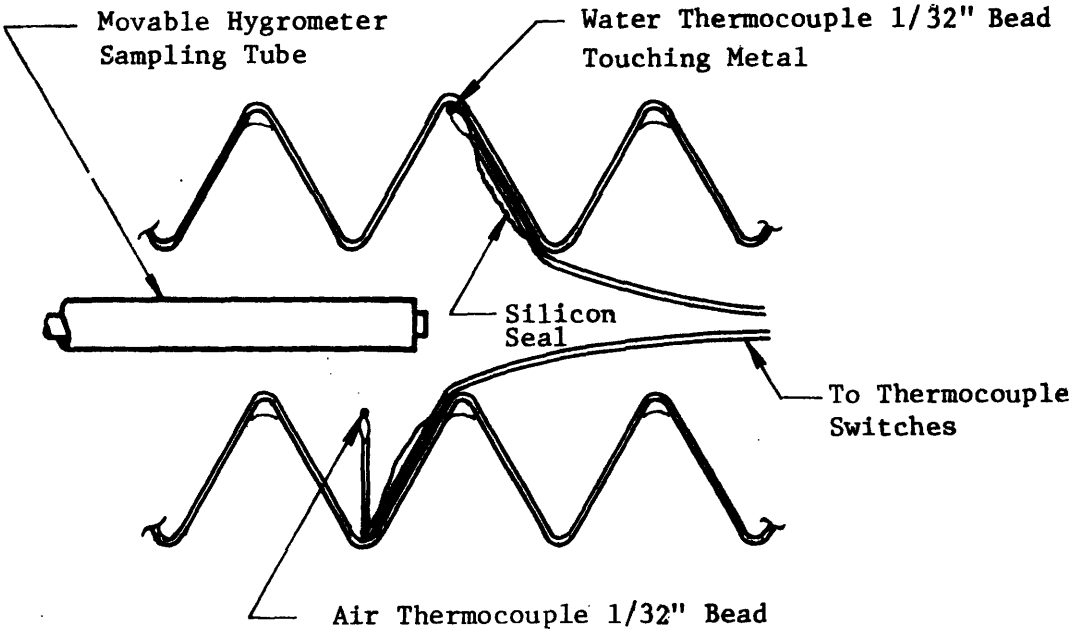

a. Detail of Instrumentation at Each Location (actual size)

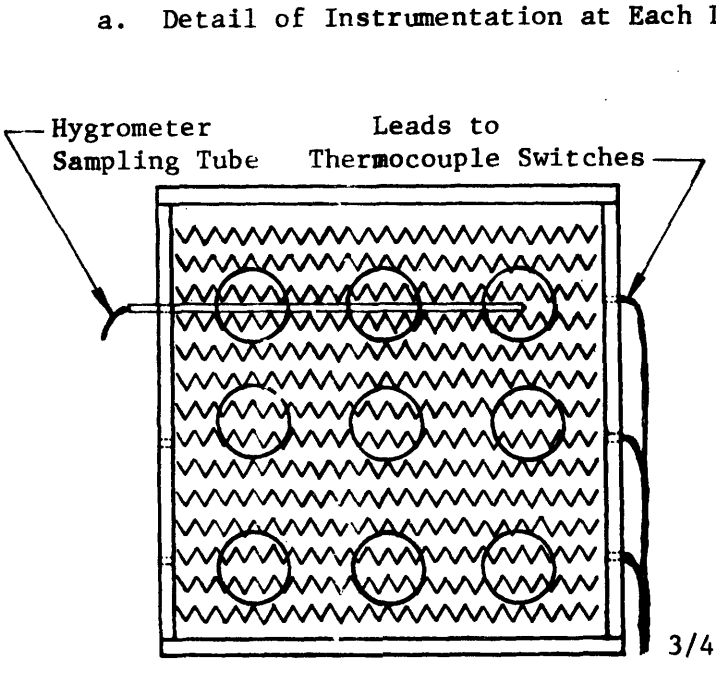

b. Instrument Locations on Tower Cross Section

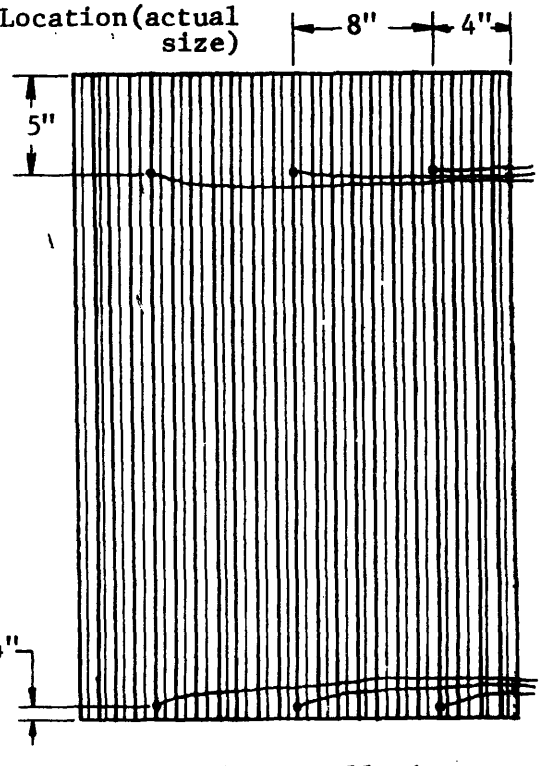

c. Thermocouple Installations on the Packing Plates (water side)

Figure 2.2 Instrumentation of the Packing Plates Including Locations of Thermocouples and Hygrometer Sampling Tube

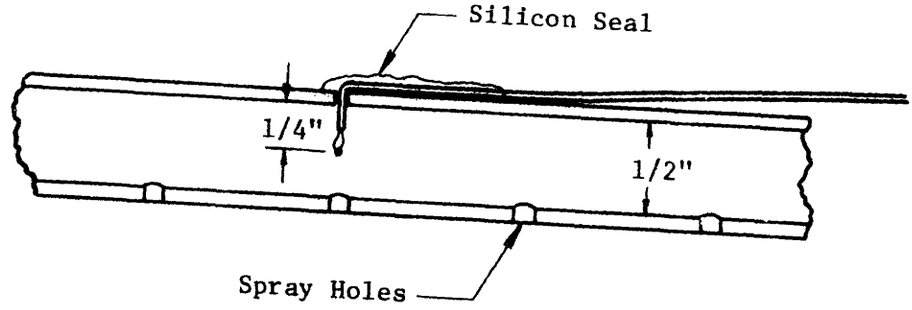

Figure 2-3 Thermocouple Installation in Distribution Pipes (Actual Size)

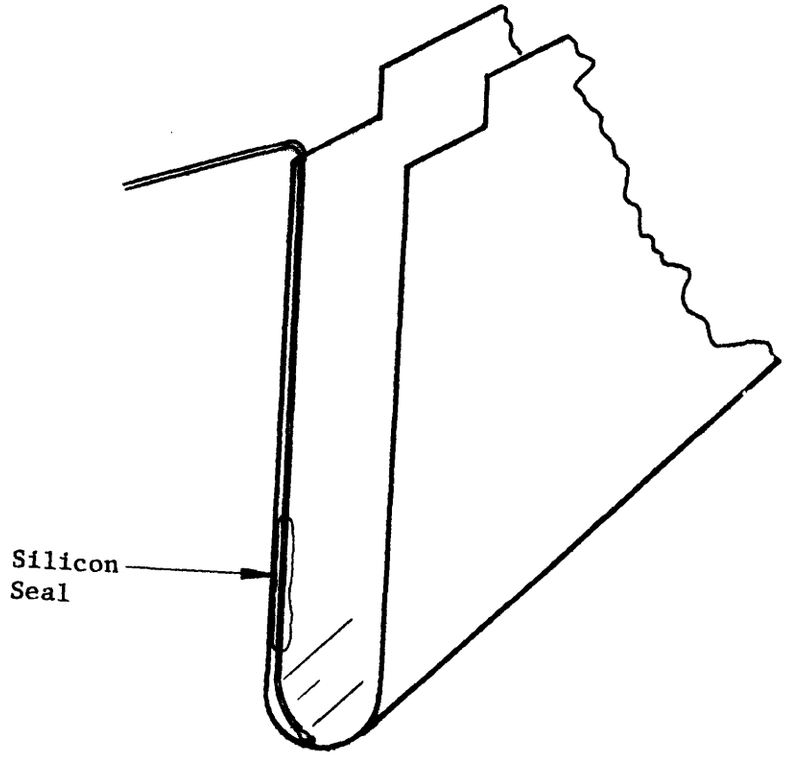

Figure 2-4 Thermocouple Installation in Outlet of Collection Channels (Approximately Actual Size)

Temperatures were measured at eight locations. The water temperature was measured inside the distribution pipes, at the top and bottom of the packing plates and at the outlet of the collection channels. The air temperature was measured below the collection channels, at the bottom and top of the packing and above the distribution pipes. To obtain an average over the cross-section of the tower, nine measurements were made at each location, except in the collection channels, where three measurements were made. The air and water temperature on the plates were measured by using nine separate thermocouples for each measurement. They were fastened at three locations at the top and bottom of three different plates. (See Figure 2-2). The temperature in the water collection channels was measured at the outlet of the channels below the plates instrumented for air and water measurements (See Figure 2-4). The thermocouples in the pipes were placed in the same nine locations as in the packing section. (Figure 2-3). The measurement of the air temperature above the pipes and below the channels was accomplished using rakes with three thermocouples (Figure 2-5). These rakes were moved to three positions as at the other tower locations. The air and water measuring thermocouples on the plates and in the troughs, were fastened in place with silicon seal. In the distribution pipes, the thermocouples were inserted through holes in the pipes and similarly cemented in place.

2.3 Evaporation Measurement

In order to determine the rate of water loss in the tower, two methods were considered. These were a direct measurement of the water in the system before and after a run, and a measurement of the air

humidity at both ends of the packing section. The first method was not used since it was decided that leakage in the tower would greatly affect the measurement of the small amount of loss expected. Several different types of hygrometers were investigated. It was determined that $\pm$ .3°F accuracy was required for a dew point measurement, to ensure less than $\pm$ 10% error in the evaporation rate, assuming that approximately .1% of the water is evaporated. Hygrometers which use variable resistance probes are in general greatly affected by wetting. They are also subject to some drift and are marginally acceptable when calibrated. An optical dew point device was found to be sufficiently accurate, as well as reliable. A demonstrator model was used for the test runs, which was found to be repeatable to at least $\pm$ .3°F (See Figure 2-2).

2.4 Flow Measurements

Two rotometers were used to determine the water flow rate through the tower, each measuring the flow to one of the plexiglass feeder tanks. Each rotometer had a capacity of approximately 20 gpm and were calibrated by means of a weight tank. They were readable to $\pm$ .2 gpm ($\pm$ 1% maximum flow). For the lowest flow rate used in the tower (5 gpm per meter) this error was $\pm$ 4%.

To speed the process by which the air flow rate was determined in the packing section, it was decided to fix a pitot tube in place between the plates and take only one measurement for each data run.

The air flow between the individual plates was assumed to be turbulent with maximum velocity at the midpoint of the separating gap. Measurements of this midpoint velocity showed that it was nearly uniform throughout the packing section.

The pitot tube was fixed between the plates about 1/3 of the way back and 1/3 of the way (Figure 2-6) in from the sides of the packing section. Great care was taken to align the tube parallel to the plates and in the center of the gap. A movable pitot tube was positioned parallel in the plenum above the packing section and used to scan the airflow at that point.

Data taken at various air flow rates were then compared and a ratio was found between bulk air flow as measured by the scanning pitot tube and mid-point air velocity measured by the fixed pitot tube.

For a pitot tube in a low velocity airstream the velocity is given by the relation:

$$1/2 \quad \rho V^2 = \Delta P \qquad (2\text{-}1)$$

Thus, for any two pitot tubes in air at the same temperature and pressure, the ratio of velocities is:

$$\frac{V_1}{V_2} = \frac{\sqrt{\Delta P_1}}{\sqrt{\Delta P_2}} = \frac{\sqrt{h_1}}{\sqrt{h_2}} \qquad (2\text{-}2)$$

and the ratio of the average velocity measured in the plenum and the velocity measured by the fixed pitot tube is given by:

$$\frac{V_{avg}}{V_{fixed}} = \frac{(\sqrt{h_1} + \sqrt{h_2} \ldots \sqrt{h_9})/9}{\sqrt{h_{fixed}}} \qquad (2\text{-}3)$$

Where $h_1 - h_9$ are the manometer heights taken at the 9 scan locations.

Eight sets of measurements were made at varying airflow and averaged to give the velocity ratio. (See Table 2-1).

For the analytic comparison,

$Re = V D_h/\nu$ $\quad V = 300$ to 500 ft/min (1.52 to 2.54 m/s)

$D_h = 0.25$ ft (.08 m)

$Re = 6400$ to 11,000

From Reference [12] by integrating the relation:

$$\frac{V_x}{V_{CL}} = (y/r_o)^{1/n} \quad \text{where}$$

Re	n	V/V_{CL}
4,000	6	0.791
110,000	7	0.817

Indicating a ratio of approximately 0.80 for this range of Reynold's numbers. This compares favorably with the experimentally measured ratio of 0.81.

2.5 Error Analysis

To determine the significance of the instrument errors, their effect on the energy balance must be shown. The energy balance for a heat exchanger reduces to [4]:

Rate of enthalpy in = Rate of enthalpy out

In the case of the cooling tower, this becomes,

TABLE 2-1

Average and Centerline Air Velocities Between Packing Plates

RUN	$\sqrt{h}_{\text{above plates avg}}$ ($\sqrt{\text{in}}$)	$\sqrt{h}_{\text{fixed}}$ ($\sqrt{\text{in}}$)	Ratio V_{avg}/V_{CL}
1	0.1213	0.1367	9.89
2	0.0779	0.1095	0.71
3	0.1232	0.1500	0.82
4	0.1406	0.1590	0.88
5	0.1397	0.1711	0.82
6	0.1176	0.1539	0.76
7	0.1186	0.1410	0.84
8	0.0864	0.1090	0.79

Average Ratio = 0.81

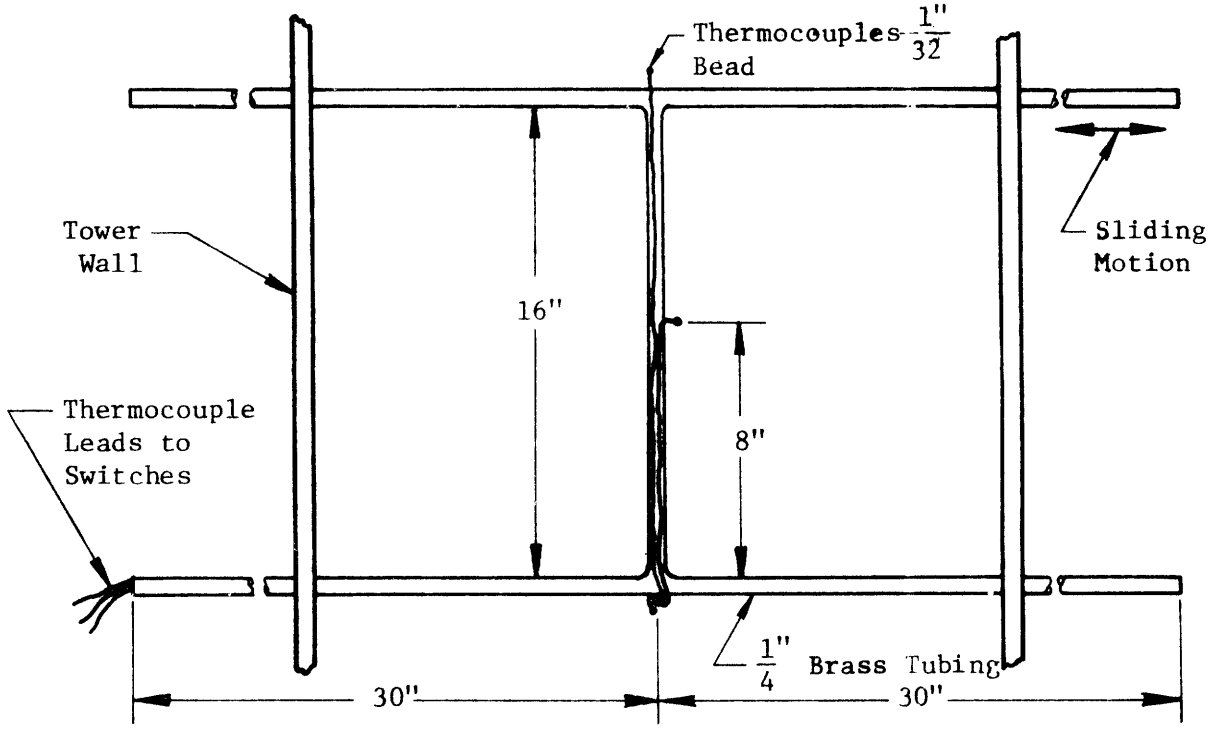

a. Top View of Rake

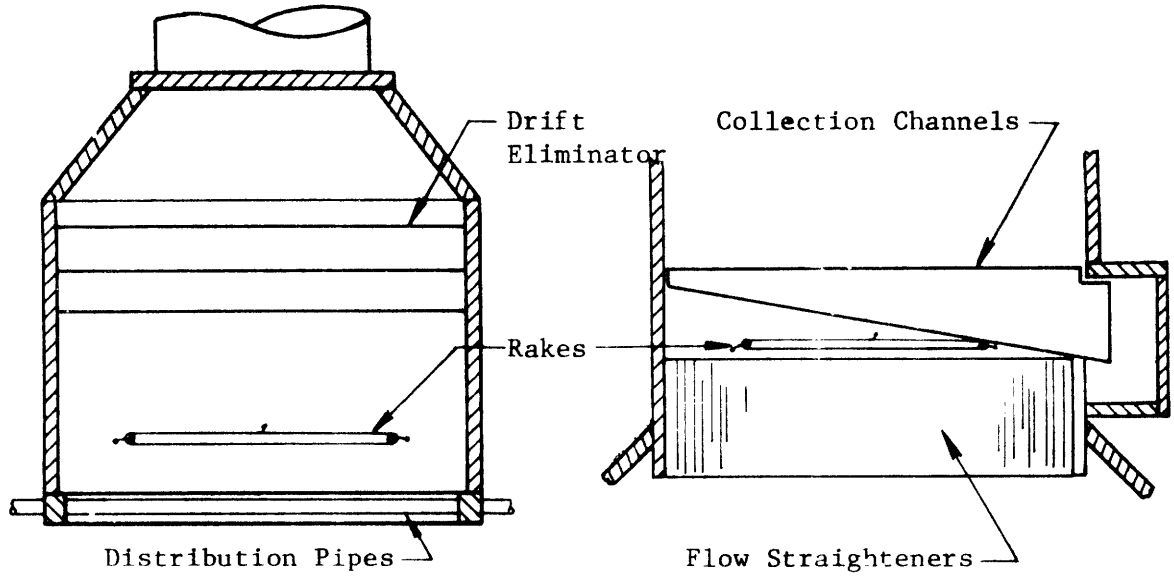

b. End View Above Distribution Pipes c. End View Below Collection Channels

Figure 2-5: Location of Sliding Rakes Used to Measure Air Temperature Above the Distribution Pipes and Below the Collection Channels

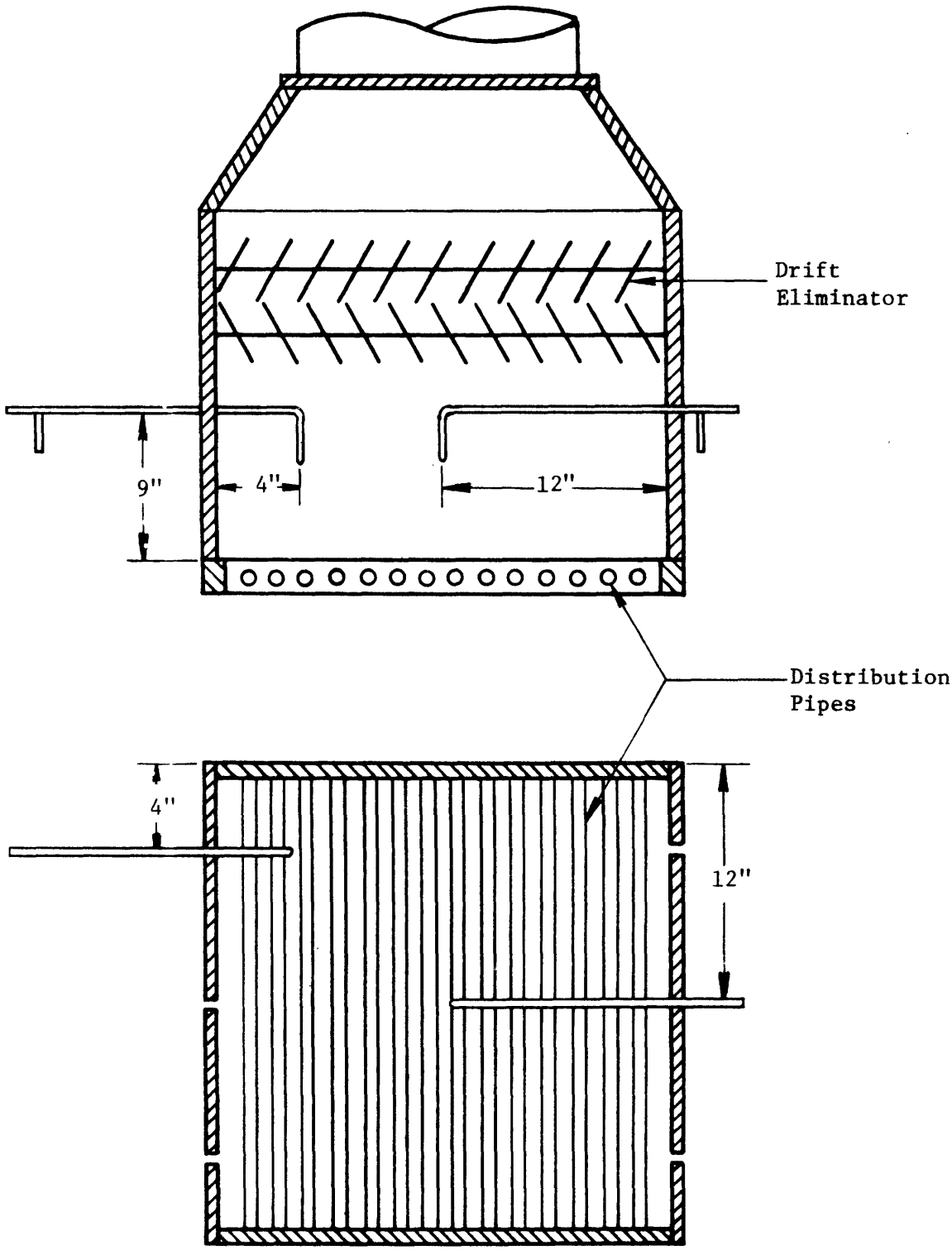

Figure 2-6: Pitot Tube Installation Showing Two Locations of the Pitot Tube

$$\dot{Q} = \dot{m}_{air} \left(h_{air_{in}} + w_{in}\, h_{vapor_{in}} - h_{air_{out}} - w_{out}\, h_{vapor_{out}}\right) =$$

$$- \dot{m}_{water}\, c_{p_{water}} \left(T_{water_{in}} - T_o\right) + \left(\dot{m}_{water} - \Delta\dot{m}_{water}\right) c_{p\ water}$$

$$\left(T_{water_{out}} - T_o\right) \qquad (2\text{-}4)$$

where $\dot{m}$, h, w, and T are mass flow rates, enthalpies, absolute humidities and temperature respectively. $\dot{Q}$ is the heat transfer rate and $c_{p_{water}}$ is the specific heat at constant pressure for water, which is assumed to be 1 BTU/lb_m°F. T_o is the reference temperature at which the enthalpies are evaluated. Here T_o is 32°F. The reference for the water vapor is liquid water at 32°F. $\Delta\dot{m}$ water is the amount of water transferred to the air stream, and is given by:

$$\Delta\dot{m}_{water} = \dot{m}_{air} \left(w_{out} - w_{in}\right) \qquad (2\text{-}5)$$

The value of $\dot{m}_{air}$ is determined by the pitot tube measurement, and is subject to the associated error. h_{air} and $h_{air_{out}}$ are determined by the air temperature measurements as are h_{vapor} and $h_{vapor_{out}}$. Errors in these values are determined by inaccuracies in the thermocouple reading, as are errors in $T_{water_{in}}$ and $T_{water_{out}}$. w_{in} and w_{out} are measured with the dew point hygrometer.

To evaluate the effect of instrument limitations, an uncertainty analysis is made using the following form of equation 2-4, combined with equation 2-5.

$$\delta\dot{Q} = \dot{m}_{air} (h_{air_{in}} + w_{in} h_{vapor_{in}} - h_{air_{out}} - w_{out} h_{vapor_{out}})$$

$$+ \dot{m}_{water} c_{p_{water}} (T_{water_{in}} - T_o) - c_{p_{water}}$$

$$(\dot{m}_{water} - \dot{m}_{air} (w_{out} - w_{in}))(T_{water_{out}} - T_o) \qquad (2\text{-}6)$$

where $\delta \dot{Q}$ is the discrepancy between the air and water sides of heat balance. The uncertainty $u_{\delta\dot{Q}}$ is calculated by the following equation [9]:

$$u_{\delta\dot{Q}} = [(\frac{\partial\delta\dot{Q}}{\partial x_1} u_1)^2 + (\frac{\partial\delta\dot{Q}}{\partial x_2} u_2)^2 + \ldots + (\frac{\partial\delta\dot{Q}}{\partial x_n} u_n)^2]$$

where $x_1, x_2, \ldots x_n$ are the humidities, enthalpies, temperatures and flow rates in equation 2-6 and $u_1, u_2 \ldots u_n$ are their respective uncertainties. The following values which satisfy the energy balance might be typical test conditions for the model tower:

$\dot{m}_{air} = 150 \pm 8$ lb_m/min

$\dot{m}_{water} = 170 \pm 1.7$ lb_m/min

Air temperature in = $90°F \pm .1°F$ (after collection troughs)

Dew point temperature in = $50°F \pm .3°F$

Air temperature out = $100°F \pm .1°F$

Dew point temperature out = $55°F \pm .3°F$

$T_{water_{in}} = 120°F \pm .1°F$

$T_{water_{out}} = 116.4°F \pm .1°F$

The heat transfer rate for this case as cauculated using equation 2-4 is 625.6 BTU/min. The uncertainty according to equation 2-7 is 46.6 BTU/min or 7.5%. To illustrate the dependence of the error in $\dot{Q}$ on the test conditions the following set of conditions is investigated:

$\dot{m}_{air} = 150 \pm 8\ lb_m/min$

$\dot{m}_{water} = 90 \pm 1.7\ lb_m/min$

Air temperature in = $90°F \pm .1°F$

Dew point temperature in = $20°F \pm .3°F$

Air temperature out = $103°F \pm .1°F$

Dew point temperature out = $33°F \pm .3°F$

$T_{water_{in}} = 140°F \pm .1°F$

$T_{water_{out}} = 132°F \pm .1°F$

In this case $\dot{Q} = 745.43$ and the uncertainty is 43.83. Even though the water temperature change and the absolute humidity may be more accurately measured for this case, the effect on the energy balance is insignificant. The error in the air flow measurement still predominates, and the uncertainty is essentially unchanged (see Appendix B). Due to an increase in $\dot{Q}$, however, the percent error is reduced to 5.9%.

Other factors which may influence the accuracy of the data, include the fact that the nine locations may not give a true average over the

cross-section. The hygrometer sampling tube may occasionally remove water droplets with the air, and the pitot tube measurements may be affected by the proximity of other tower components such as the distribution pipes and the drift elminators. (See Fig. 2-6). The magnitude of these possible errors is difficult to predict analytically.

CHAPTER 3

COMPARISON OF TEST RESULTS AND COMPUTER PROGRAM

3.1 Computer Program

The computer program (Appendix H) was the same as given in reference [1], modified to match measured values of the dry plate surface heat transfer coefficient and the wet-to-dry surface area ratio.

The basic equations were taken from a paper by G. Yadigaroglu which was concerned with totally wet towers with flat packing plates. They were then modified to include heat transfer from the dry surface. The solution involves choosing values for the temperatures, water flow rates, absolute humidity and heat transfer rates and solving for the incremental changes. These changes are then added to the initial values and the solution found in a "marching out" or Euler process.

The expressions for the water surface and dry plate heat transfer coefficinets h and h_{DP} are taken from the Dittus-Boelter relation as used by Yadigaroglu [2].

$$Nu = .022\ Pr^{0.6}\ Re^{0.8} \qquad (3\text{-}1)$$

For calculating fin efficiency, the packing plates were modeled as simple plate fins (shown in Fig. 2-3). Fin efficiency was then calculated from the expression:

$$\eta_{fin} = \frac{\tan h\sqrt{Z^2 h/kt}}{\sqrt{Z^2 h/kt}} \qquad (3\text{-}2)$$

taken from reference [12].

The mass transfer coefficient is derived from the Chilton-Colburn analogy between heat and mass transfer may be written: [1]

$$h_{D_{\text{wet surface}}} = \frac{h_{\text{wet surface}}}{\rho_{mix} C_{mix}} (Pr/Sc)^{2/3} \qquad (3\text{-}3)$$

where ρ_{mix}, C_{min} and Sc are the density, specific heat and Schmidt number of the air-water vapor mixture. The characteristic length used for these relations is the hydraulic diameter of the air flow channel between the packing plates [12].

Provision was also made to allow the program to run for a completely wet and completely dry surface area. Comparison with previously published results provided a check on the program's validity [1].

Physical properties of air, liquid water and water vapor were approximated by correlating equations [4 and 5] and/or simple curve fits [1], and may be seen in the computer listing (Appendix H).

Overall heat transfer is given by the equation:

$$Q_{tot} = (T_{\ell_{in}} - T_{\ell_{out}})\dot{m}_{\ell_{out}} + \dot{m}_a(w_{out} - w_{in})(T_{\ell_{in}} - T_o) \qquad (3\text{-}4)$$

And evaporative heat transfer given by:

$$Q_{evap} = (m_{\ell_{in}} - m_{\ell_{out}})[h_{f_{gT_{\ell_{in}}}} - C_a(T_{\ell_{in}} - T_{\ell_{out}})] \qquad (3\text{-}5)$$

Where T_o is the temperature at which the enthalpy of the saturated liquid to be zero, in this case $T_o = 32°F(0°C)$ so as to remain consistant with published psychrometric charts and tables.

3.2 Determination of Surface Transfer Coefficients

Certain parameters of the packing section were unknown functions of geometry and flow conditions. Two of these, the wet-to-dry surface area ratio and the dry plate surface heat transfer coefficient, were determined in auxiliary experiments and these values used to modify the analytic predictions in the computer analogy.

The determination of A_{wet}/A_{dry} was done twice, before and after painting the packing plates. (See Appendix E).

Before painting the deposit buildup was easily visible on the surface and its width could be directly measured with a scale. This was assumed to be the entire extent of the wet surface area due to the "blotter effect" noted in Appendix E. Using the observed deposit width of 0.25 in (0.6 cm) from the trough bottom and the water free surface width as 0.125 in. (0.3 cm) gives a calculated A_{wet}/A_{dry} of 11%.

After painting the plates a photographic method was necessary as there was no longer a measureable deposit line. The paint used was non-reflecting and black. A columnated light source was shone down into the trough from the side. Any reflection seen would have to come from the water surface, since the water did not wet the plate and could not "climb" up the side of the trough. The reflection was recorded by a high quality single-lens reflex camera using close-up lenses for magnification. Enlargements of the photographs showed a clear separation between water surface and plate area. These photographs, after correction for depth-of-field, show a water surface area width of 0.134 in (0.34 cm). This corresponds to a wet-to-dry surface area ratio of 4%. This was later increased to 5.5% as it became evident that the same non-wetting characteristics that helped cut the

total wetted surface area were now letting the water streams wander on the upper portion of the packing plates.

This area ratio did not change significantly over the available range of water flow rates.

The dry surface heat transfer coefficient of the packing plates was checked by evaluation of the transient response of the plate temperature to a step change in air temperature. The packing plates were cooled 15 to 20°F (8-11°C) below ambient (intake)air temperature. The apparatus exhaust fan was then started, pulling the warmer ambient air into the packing section at a known rate of flow. Local plate and air temperatures were recorded at 10 second intervals until plate temperature approached intake air temperature.

Analysis (Ref. [8], Chapter 3) of this data (See Appendix J) indicated a dry plate surface heat transfer coefficient equal to 3.3 BTU/hr-ft^2°F (160/kal/h-m^2°C). This value was approximately 1.5 times higher than the value predicted by equation 3-1 when corrected for entrance effects [16]. This increase was attributed to the highly irregular flow channel and the high inlet turbulence from the flow straighteners and collection channels (Figure 2-1).

Two other paramters, the wet surface heat and mass transfer coefficients could not be experimentally measured but were increased by a factor of 1.5 also. This was done as the wet surface heat and mass transfer coefficients depend on the same flow conditions as the dry heat transfer coefficient (except for the relative Reynolds number between the air and the moving water surface).

3.3 Summary of Test Data and Computer Predictions

The summary charts (Tables 3-1, 3-2) list the major points of comparison between the computer prediction and the model tower test results. For the model tower tests both air side and water side enthalpy change was calculated. On the air side:

$$\Delta H_a = \dot{m}_a[w_{out}(h^o_{fg} + \int_{T_o}^{T_{a_{out}}} C_v dT) - w_{in}(h^o_{fg} + \int_{T_o}^{T_{air_{in}}} C_v dT) + \int_{T_{a_{in}}}^{T_{a_{out}}} C_a \, dT] \quad (3.6)$$

Where T_o is the reference temperature where the enthalpy of saturated liquid is taken as zero, and where h^o_{fg} is the latent heat of vaporization at the reference temperature. In practice the air side enthalpy change was evaluated from tabulated values [6] of dry air and water vapor enthalpy. These tables were based on T_o = 32°F (0°C) and for consistency this value of T_o will be used in all calculations.

On the water side:

$$\Delta H = \dot{m}_{\ell_{out}} \int_{T_{\ell_{out}}}^{T_{\ell_{in}}} C_\ell dT - \dot{m}_a(w_{out} - w_{in}) \int_{T_o}^{T_{\ell_{in}}} C_\ell dT \quad (3-7)$$

Where the second term on the righthand side of the equation represents the enthalpy loss due to mass transfer. In practice, the heat capacity of water was taken to be a constant, 1 BTU/lbm-°F (1 kcal/kg-°C) and ΔH_ℓ evaluated directly from the measured inlet and outlet conditions.

For energy balance calculations, the error was calculated from the equation:

$$\text{Error} = \frac{\Delta H_a + \Delta H_\ell}{1/2\ (\Delta H_a - \Delta H_\ell)} \quad (3-8)$$

where $1/2(\Delta H_a - \Delta H_\ell)$ is the average of the air and water side enthalpy changes and appears in Tables (3-1, 3-2) as Q_{total} for the model tower tests.

Q_{evap} was evaluated for the model tower tests from the inlet and exhaust conditions based on the thermodynamic relations:

$$Q_{evap} = \dot{m}_a(w_{out} - w_{in})[h_{fg}^o + \int_{T_o}^{T_{a_{out}}} C_v dT - \int_{T_o}^{T_{water_{in}}} C_\ell dT] \quad (3\text{-}9)$$

Assuming constant C_v and rearranging this can be written as:

$$Q_{evap} = \dot{m}_a(w_{out} - w_{in})[h_{fg}^{T_{\ell_{in}}} - C_v(T_{\ell_{in}} - T_{a_{out}}) \quad (3\text{-}10)$$

Where C_v was taken to be 0.4458 BTU/lbm°F (0.4458 kcal/kg°C) and $h_{fg}^{T_{\ell_{in}}}$ was taken from tabulated values [6].

The values of Q_{evap} and Q_{total} for the computer model were calculated from the exhaust conditions predicted by the program and are presented in the tables for each test run. A specific discussion of each table follows below.

The energy balance ($\Delta H_\ell + \Delta H_a = 0$) provides an indication of the validity of the experimental process. Analysis (see Section 2.5) of this particular experiment showed a maximum possible error of 15% (as defined above) based on individual instrument repeatability. In practice this limit was exceeded on several occasions. These descrepencies have been attributed to changing flow conditions. Data measurements for a typical run required approximately one hour. Water temperatures were observed to remain fairly constant during this time as were, to a lesser extent air temperatures. The greatest problem was encountered in the humidity

data. The optical dewpoint hydrometer, while highly repeatable, was slow reading and as much as 20 to 30 minutes could elapse between beginning to scan the inlet section and finishing the scan of the outlet section. Water sprays, steam jets and other watery experiments in the laboratory had a noticeable effect on the air humidity content. Efforts to reduce this interference included running at odd hours and attempting to control local sources of humidity. Reasonable energy balances were thus obtained with the larger errors blamed on unobserved humidity and air temperature transients.

This summary is divided into two parts, 5 data runs completed before painting the packing plates and 4 runs done since that time (see Appendix E). Program inputs for the first part consist of ambient inlet conditions to the model tower packing section plus these approximate parameters (see Section 3-2):

A_{wet}/A_{dry} = 11%

$h_{dry\ plate}$ = 3.3 BTU/hr-ft^2°F (16.1 kcal/h-m^2°C)

$h_{wet\ surface}$ = 3.6 BTU/hr-ft^2°F(18.0 kcal/h-m^2°C)

$h_{D_{wet\ surface}}$ = 240 ft/hr (75 m/h)

As can be seen from the summary chart (Table 3-1), only once does the predicted evaporative heat transfer rate differ by more than 10% of the measured rate and never does the total heat transfer rate fall outside the measured air and water side heat transfer rates.

Corrosion noted on the plates after the initial series of data runs eventually necessitated the coating of the packing plates with an acrylic protective paint (App. E). After painting the plates the A_{wet}/A_{dry} ratio

was found to be 5.5% (Section 3-2). An order of magnitude analysis shows that the resistance to heat transfer added by painting the surface is very small when compared to the convective heat transfer coefficient. Since the wet surface characteristics have been assumed to remain the same as before the painting, (except for the surface area ratio) all the transfer coefficients have been left as in the previous runs.

Refering to the summary chart, Table 3-2, the four runs produced good energy balances, however the correlation between measured and computer-predicted total heat transfer is not as close as in the previous series. The experimentally measured heat transfer rate is consistently low in each of the four cases, but moves closer to the computer-predicted value in consecutive runs. By the last run (on 6/24) the difference is much less than 10% of the measured value and the predicted value well within the measured air and water side heat transfer rates.

It was speculated that a temporary resistance to heat transfer was caused by incomplete wetting of the newly painted plates. The approach of measured to predicted heat transfer can be a "wearing in" period during which the non-wetting characteristic declined. There was no noticeable change in the wet-to-dry surface area ratio.

As Table 3-2 shows, the evaporative heat transfer predictions match closely with the measured values in each run.

From these results it was concluded that the agreement between the analytic (computer) model and the heat transfer model tower test results were good enough to permit the use of the computer program (listed in Appendix H) to generate data for the comparisons in Chapter 4.

TABLE 3-1

Comparison of Computer Program and Model Tower Test Results - Unpainted Packing Plates A_{wet}/A_{dry} = 11%, Galvanized Plates

Run Date	ITD (F)	Q_{total} BTU/min	Q_{evap} BTU/min	Air Side Heat Transfer(BTU/min)	Water Side Heat Transfer(BTU/min)	$\frac{Q_{tot}}{Q_{evap}}$ (%)	Energy Balance Error(%)
3/19							
measured	43.7	839	405	738	939	48	24
computer		875	460			53	
3/22							
measured	36.7	677	336	638	727	50	13
computer		700	358			51	
3/23 am							
measured	38.1	759	427	750	768	56	2
computer		765	402			53	
3/23 pm							
measured	43.3	935	490	835	1017	52	18
computer		955	526			55	
3/25							
measured	44.5	877	463	844	909	55	7
computer		900	481			54	

TABLE 3-2

Comparison of Computer Program and Model Tower Test Results - Painted Packing Plates

A_{wet}/A_{dry} = 5.5%, Plates coated 0.001 in Crylon^{R} paint

Run Dates	ITD (F)	Q_{total} BTU/min	Q_{evap} BTU/min	Air Side Heat Transfer(BTU/min)	Water Side Heat Transfer(BTU/min)	$\frac{Q_{total}}{Q_{evap}}$ (%)	Energy Balance Error(%)
5/6							
measured	42.3	544	279	518	571	51	10
computer		654	278			43	
5/11							
measured	53.7	755	440	812	697	58	15
computer		366	371			43	
5/25							
measured	52.8	701	316	653	749	45	14
computer		771	305			40	
6/24							
measured	28.0	380	195	413	346	51	17
computer		400	171			43	

CHAPTER 4

PERFORMANCE COMPARISON FOR VARIOUS COOLING TOWER COMBINATIONS

This chapter compares the performance for a given power plant of the two most widespread types of cooling towers used today, the evaporative (wet) and the non-evaporative (dry), with that of the V-trough packing design developed in this project (wet-dry) (see Section 2-1). To generate the data necessary for these comparisons an idealized design has been made of each tower type (Appendix D). Each of these designs is sized to give the same hot water temperature drop and total heat transfer rate for a set of fixed design inlet conditions. The designs have then been evaluated by computer analogy under a number of differing inlet conditions and the results (evaporation rate, heat transfer rate, exit air conditions) used as a basis for the following comparisons.

Also included are the combination-type towers used by some designers to overcome the disadvantages of single wet and dry systems. Studies of these [13] systems are very promising and the main thrust of this chapter is directed toward the analysis of these systems.

4.1 Description of Combination-Type Systems

A combination tower design consists of two individual cooling towers in parallel or series connection, each bearing a share of the heat load requirement. Towers can be inter-connected in several different ways (Figure 4-1), but for simplicity it was assumed that each tower acted independently and received its share of the hot water to be cooled at the same temperature as in Figure 4-1C. In this analysis, the designs use a dry tower sized so that it alone can handle the required heat load

Fig. 4 -1 A

Fig. 4 -1 B

Flow Configurations for
Combination Cooling Towers

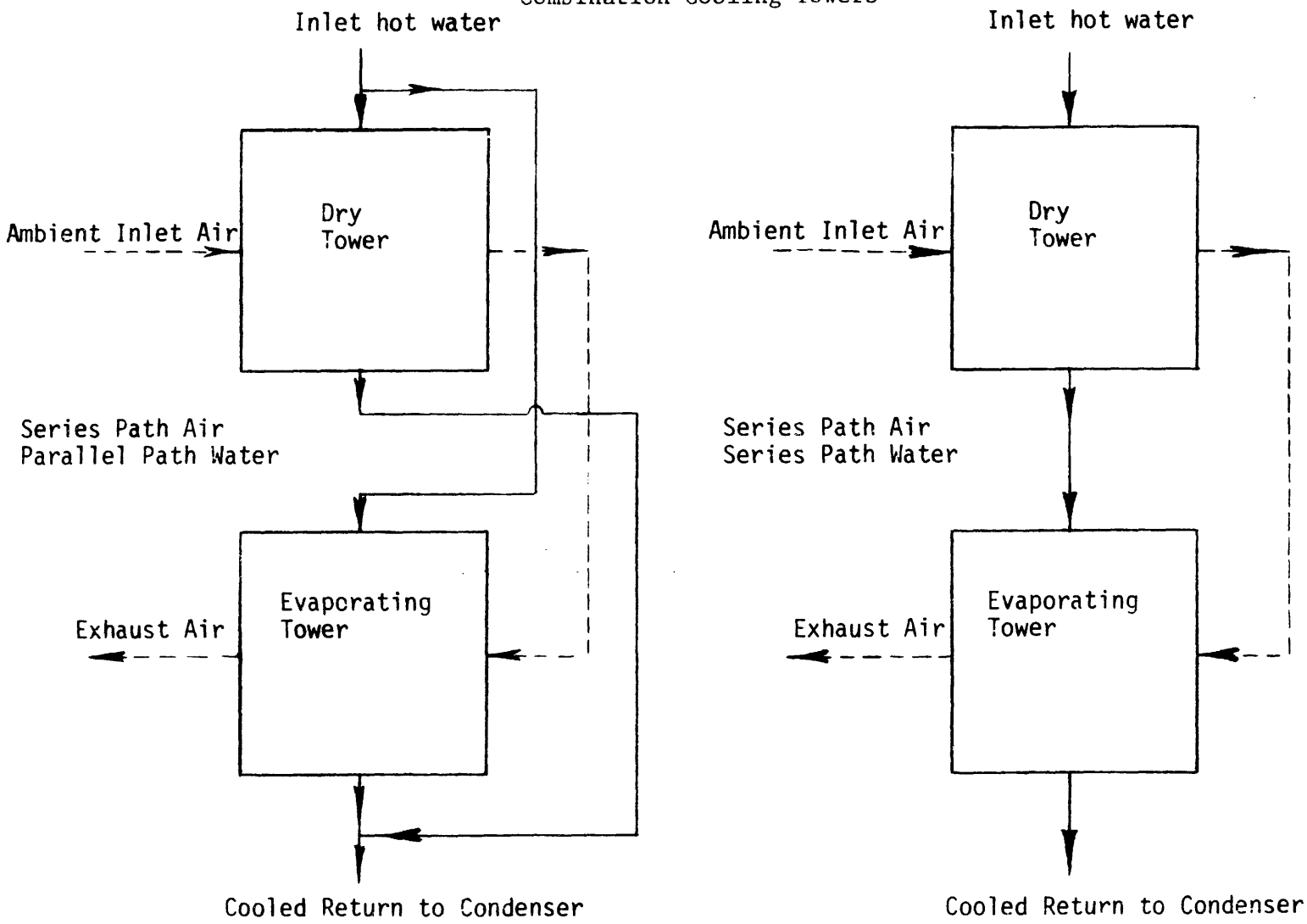

Fig. 4 -1 C

Flow Configurations for
Combination Cooling Towers

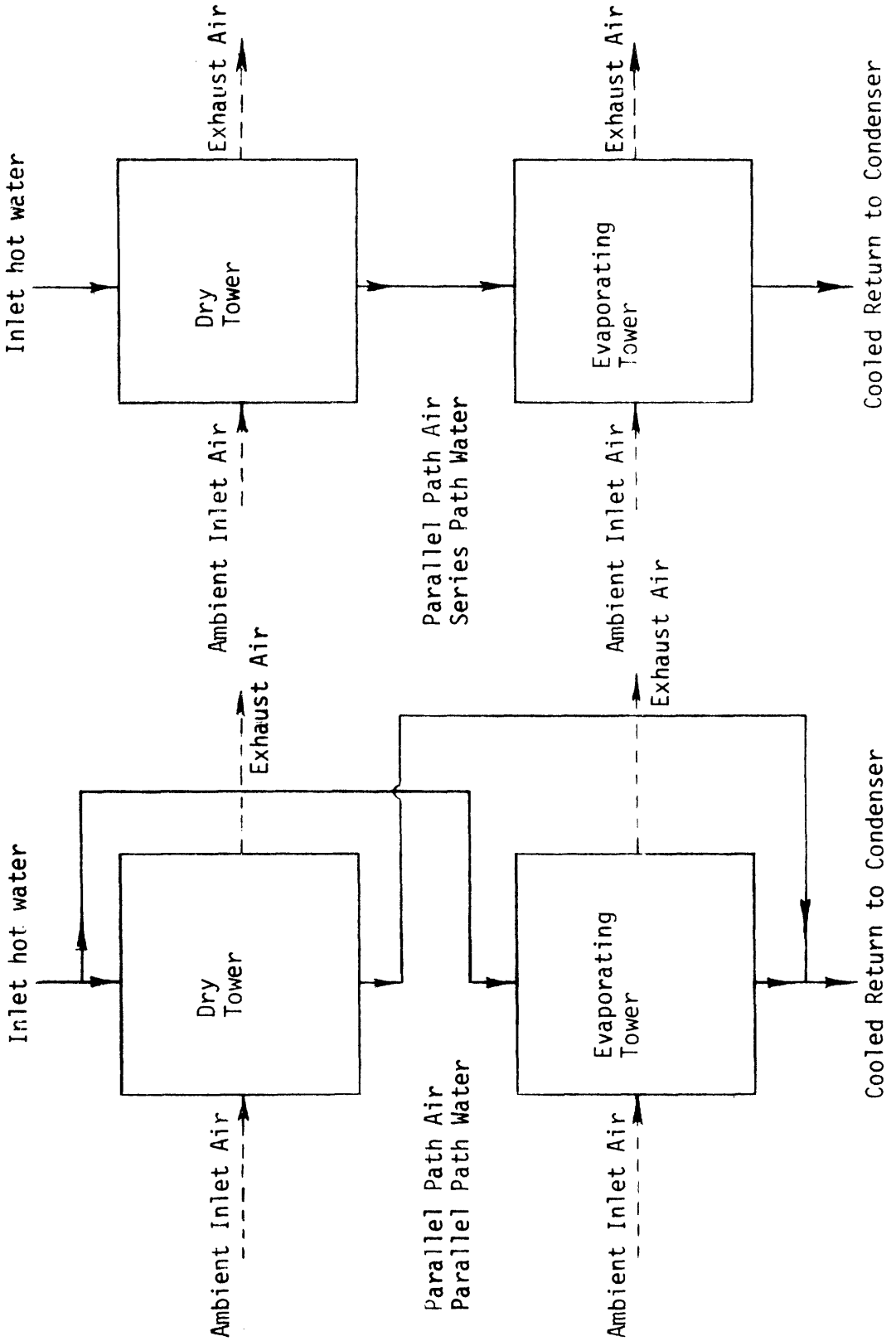

Fig. 4 -1 D

below a certain ambient dry-bulb temperature, and a wet tower which is added only at higher ambient temperatures when the dry tower is unable to carry the entire heat load alone. This design has the advantages of being much lower in cost than a single dry tower sized to handle the fixed heat load at all operating conditions [13] while evaporating much less water than a single, equivalent wet tower.

The advantages of this concept are such that it was decided to include combinations of dry and wet-dry concept towers (described in this work) which would also reflect some of the advantages of the conventional dry and wet tower combination systems.

For the purposes of this comparison, it was assumed that the basic component towers (dry, wet, wet-dry) could each be linearly employed; that is, if a certain tower could transfer heat at a rate Q under one set of ambient conditions, and at a rate 2Q at some other ambient condition, it would be possible to simply take one-half of the tower out of service to keep the heat transfer rate constant at this second set of conditions. The fan power and water loss would also be reduced by the same fraction. This assumption is more accurate when applied to large cooling tower systems which consist of many controlable units than when applied to a single tower.

The following eight representative combinations will be compared and referred to by the names listed here.

1) DRY tower: completely non-evaporative, this tower transfers all heat by forced convection;
2) WET tower: deluge-type packing, this tower transfers approximately

85% of its heat load through latent heat of evaporation with the remaining heat transfer due to convection from the water surface;

3) WET/DRY tower: V-trough type packing with a wet-to-dry surface area ratio of 5%. This configuration is similar to the model tower which was built and evaluated at M.I.T. within the last year.

4) WET + DRY @ 80°F: a DRY tower sized to handle the design heat load below 80°F dry-bulb (27°C) inlet air and a WET tower to help carry the design heat load at higher ambient temperatures.

5) WET + DRY @ 60°F: similar to (4), with the DRY tower sized at 60°F(16°C) inlet air and the WET tower added at higher ambient temperatures.

6) WET + DRY @ 40°F: similar to (4), with the DRY tower sized at 40°F (4°C) inlet air and the WET tower added at higher ambient temperatures.

7) WET/DRY + DRY @ 60°F: a DRY tower sized to handle the required heat load at 60°F (16°C) inlet air and a WET/DRY tower to help carry the design heat load at higher ambient temperatures.

8) WET/DRY + DRY @ 40°F: similar to (7), with the DRY tower sized at 40°F (4°C) inlet air and the WET/DRY tower added at higher ambient temperatures.

Performance for each of these configuations was evaluated by means of the computer program listed in Appendix H using the individual design parameters given in Appendix D.

4.2 Performance Predictions

The following sections and figures compare various aspects of performance for the combination cooling towers described above. For the most part these comparisons are based on a constant rate of heat rejection and a constant inlet hot water temperature for each system being evaluated. At high ambient temperatures both components of a combination system share the heat load, with the DRY component operating at its maximum capacity for those conditions and the evaporating (WET or WET/DRY) component making up the rest of the requirement.

As the ambient temperature decreases, the DRY component carries an increasing portion of the fixed heat load as the evaporating tower is cut back to hold the system heat rejection rate constant. When the DRY component sizing temperature is reached, the DRY tower carries the entire heat load and the WET component is completely shut down. Only for temperatures below this point is the DRY component capacity reduced in order to maintain a constant system heat rejection rate.

Use of these graphs must be tempered with the knowledge that each basic tower type (DRY, WET, WET/DRY) has a different mechanism for heat transfer. Usual heat exchanger performance comparison parameters may be misleading when applied to a WET or WET/DRY tower due to the portion of heat transferred by evaporation. For this reason, no attempt has been made to consolidate the findings into a single figure or section, but rather many views of system performance are presented, with overall conclusions appearing below.

4.2.1 Heat Transfer Rate

Figure 4-2 shows the variation of the overall heat rejection capabilities of the three basic designs with inlet dry bulb temperature. These and the following performance curves were taken from data calculated by the comptuer program listed in Appendix H.

DRY tower heat transfer rate under these conditions is linearly dependent on the initial temperature difference (ITD) between the ambient air and the inlet hot water. Thus the total heat rejection rate at T_{amb} = 90°F (32°C), ITD = 40°F (22°C), would be half that at T_{amb} = 50°F (10°C), ITD = 80°F (44°C), etc.

The WET tower has two heat transfer mechanisms which must be taken together to determine the overall heat transfer rate. One, dry convection from the hot water surface is essentially the same as that of the dry tower above, decreasing linearly to zero as $T_{amb} = T_{\ell_{in}}$. This mechanism, however, makes up only 15% of the total heat rejection on the average and thus has small influence on the total performance of the tower. The major portion of the heat load is transferred by evaporation which varies linearly as to the difference of the partial water vapor pressures of the ambient air and inlet hot water. For most of the operating range of the WET tower, this difference is a strong function of the inlet hot water temperature due to the non-linearity of the temperature-saturation pressure curve for water. Only at ambient temperatures close to the inlet hot water temperature, does the moisture content of the ambient air become an important parameters (Figure 3-3).

The combined result of these two mechanisms gives the WET tower a fairly flat performance curve over most of its operating range.

Fig. 4-2 A

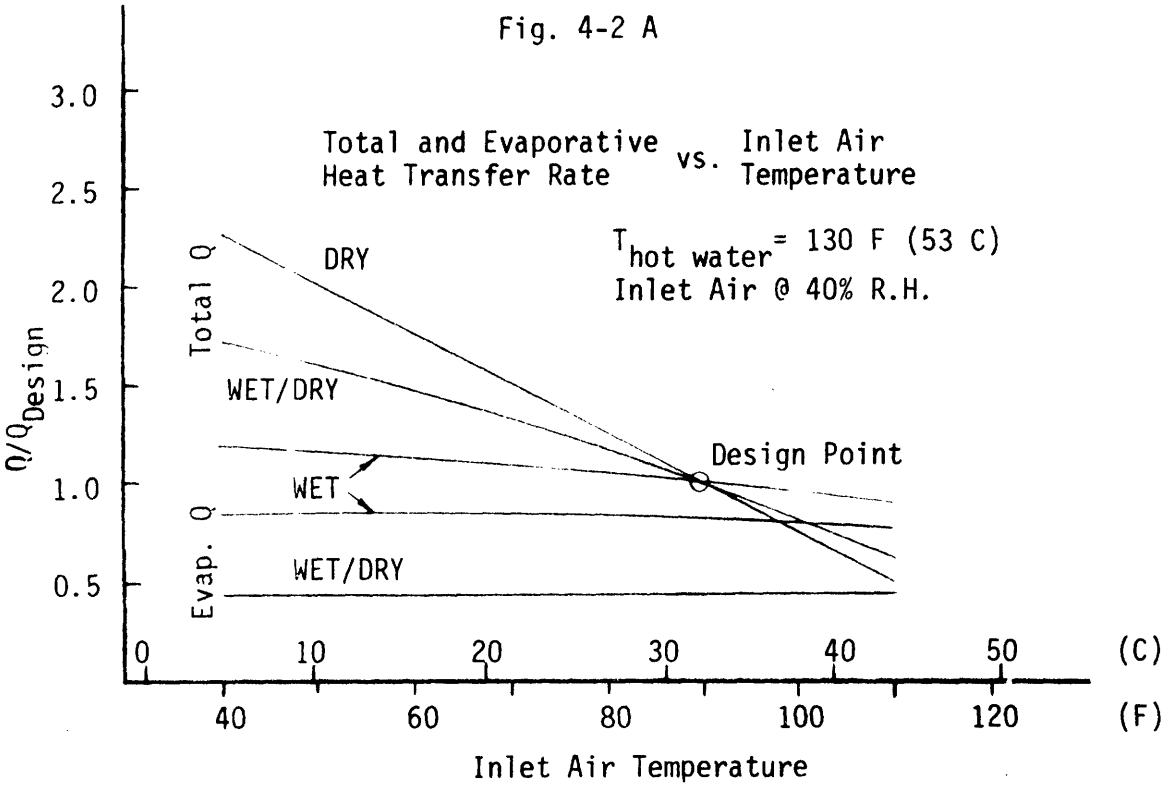

Fig. 4-2 B

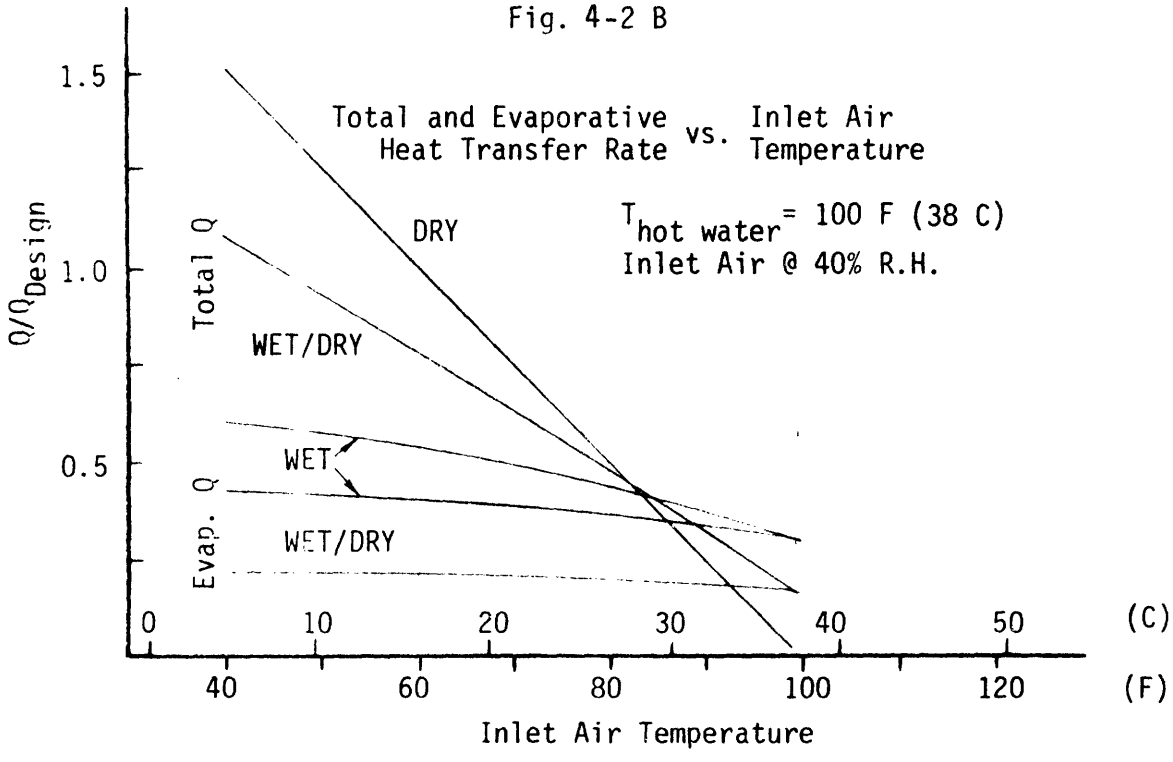

Fig. 4-2 C

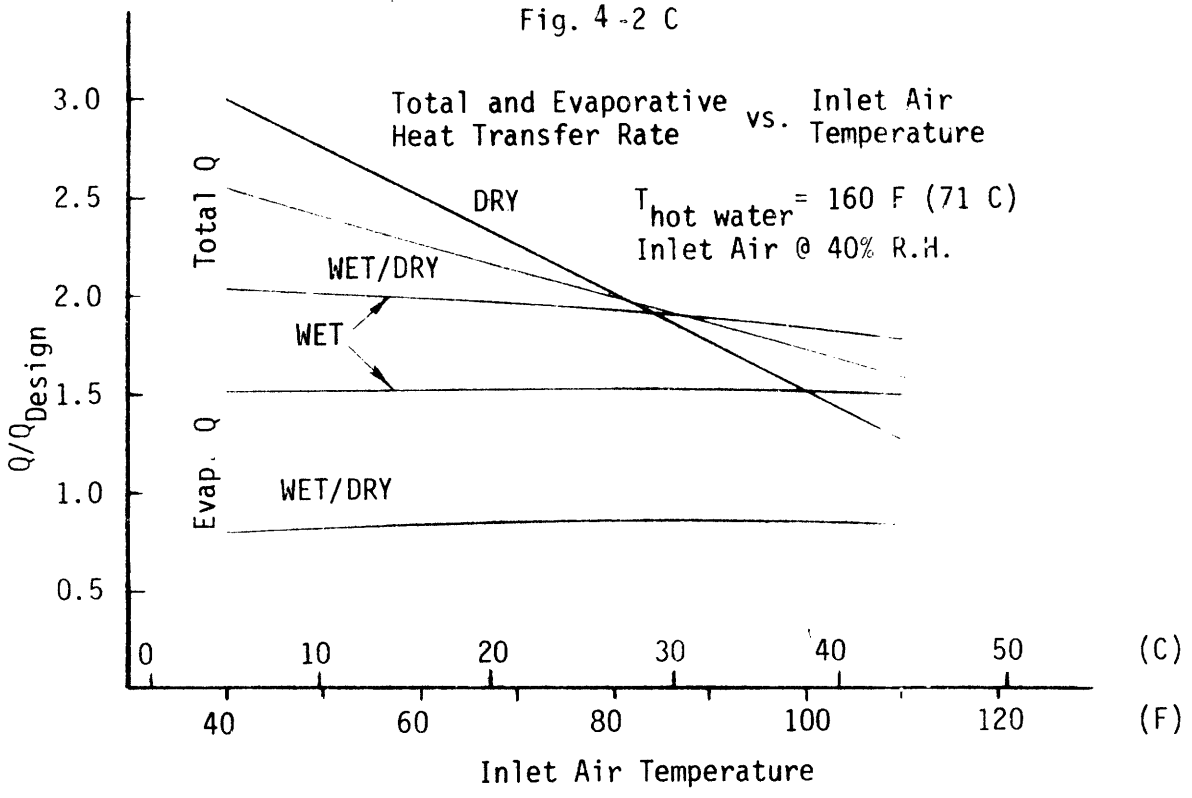

Fig. 4-3

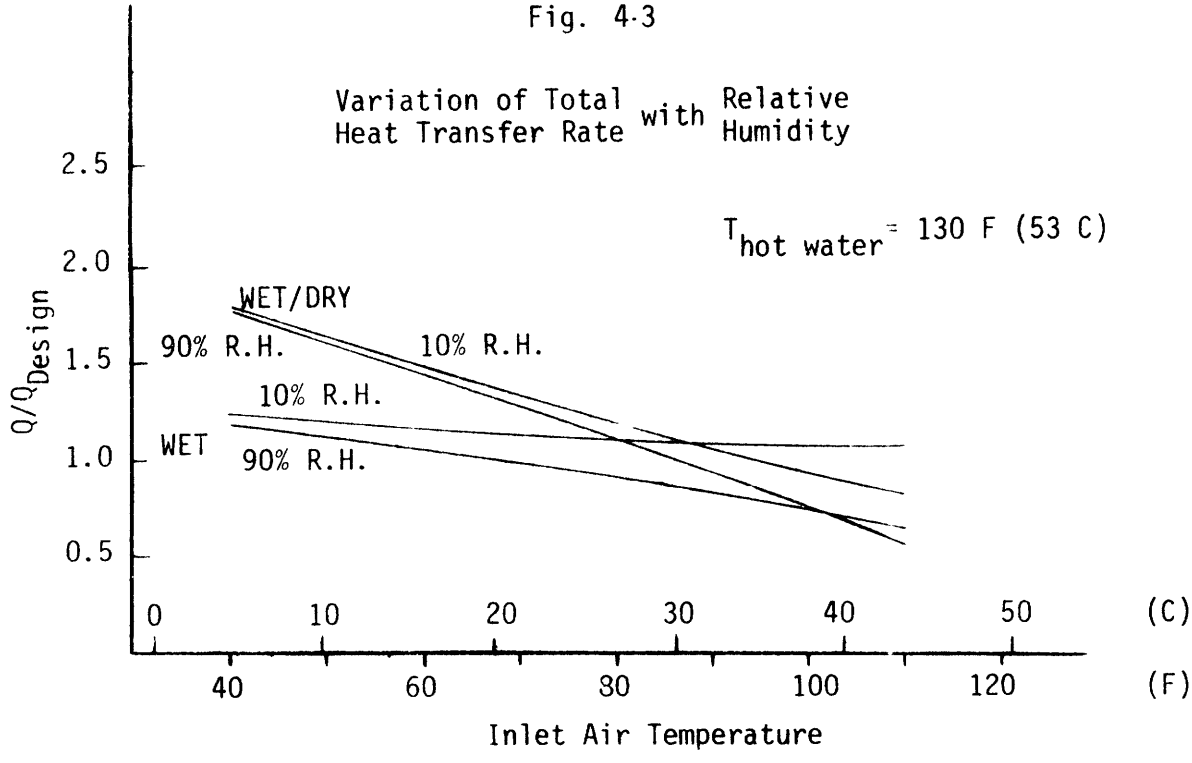

For the WET/DRY tower, the same two mechanisms for heat transfer are also operating, but their proportional share of the heat load has been changed. On the average about 60 to 70% of the heat load is rejected by dry convection with the remaining 30 to 40% rejected through evaporation. Thus the WET/DRY tower seems to behave much more like the DRY tower, where overall capacity increases with the ITD. The WET/DRY tower is also less affected than the WET tower by ambient air moisture content at high ambient air temperatures (Figure 4-3).

4.2.2 Air Flow Requirements

Figure 4-4 compares the required air mass flow rates of the various designs using a purely WET tower as a basis. Heat load is held constant here at Q_{design} and the combination towers are employed as described in Sec. 4.1. Air mass flow is proportional to fan equipment and power consumption as well as overall tower size.

For a DRY tower the necessary air mass flow increases rapidly as the initial temperature difference is reduced.

The WET + DRY combination towers behave as a purely DRY tower until they reach the temperature for which the DRY portion was sized. Above this design point the rate of increase of the air flow rate is reduced as the WET portion now takes a growing share of the heat load.

The WET/DRY tower operated above the WET tower flow rate, but well below those of the WET + DRY towers in all cases. It also exhibits much less of a tendency to rise at higher temperatures than does the DRY tower.

The WET/DRY + DRY towers require slightly more air flow than the WET + DRY towers with the same all-dry design temperature. This was due to the reduced evaporative share of the heat load and the higher air flow requirements of the WET/DRY tower over a WET tower.

Fig. 4-4

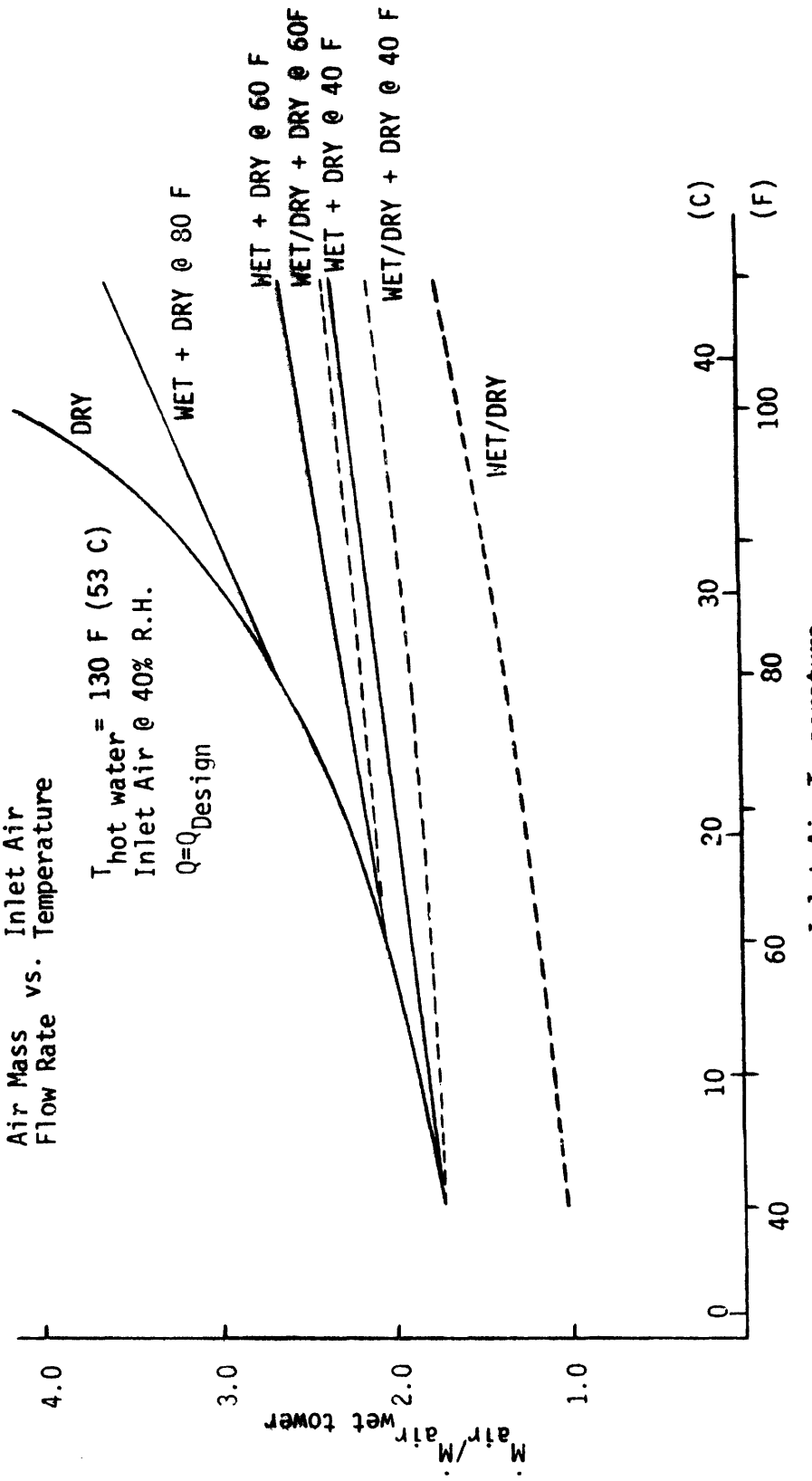
Air Mass Flow Rate vs. Inlet Air Temperature
$T_{hot\ water}$ = 130 F (53 C)
Inlet Air @ 40% R.H.
Q=Q_{Design}
DRY
WET + DRY @ 80 F
WET + DRY @ 60 F
WET/DRY + DRY @ 60F
WET + DRY @ 40 F
WET/DRY + DRY @ 40 F
WET/DRY
$\dot{M}_{air}/\dot{M}_{air_{wet\ tower}}$
4.0
3.0
2.0
1.0
0
10
20
30
40
(C)
40
60
80
100
(F)
Inlet Air Temperature

This graph does not take into account air pressure drop across the tower which is an essential parameter of pumping power costs.

4.2.3 Water Consumption

Figure 4-5 compares the rate of water consumption of the various towers for a fixed heat rejection rate using a purely WET tower continuously operating at 90°F dry-bulb (32°C), 40% R.H. for comparison. Inlet hot water for all towers was assumed to be constant at 130°F (54°C).

The combination towers of both WET + DRY and WET/DRY + DRY configurations consume no water until inlet conditions rise above the DRY component design temperature at which time the evaporating component must be brought into service. The water consumption rates for all designs then rise to meet where T_a = 130°F (54°C), at which point all heat transfer must be done by evaporation.

The WET/DRY tower has a relatively constant consumption rate in the lower operating ranges, but begins to consume more water as inlet air temperature increases and the convective heat transfer rate is reduced.

All the combination towers and the WET/DRY tower consume much less water than a WET tower under the same conditions. All WET/DRY + DRY systems consume far less water than similar WET + DRY systems having the same DRY tower design temperature.

The variation of water consumption rate with ambient and inlet hot water temperature was investigated as one means of optimizing the wet-dry design. The WET/DRY tower used in the previous comparisons was evaluated

Fig. 4-5

Water Consumption Rate vs. Inlet Air
for Combination Towers Temperature

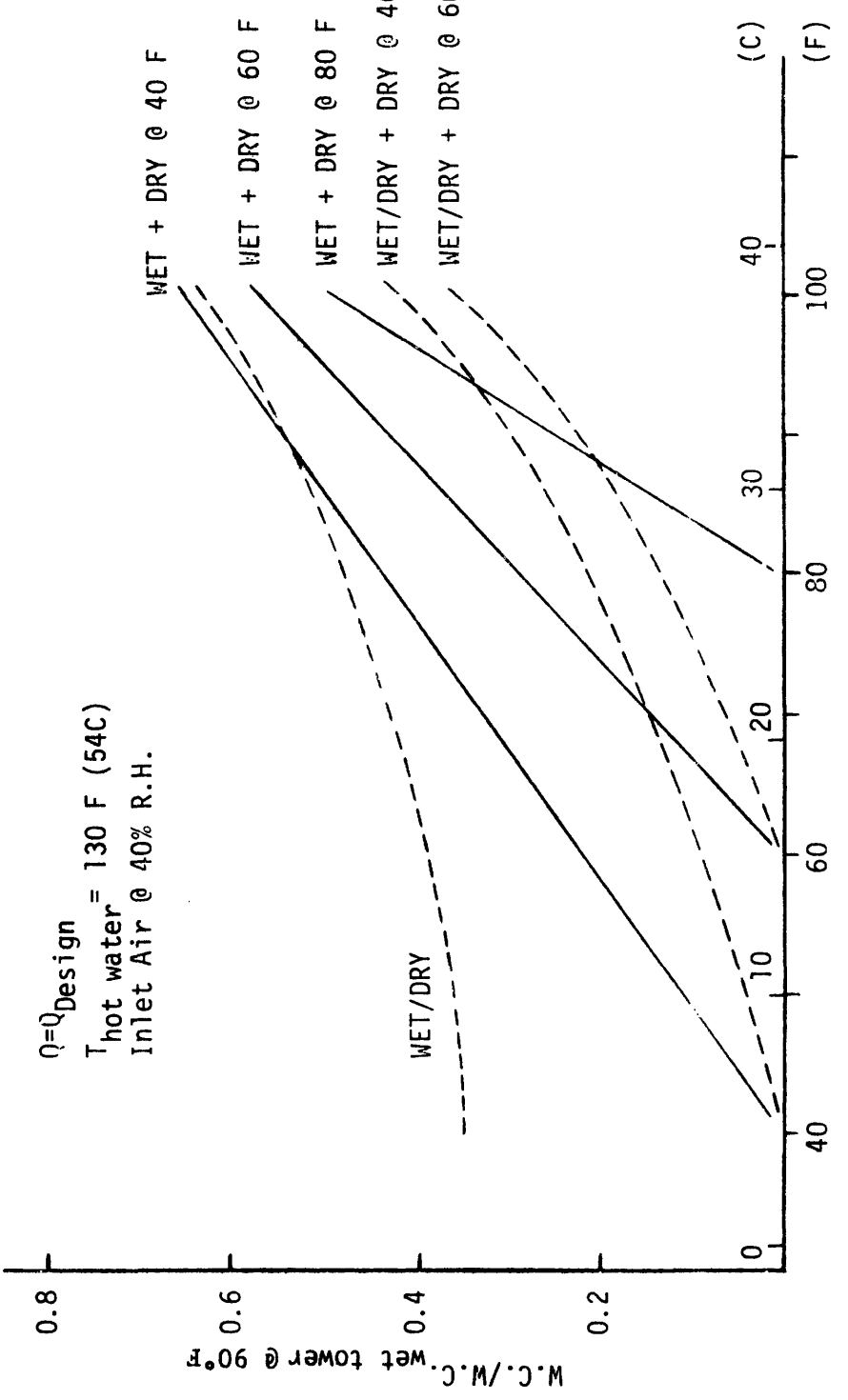

with varying inlet temperatures and fixed heat load. The results appear in Figure 4-6.

As an example, for the $T_{\ell_{in}}$ = 130°F (54°C) curve, water consumption is seen to rise with ambient air temperature as more of the tower comes on line and evaporation takes over a growing share of the heat load. Finally, at 90°F (32°C), the WET/DRY tower is operating at full capacity. Any further increase in ambient air temperature would cause the tower heat transfer rate to drop below the fixed heat load consumption of the WET/DRY tower for fixed hot water inlet temperature of 130°F (54°C) over a range of inlet air temperatures.

The same procedure was followed for $T_{\ell_{in}}$ = 120°F (49°C), 110°F (43°C), and 100°F (38°C) with the same tower design. These curves also appear in Figure 4-5. The endpoints and the dashed line represent water consumption and inlet air temperature when the design is allowed to run continuously at full capacity under a fixed heat load.

A WET/DRY tower system, optimized for minimum water consumption, would therefore be run at maximum capacity whenever possible, and only cut back when $T_{\ell_{in}}$ (and thus turbine back pressure) falls below an acceptable level. This also minimized turbine back pressure under all operating conditions and increases power plant gross output.

Running the tower system at full capacity also means higher operating and maintenance costs, but these should be more than offset by reductions in power generating costs.

Fig. 4-6

Variation of Water Consumption Rate
with Inlet Air and Water Temperature

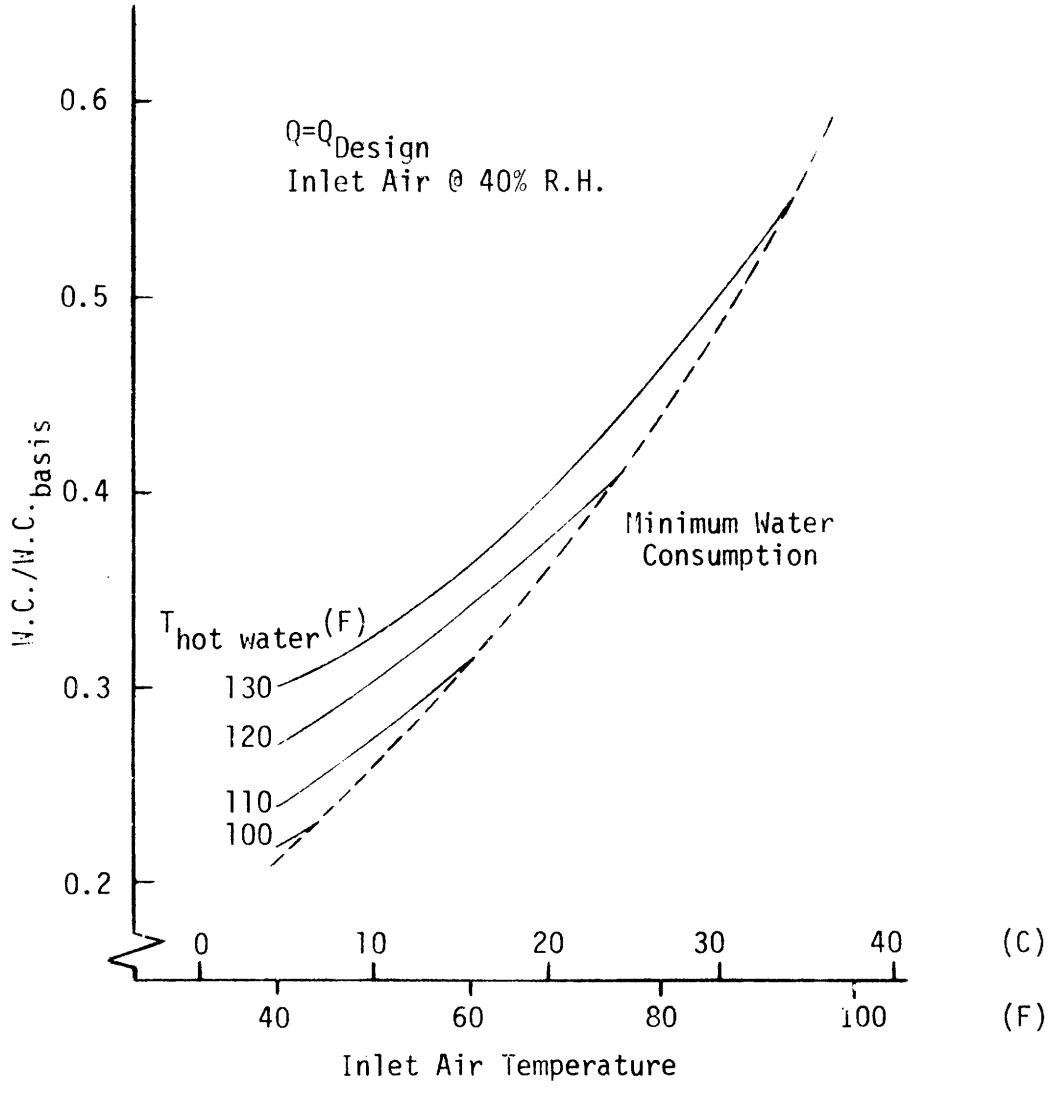

Figures 4-7 A,B,C,D compare the monthly water consumption rates of the various systems for locations around the country. All systems had a constant heat load,inlet hot water of 130°F (54°C), and were again compared using a WET tower working at 90°F (32°F) for a basis.

Water consumption for all designs in general climbs during the summer months and declines during the winter. It can also be seen that the WET + DRY @ 60°F and the WET/DRY + DRY @ 40°F designs have approximately equal water consumption in each location.

Climatic data were summarized from reference [14] and individual configuration performance under various conditions (evaporation rate, heat transfer rate, etc) taken from the preceeding figures. This use of hourly temperature distributions gives an accurate description of the weather conditions under which towers would be operating and makes possible this sort of analysis.

Please note that each value is a monthly consumption, independent of the preceeding and following months. For clarity the curves are continuous rather than stepped.

Figures 4-8 A,B represent the yearly totals of the monthly water consumption values shown in figures 4-7 A,B,C,D.A WET tower operating at 90°F (32°C) was again the basis.

The WET/DRY tower is shown to consume approximately 60% less water than a WET tower under the some conditions. The consumption totals for the WET + DRY @ 40°F are also fairly close for most locations, and about 90% lower than a comparable WET tower.

Fig. 4-7 A

Seasonal Variation of Water Consumption Rate
for Albuquerque, N.M.

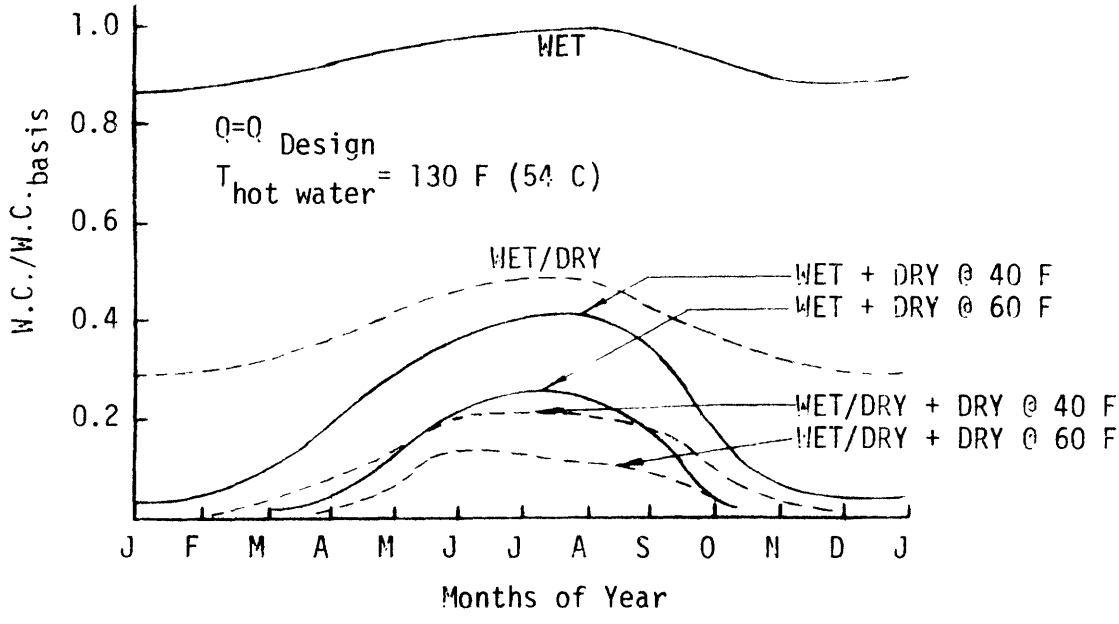

Fig. 4-7 B

Seasonal Variation of Water Consumption Rate
for Boston, Mass.

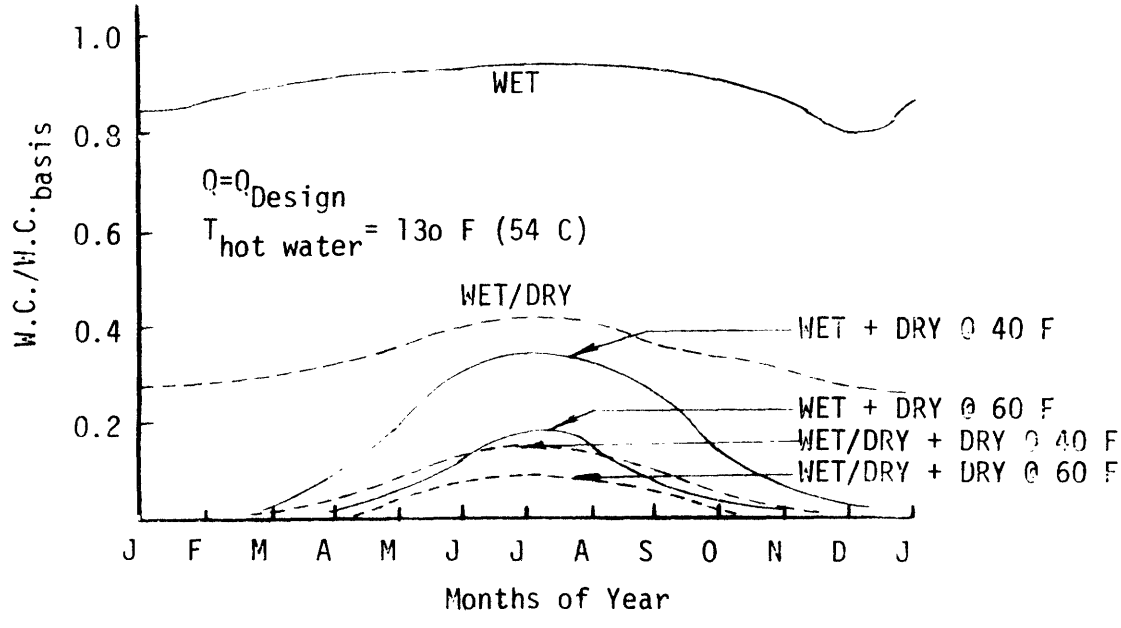

Fig. 4 -7 C

Seasonal Variation of Water Consumption Rate
for New, N.Y.

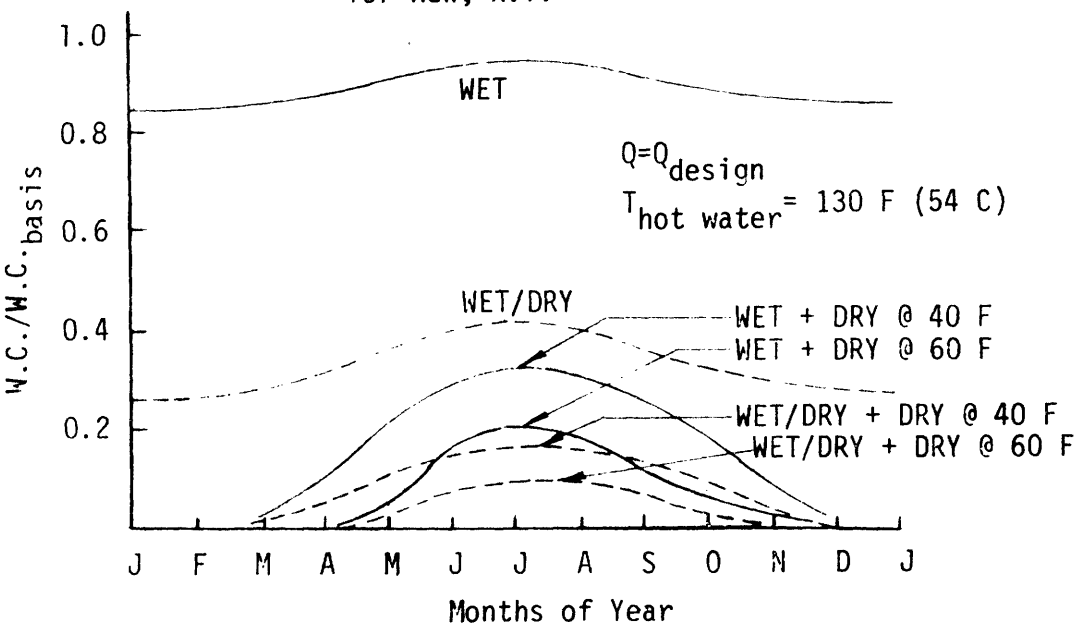

Fig. 4 -7 D

Seasonal Variation of Water Consumption Rate
for Los Angles, California

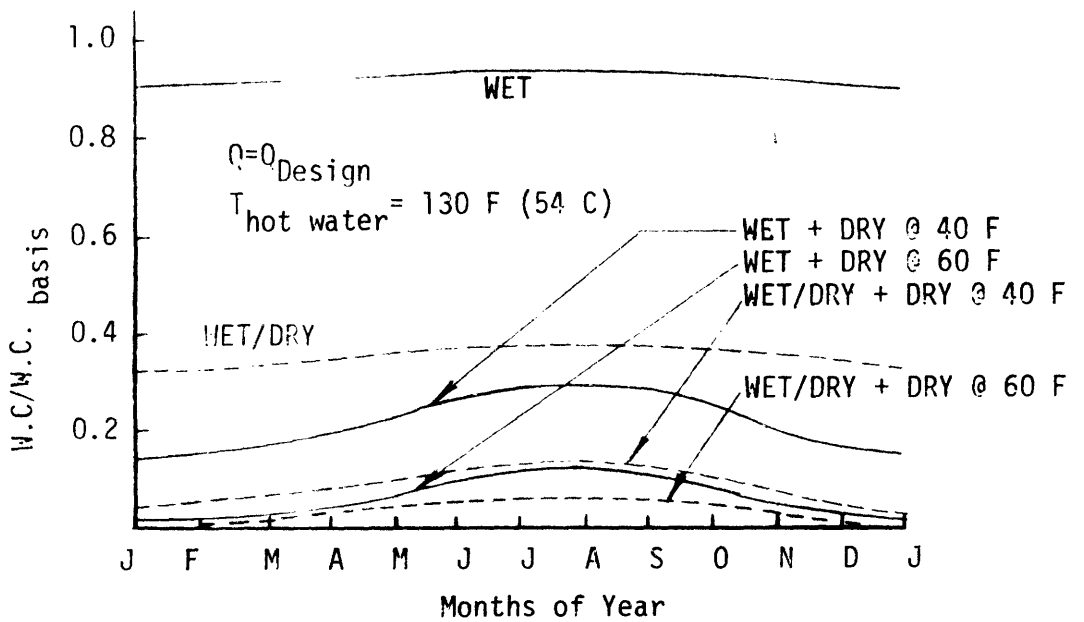

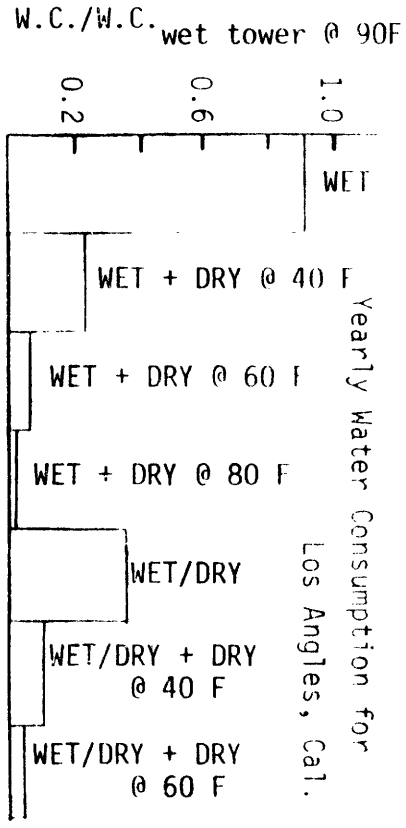
W.C./W.C. wet tower @ 90F
0.2
0.6
1.0
WET
WET + DRY @ 40 F
WET + DRY @ 60 F
WET + DRY @ 80 F
WET/DRY
WET/DRY + DRY @ 40 F
WET/DRY + DRY @ 60 F
Yearly Water Consumption for Los Angles, Cal.

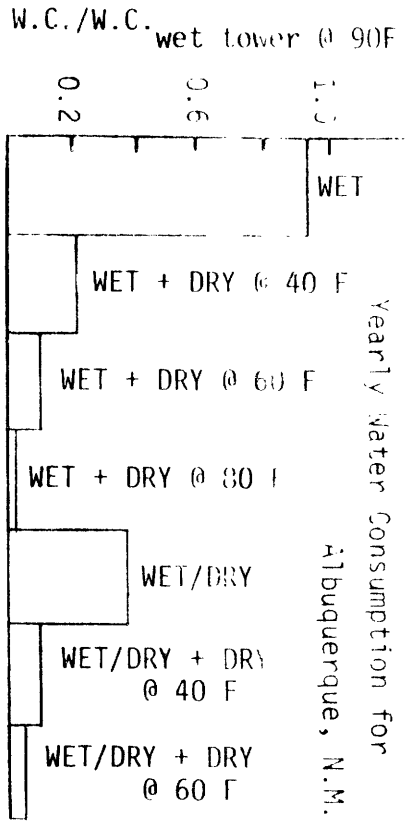
W.C./W.C. wet tower @ 90F
WET
WET + DRY @ 40 F
WET + DRY @ 60 F
WET + DRY @ 80 F
WET/DRY
WET/DRY + DRY @ 40 F
WET/DRY + DRY @ 60 F
Yearly Water Consumption for Albuquerque, N.M.

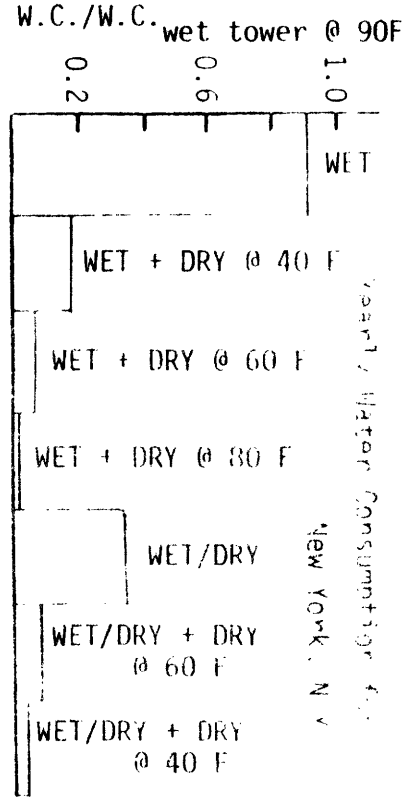
W.C./W.C. wet tower @ 90F
0.2
0.6
1.0
WET
WET + DRY @ 40 F
WET + DRY @ 60 F
WET + DRY @ 80 F
WET/DRY
WET/DRY + DRY @ 60 F
WET/DRY + DRY @ 40 F

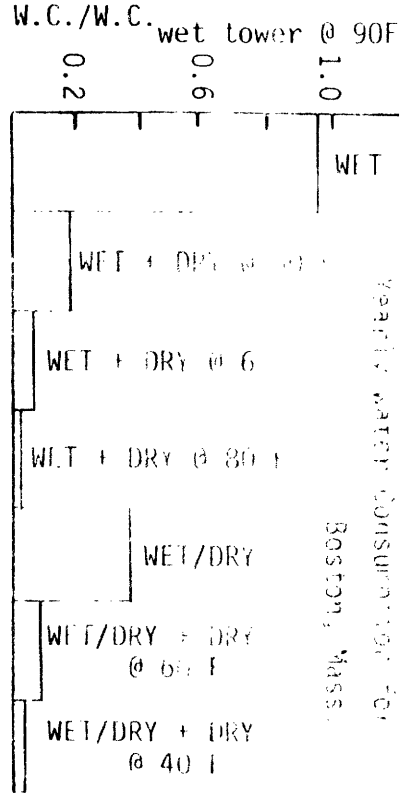
W.C./W.C. wet tower @ 90F
0.2
0.6
1.0
WET
WET + DRY @ 6
WET + DRY @ 80 F
WET/DRY
WET/DRY + DRY @ 40 F

Fig. 4-8

4.2.4 Minimum Turbine Back Pressure

Figure 4-9 shows the variation of condenser pressure with inlet air temperature for the three basic component towers. At lower ambient temperatures it is possible, by running the towers at full capacity, to reduce the hot inlet water temperature while maintaining the design heat rejection rate.

The inlet hot water temperature is related to the turbine back pressure and overall power plant efficiency. Modern turbines can have an operating range from 1.5 up to 15 in. of Hg (300-1300 N/m^2) back pressure with efficiency decreasing and capital costs increasing very rapidly for designs above 5 in. of Hg. (600 N/m^2). Most turbines now being installed are low back pressure designs.

Note that the DRY tower is extremely sensitive to ambient temperature and requires very hot water above the design point of 90°F (32°C) inlet air. The WET/DRY and WET towers are respectively less sensitive and could continue to deliver full service at higher temperatures.

In practice, the inlet hot water temperature would be allowed to "float" with ambient conditions, rising or falling until the turbine design limit is reached. At low ambient temperatures where the turbine back pressure is likely to drop below the design limit, the tower system capacity would be reduced to maintain the minimum back pressure. At high ambient temperatures where maximum turbine back pressure would be exceeded, the generating turbines would be throttled back to reduce the total heat load requirement to within the capacity of the tower system under the prevailing ambient conditions.

Fig. 4-9

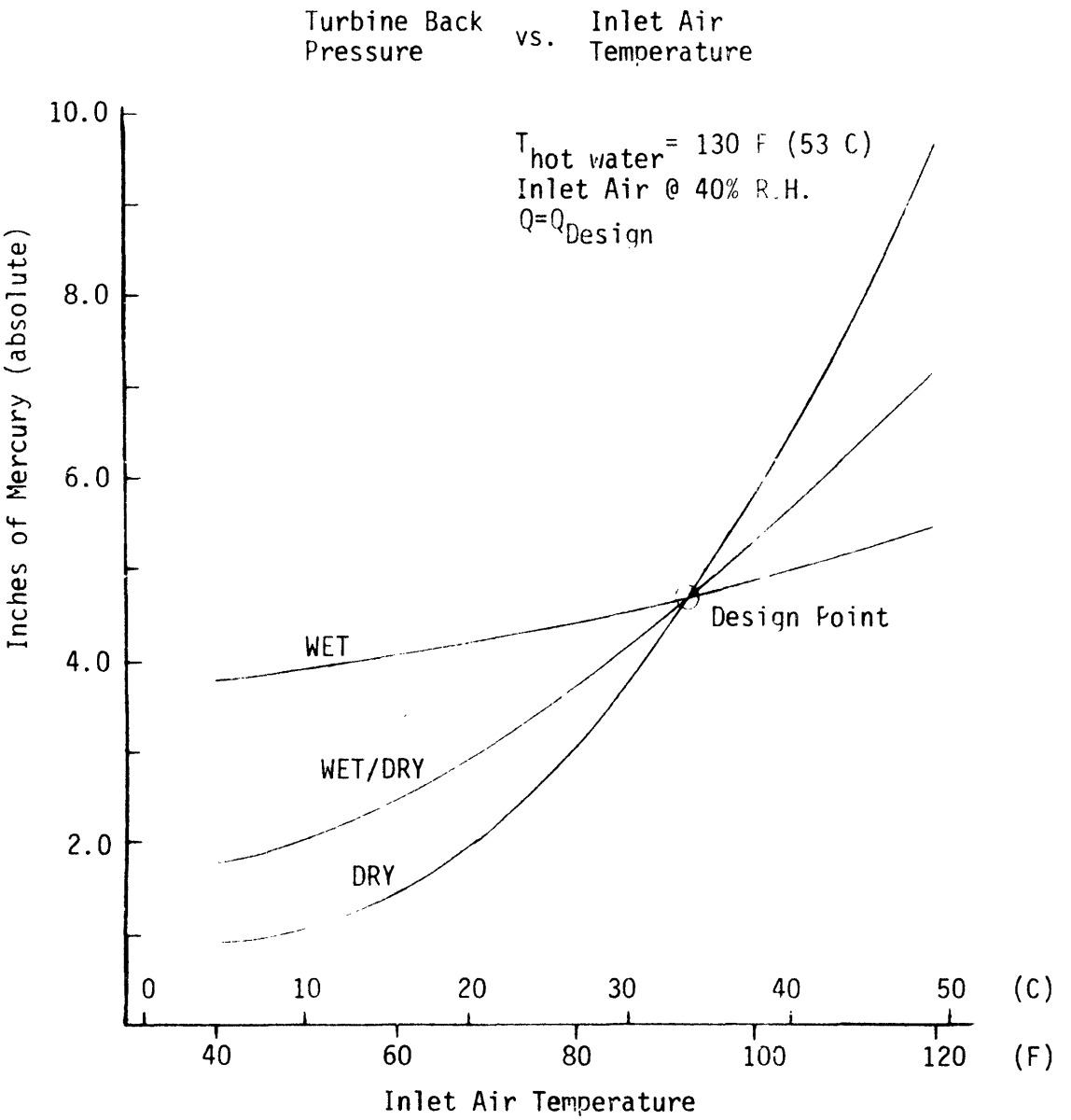
Turbine Back Pressure
vs.
Inlet Air Temperature
$T_{hot\ water}$ = 130 F (53 C)
Inlet Air @ 40% R.H.
$Q=Q_{Design}$
Design Point
WET
WET/DRY
DRY
Inches of Mercury (absolute)
10.0
8.0
6.0
4.0
2.0
0
10
20
30
40
50
(C)
40
60
80
100
120
(F)
Inlet Air Temperature

4.2.5 Incidence of Fogging

Figures 4-10,11 show the exhaust air conditions (temperature, for each relative humidity, specific humidity of the three basic tower designs.

Inlet conditions (ambient air temperature and hot water temperature) were varied over the normal operating range of a cooling tower system, while ambient air relative humidity was set at 90%.

Except at high ambient temperature conditions, the WET tower exhausts air at over 100% relative humidity, i.e. with entrained air droplets. This indicates the immediate presence of a fog plume. At air exhaust conditions of less than 100% R.H. fogging may occur depending on the mixing conditions of the ambient air and the tower exhaust. If the mixture passes through the saturation region for water vapor during mixing, fog will form in the area around the tower.

The WET/DRY tower, with its reduced evaporative heat transfer, does not produce a fog plume even under the most unfavorable ambient conditions.

Some types of WET+DRY combination tower systems mix the exhaust air from each component before discharging it to the atmosphere. This will reduce the incidence of fogging by allowing the wet tower exhaust to premix with hot air at ambient humidity before being discharged.

However, due to cost and land use considerations, the more recent trend in combination systems has been to build two separate towers, each exhausting separately into the atmosphere. In this case the individual towers would be described as in figures 4-10 and 4-11.

Fig. 4-10 A

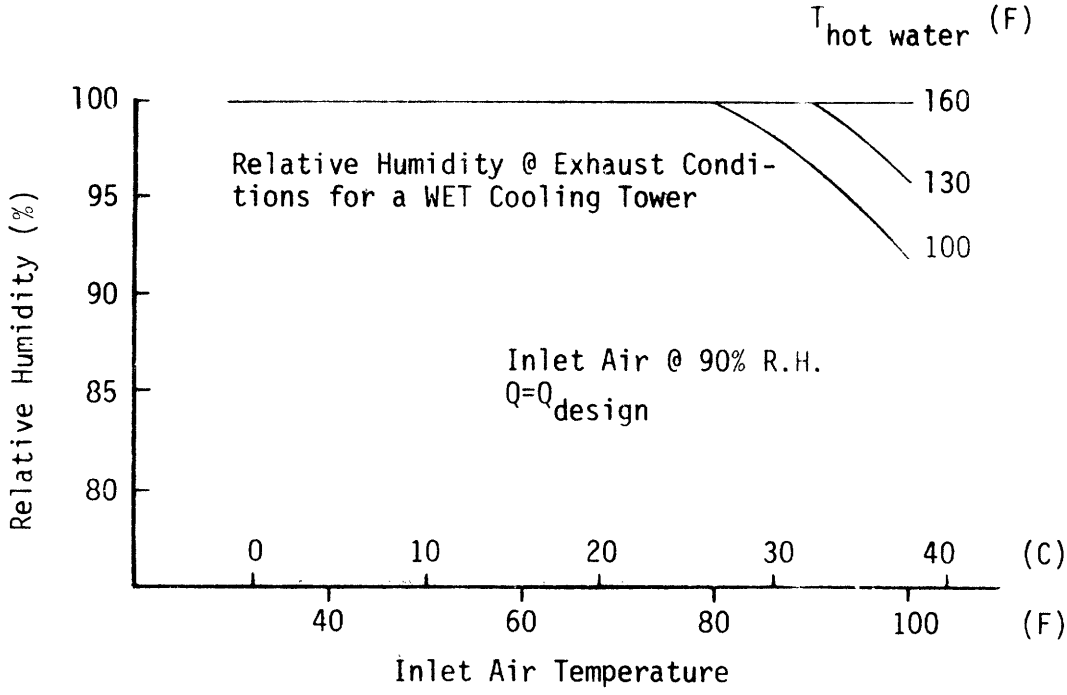

Fig. 4-10 B

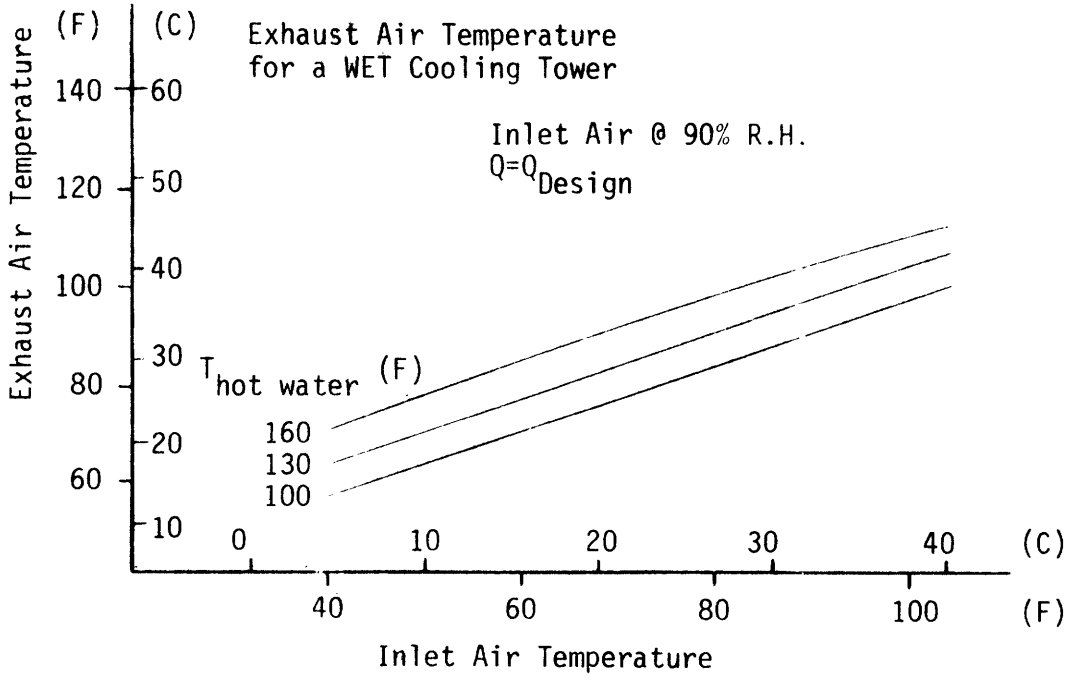

Fig. 4-10 C

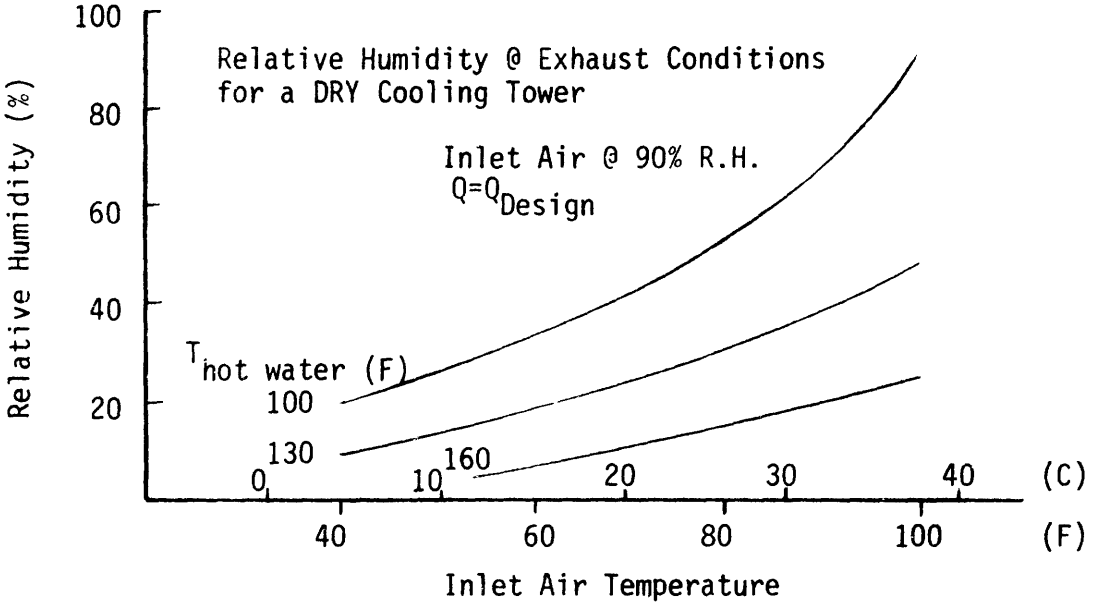
Relative Humidity (%)
100
80
60
40
20
Relative Humidity @ Exhaust Conditions
for a DRY Cooling Tower
Inlet Air @ 90% R.H.
Q=Q Design
T hot water (F)
100
130
160
0
10
20
30
40
(C)
40
60
80
100
(F)
Inlet Air Temperature

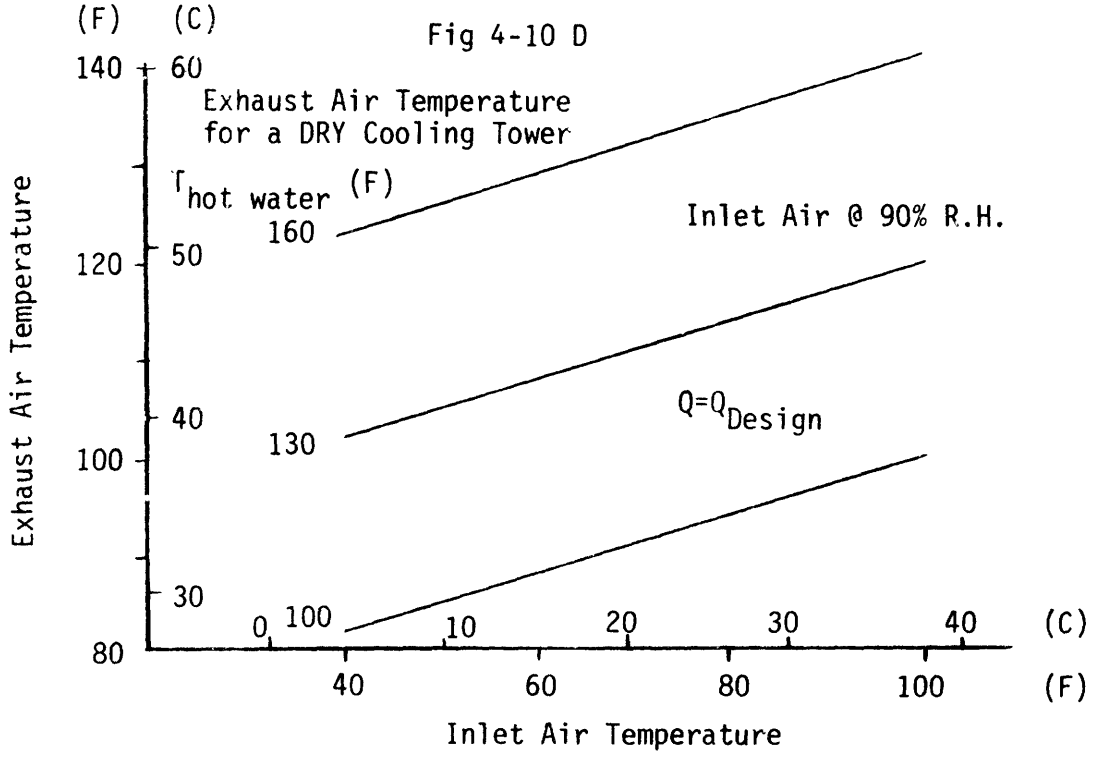
(F)
(C)
Fig 4-10 D
140
60
Exhaust Air Temperature
for a DRY Cooling Tower
T hot water (F)
160
50
Inlet Air @ 90% R.H.
120
40
Q=Q Design
130
100
30
0
100
10
20
30
40
(C)
80
40
60
80
100
(F)
Exhaust Air Temperature
Inlet Air Temperature

Fig. 4-10 E

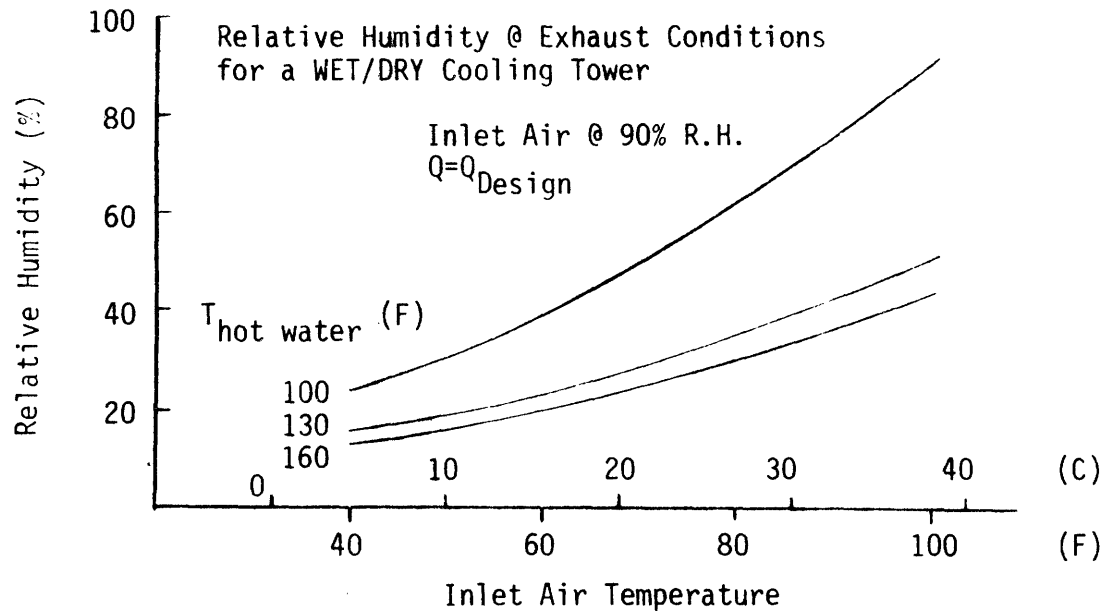

Fig. 4-10 F

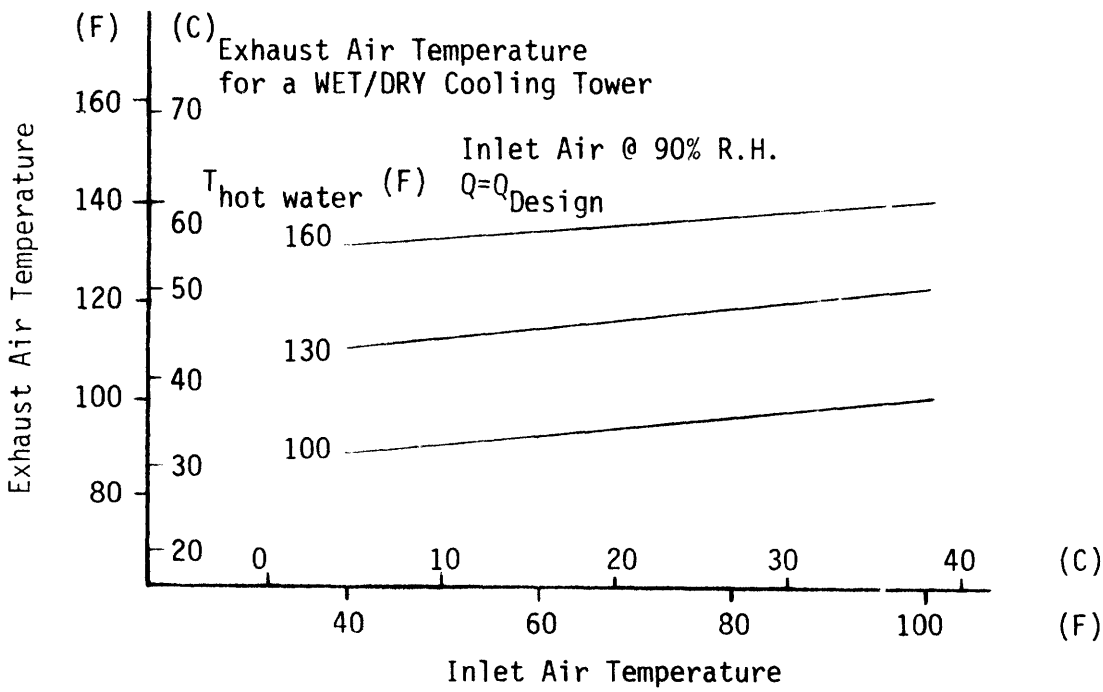

Fig. 4-11 A

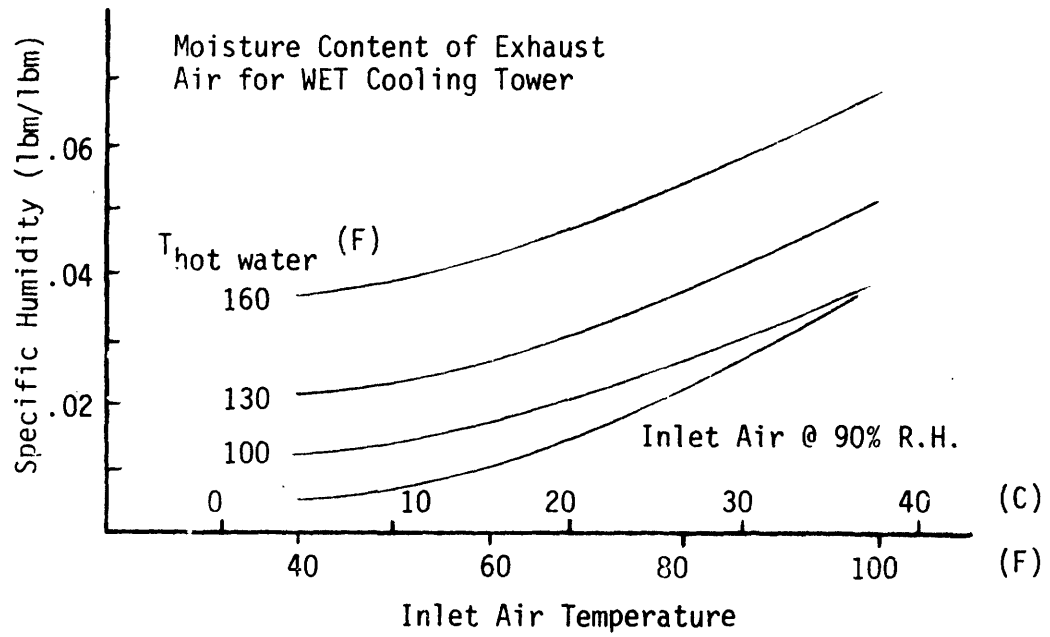

Fig. 4-11 B

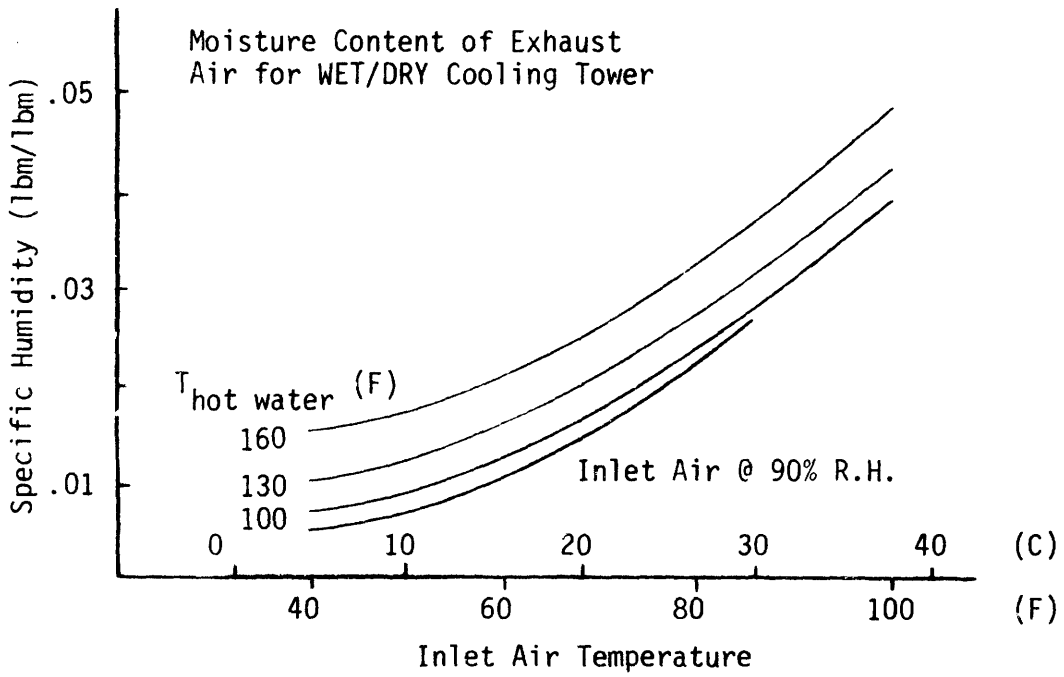

CHAPTER 5

CONCEPTUAL DISCUSSION OF CROSSFLOW CONFIGURATION

5.1 Need for a Crossflow Design

Early in the project it was recognized that the counterflow configuration would pose difficult design questions which would have to be answered before the concept could be used in practice.

The present design has the cool air entering at the bottom of the packing section and exiting at the top [1]. The hot water is distributed over the packing plates at the top of the section and collected at the bottom, hence the designation counterflow. Since the distribution and collection of the water is done in the airstream, great care had to be taken in the original design to reduce the amount of evaporation which would take place.

This was eventually done by distributing the hot water by rows of copper pipes with evenly spaced holes drilled along their length. These were arranged so as to provide one stream of water for each channel on each packing plate. Collection was accomplished by large sheet metal gutters at the bottom of each packing plate which would catch the cooled water and channel it quickly aside out of the air flow (Figure 2-1).

On an experimental level, this design presented several problems. Alignment of both the pipes and gutters was difficult and had to be done very closely to avoid splashing and dripping of water in the airstream. The distribution pipes became clogged with impurities and

had to be individually cleaned [1]. The collection gutters were large enough to warm theincoming air about 10°F (6°C) or more before it reached the packing section, thus precluding low air temperature tests. Despite the above precautions, in some tests the humidity change across the distribution system matched the change across the entire packing seciton.

For a full-size tower the size of the pipes and gutters would have to be increased to account for the greater width of the tower. Clogging and alignment would be an evern greater problem, while the larger pipes and gutters would decrease the airflow area and require more fan power for an equivalent rate of heat transfer. Evaporation in the distribution section would continue at what is considered an unacceptable level.

The solutions to each of these problems of the counterflow design would be costly and complicated. In an effort to keep the design both simple and effective, it was decided to investigate another configuration.

Instead of having the air flow from the bottom of the packing section to the top, the proposed design would have the air flowing across the plates horizontally, thus "crossflow".

This idea has several advantages:

1) It is possible to distribute and collect the hot water in an enclosed space, out of the airflow. This would eliminate most of the unwanted evaporation,

2) The distribution and collection are simplified. It would be possible to distribute the water with large spray nozzles

and collect it in a simple catch basin, thus cutting both fabrication and maintenance costs,

3) The elevation profile is reduced. There would be no need for an air inlet space under the packing section or for exhaust fans or ducting mounted above the packing section.

4) Air pressure drop can be adjusted by varying the width of the plates in addition to plate length and plate spacing. This would help in the optimization of the final design.

Disadvantages of this design include:

1) Reduced theoretical efficiency in heat transfer due to the change from counterflow to crossflow configuration.

2) Lack of knowledge of the heat and mass transfer characteristics of the V-trough packing plate under these conditions.

3) The need for major modification of the model tower presently in use if this configuration is to be tested.

5.2 Feasibility and Computer Program

In order to provide an estimate of the reduction in heat transfer rate caused by the change to crossflow configuration, a new computer program (listed in Appendix I) has been written. This program follows the analogy developed for the counterflow program (Appendix H, [1]) except for some minor bookeeping changes.

The crossflow packing is modeled by the program as a grid of series exchangers each of whichhas a small enough property change to be approximated by a counterflow heat exchanger. The program starts in the upper corner of the grid where both air and water inlet conditions are known. Using the method described in Chapter 3, the outlet conditions of this section are calculated and the results used as inlet conditions for the grid sections below and directly to the side. By moving downward one column at a time, using the previously calculated outlet

conditions from the adjoining grid squares it is possible to calculate the performance of the entire packing section.

The accuracy of this calculation depends on the number of grid squares employed. Trial runs for completely dry packing sections give results within 5% of published [15] solutions when a 25 x 25 grid is used. Further increase in the number of grid squares does give some better agreement, but the calculating time is greatly increased.

The program also contained provision for mixing the ccoling air as it passed through the packing section. However the difference in heat transfer rate between well-mixed and unmixed airflow was found to be very small (5%) for the operating range of an atmospheric tower.

Using the program described above a wet-dry crossflow tower was sized in the same way as the component towers used for the comparison in Chapter 4. This crossflow wet-dry required about 6% more surface area than the comparable counterflow WET/DRY tower where both were sized to carry the same heat load under 90°F (32°C), 40% R.H. conditions.

Performance curves under varying ambient air conditions for the tower designs are quite close and are shown in Figure 5-1.

Although these initial estimates are very rough and were not optimized in any way, they do indicate that the necessary increase in heat transfer surface for the crossflow design is not unreasonable. The savings in design and production costs would well offset the cost of the additional surface area.

Fig. 5-1

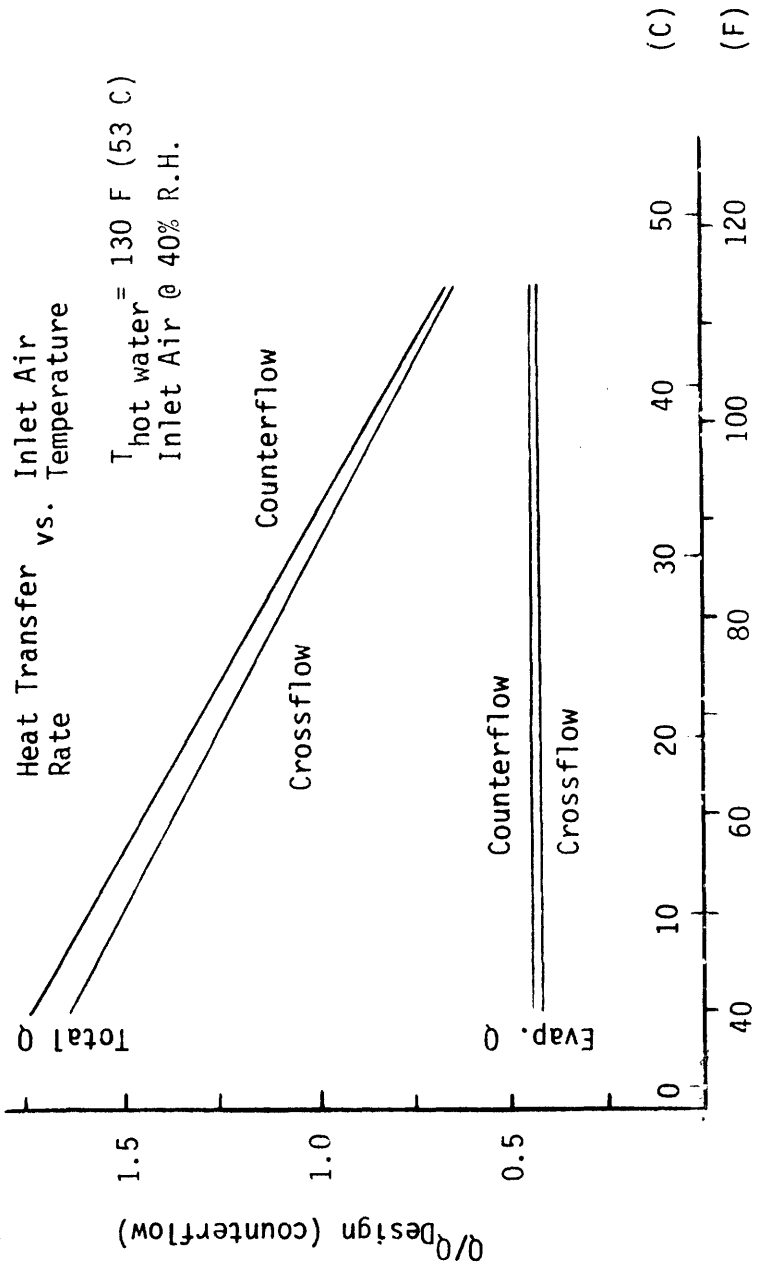
Heat Transfer Rate vs. Inlet Air Temperature
$T_{hot\ water}$ = 130 F (53 C)
Inlet Air @ 40% R.H.
Counterflow
Crossflow
Counterflow
Crossflow
Total Q
Evap. Q
$Q/Q_{Design\ (counterflow)}$
1.5
1.0
0.5
0
10
20
30
40
50
40
60
80
100
120
(C)
(F)
Inlet Air Temperature

5.3 Visualization of Large Crossflow Towers

The full size crossflow module shown here (Figure 5-2) is meant to give the reader a feel for the general size and shape of such a system. The module is approximately the same size as a mechanical draft wet tower module, with the packing section about 30 ft (9.19 m) high and 20 ft (6.1 m) thick. The air intake area is about 4300 ft^2 (400 m^2) and requires a fan of about 160 hp. Approximately 60 of these modules would be required to cool a 1000 MWe fossil fuel plant.

Part 2 of this report, printed under separate cover, will discuss the construction, instrumentation, testing and analysis of a crossflow model. Also included are project conclusions and recommendations for future investigation.

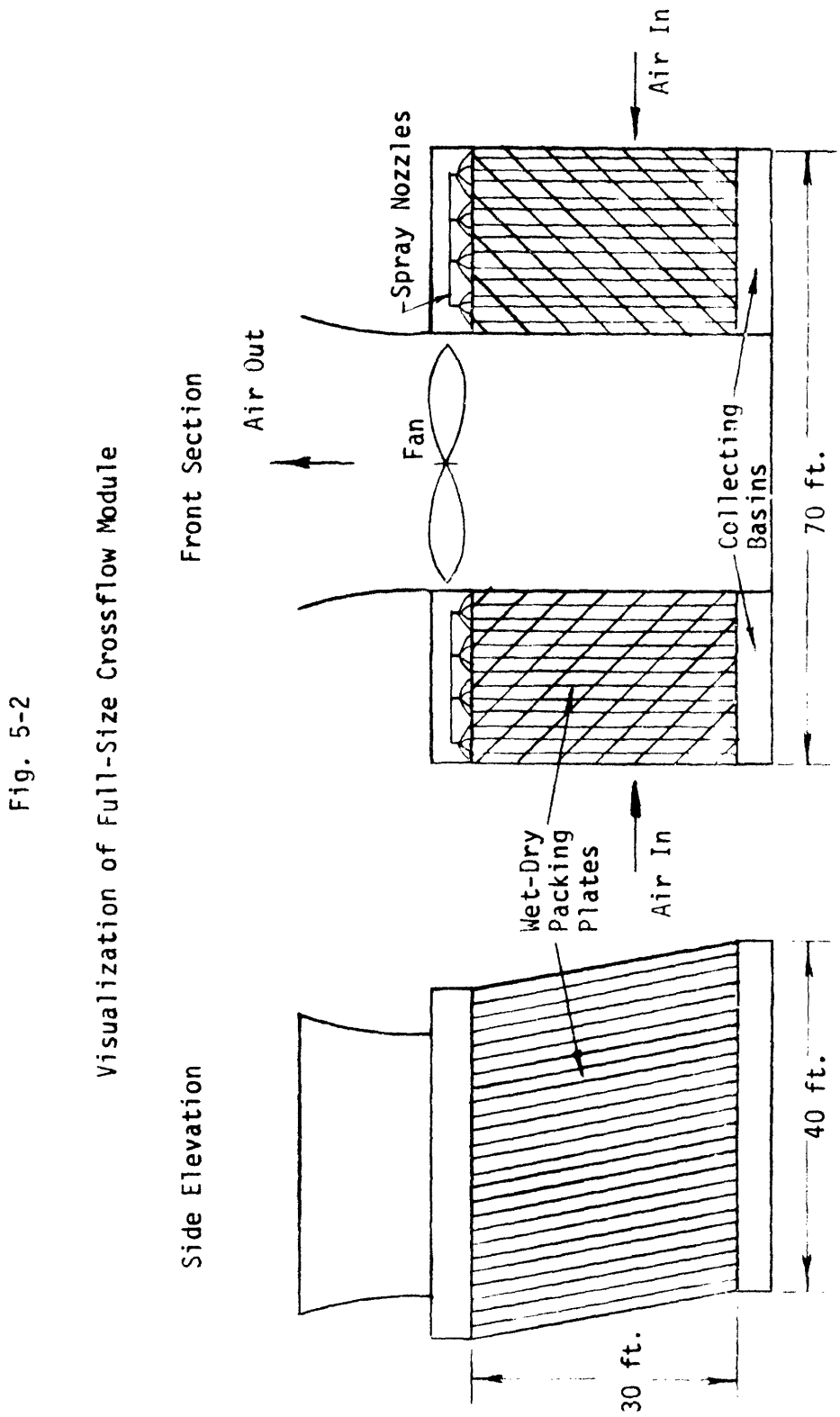

Fig. 5-2

Visualization of Full-Size Crossflow Module

CHAPTER 6: PRELIMINARY COST COMPARISON

This chapter presents a preliminary cost estimate of the wet-dry cooling tower concept and compares it with estimates for non-evaporative (dry) and evaporative (wet) cooling systems. Due to lack of operating experience with the wet-dry concept this analysis will rely heavily on previous economic comparisons [16] of cooling systems from which the wet-dry costs will be approximated.

Please note that the wet, dry and wet-dry performance models summarized in Sec. 6.2 are not the same as those presented in Appendix A and used in Chapter 4. The dry and wet system design parameters and total costs have been taken directly from the WASH-1360 report [16]. These designs are optimized for a 1000 Mwe fossil fuel plant at a fictional location designated as Middletown, USA. The wet-dry performance module has been designed to match certain parameters (airflow, water loading, exterior dimensions) of the wet system module, roughly optimized for minimum capital costs.

Section 6.1 will describe the economic models developed in Ref. [16] and used here for the calculation of capital and penalty costs for each type of cooling system. Section 6.2 summarizes the design parameters of the wet-dry design and sketches its performance at a few inlet conditions. A step-by-step description of the wet-dry cost evaluation and a short discussion of results will be found in Sec. 6.3 and 6.4, respectively. A more complete discussion of the cost evaluation method and optimization procedure for the dry and wet systems can be found by consulting Ref. [16].

6.1 Economic Model

The cooling system of a power plant determines the heat rejection temperature of the thermodynamic cycle and hence overall efficiency [12]. Cooling system performance is a function of a wide variety of factors including geographic location, ambient weather conditions, cooling system type and capacity, etc. Thus the determination of the true cost of a cooling system must include not only the initial and maintenance costs, but also an assessment of costs based on the performance of the cooling system.

The economic model consists of 1) the capital costs of the cooling system, 2) various economic penalties to account for the effects of changes in ambient conditions and other variables of cooling system and power plant operation, and 3) a total evaluated cost of the cooling system.

6.1.1 Capital Costof Cooling System

The capital cost of a cooling system includes all expenditures for parts and labor on the system. The major equipment for the systems under consideration here includes condensers, circulating pumps, piping, makeup and blowdown equipment, and the terminal heat sink, e.g. the cooling tower structure. Indirect costs include engineering and contingency charges.

6.1.2 Economic Penalties of Cooling Systems

The method of placing a dollar value on the performance of a

cooling system is to assign economic penalties to this cooling system [16]. Two major penalties are the loss of capacity and the cooling system auxiliary power requirement. In assessing the capacity penalty, the actual capacity of a plant and the corresponding energy produced by the plant are compared to a base capacity and its corresponding energy. Deviations below base values are charged to the cooling system as penalties, whereas deviations above the base values are taken as credits. The auxiliary power requirement is charged to the system according to the costs of the energy consumed.

Six penalties, in captialized dollars, have been assigned to the economic models. They are as follows [16]:

P1 = Capacity penalty cost due to highest turbine back pressure
P2 = Replacement energy cost due to turbine back pressure variation
P3 = Cost for operating circulating pumps
P4 = Cost of supplying makeup water to the cooling system
P5 = Cost for operating the terminal heat sink
P6 = Cost of operating and maintaining the cooling system

The equation used to evaluate the capacity penalty is:

$$P1 = (K)\,(\Delta KW_{max}) \qquad (6-1)$$

where: K = Capacity penalty charge rate ($/kwe)

ΔKW_{max} = Maximum loss of capacity at the worst ambient condition as compared to base plant capacity (kwe)

This penalty is treated as a capital expenditure and represents the cost of supplementing the capacity loss as compared to the base capacity, perhaps by the addition of gas turbine generating units.

The base capacity discussed here is arbitrarily defined. This capacity was chosen to correspond to an exhaust pressure of 1.5 in. of Hg ($5080 N/m^2$), a common design point for a power plant using a once - through cooling system [16].

A levalized capacity factor of 0.75 is introduced into the maintenance and operating cost equations. This factor assumes the plant will run at maximum power for 75% of the year and otherwise be at zero load. This is believed to be an adequate representation of central station base load power plants which are usually run at full capacity due to their low operating costs.

The replacement energy penalty, P2, and the cooling system auxiliary requirement energy penalties P3 and P5 are evaluated as follows [16]:

$$P2 = Cap \left(\frac{1}{afcr}\right) \int_0^{8760} (R)\ [\Delta KW(T)]\ dt \qquad (6\text{-}2)$$

$$P3 = (K)(HP_w)_{max} + Cap \left(\frac{1}{afcr}\right) \int_0^{8760} (R)\ [HP_w(T)]\ dt \qquad (6\text{-}3)$$

$$P5 = (K)(HP_t)_{max} + Cap \left(\frac{1}{afct}\right) \int_0^{8760} (R)\ [HP_t(T)]\ dt \qquad (6\text{-}4)$$

where:

afcr = Annual fixed charge rate

Cap = Levalized capacity factor

R = Replacement energy charge rate ($/kw-hr)

KW(T) = Loss of capacity due to variation in ambient conditions i.e., (plant capacity at ambient conditions) - (Base plant capacity) (kwe)

$(HP_w)_{max}$ = Maximum power requirement for pumping cooling water (kwe)

$HP_t(T)$ = Power requirement for operating the terminal heat sink at ambient condition (kwe)

$(HP_t)_{max}$ = Maximum power requirement for operating the terminal heat sink at the worst ambient condition (kwe)

t = Time (hrs)

Note that P3 and P5 both have two components, i.e., the capital expenditure of additional generating equipment and the capitalized replacement energy costs.

Penalty P4 is the makeup water costs for the system given by:

$$P4 = (G_m)\ (C_w)\ (1/afcr) \tag{6-5}$$

where;

G_m = Yearly makeup requirement (gal/yr)

C_w = Cost of makeup water ($/gal)

The annual operation and maintenance cost P6 of the system is based on the total capital cost and the amount of rotating machinery.

6.2 Performance Model

The cost of heat rejection from a 1000 Mwe fossil fuel generating plant will be considered. Figure 6-1 shows the heat rate correction for this type of plant using low exhaust pressure turbines.

The wet and dry systems compared in the following section (6.3) are taken directly from the WASH-1360 report. These two systems are the results of an extensive cost and performance optimization procedure based on the economic model described in Sec. 6.1. The wet-dry system used in this economic comparison is the result of a very rough optimization procedure which is described below.

6.2.1 Optimization of the Wet-Dry System

Due to the large number of variable parameters in the wet-dry concept, a few major assumptions have been made about the final design model, and an optimum found for the remaining variable.

These major initial assumptions include:

1) Air flow per system module equal to 1.5×10^6 ft^3/min ($710\ m^3/s$), based on fan limitations.
2) Pressure drop of 0.5 in H_2O ($125\ N/m^2$) across packing section, based on fan limitations.
3) Individual water channel loading of 1 lb_m H_2O/min (0.008 ℓ/s), based onobserved model tower performance.
4) Packing plate spacing of 1.5 in (3.8 cm), based on consideration of fabrication limitations.

Fig. 6-1

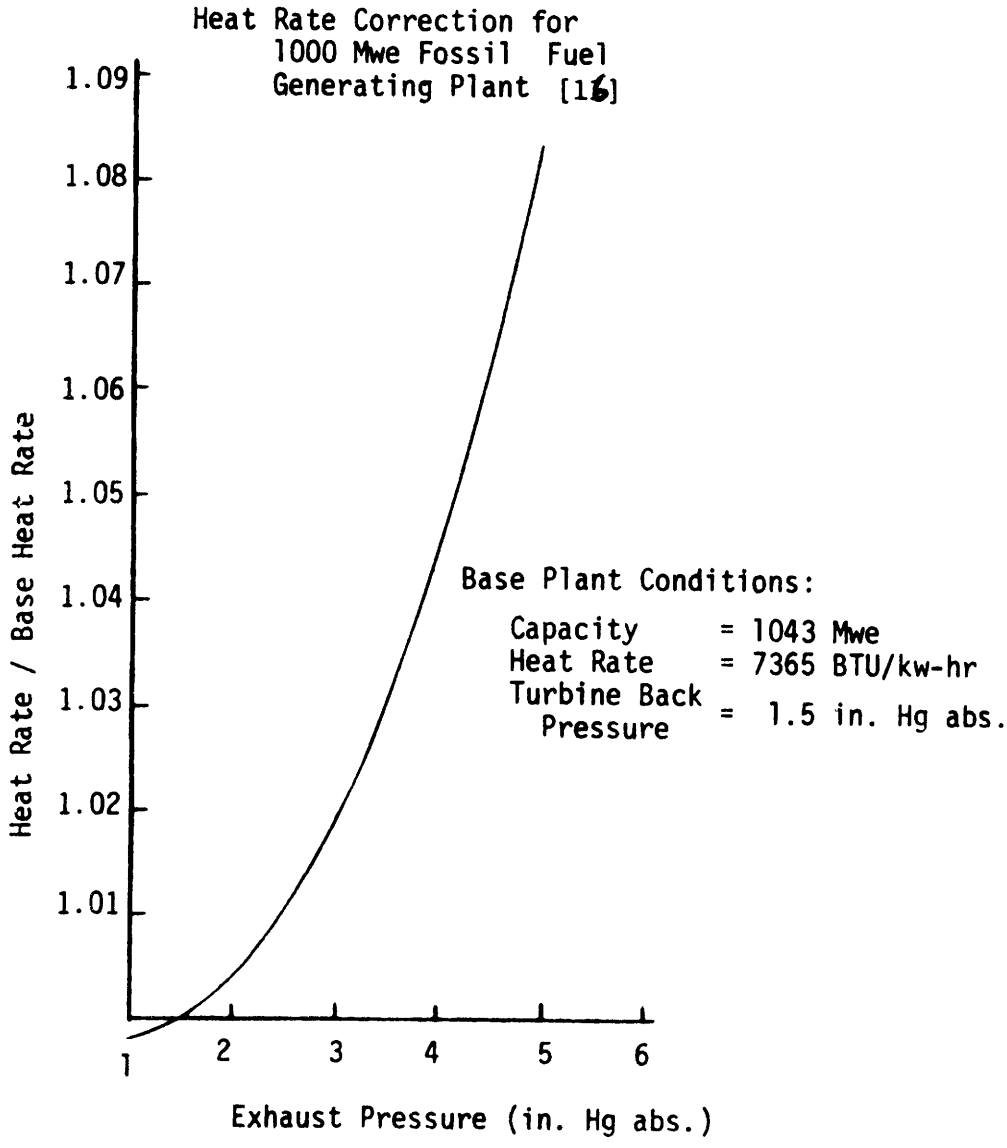
Heat Rate Correction for
1000 Mwe Fossil Fuel
Generating Plant [16]
Heat Rate / Base Heat Rate
1.09
1.08
1.07
1.06
1.05
1.04
1.03
1.02
1.01
1
2
3
4
5
6
Exhaust Pressure (in. Hg abs.)
Base Plant Conditions:
Capacity = 1043 Mwe
Heat Rate = 7365 BTU/kw-hr
Turbine Back Pressure = 1.5 in. Hg abs.

5) Plate length in direction of water flow of 30 ft (9.1 m) based on comparably sized wet modules.

6) Air and water flow streams in crossflow configuration for design considerations discussed in Chapter 5.

As in the case of both wet and dry systems, the wet-dry cooling system is made up of a number of modules, all identical in construction and performance. The number of modules necessary for a given cooling load is then determined by the heat rejection capacity at a given design temperature. The optimization presented here first determines the remaining design variable, packing surface area per module, then seeks an optimum design point for sizing the final tower system.

Using the above assumptions tower modules with packing widths of 10, 20 and 30 ft were optimized on the basis of minimum capital investment in the terminal heat sink. The cost of each module is broken down into three groups, fans and motors (identical in cost for all designs), structure and piping (here based on data from Ref. [16] and the ground area of individual modules) and packing material cost (based on packing surface area and material and fabrication costs discussed in Sec. 6.3.2). For determining the number of modules for a full size system a design point of 93 F (34 C) ambient air temperature and 121 F (40 C) hot water temperature has been assumed. The following costs in thousands of dollars can now be estimated for each module.

TABLE 6-1 MODULE COST OPTIMIZATION

Component Cost in thousands of dollars	Packing Width		
	10 ft	20 ft	30 ft
Fans and Motors	19.2	19.2	19.2
Structure and Piping	35.7	52.8	61.0
Packing Material and Fabrication	37.4	106.6	194.4
Cost per module	92.3	179.0	276.0
Number of modules needed for 1000 MWe facility	138	65	46
Total cost of Terminal Heat Sink (millions of dollars)	12.7	11.6	12.7

As shown in Table 6-1, the 20 ft wide packing section design is the optimum. Next the design inlet hot water temperature was optimized. A higher design inlet hot water temperature would require fewer modules at higher ambient temperatures to reject the same heat load as a system sized to a lower design water temperature. The reduced capital costs would be offset, however, by an increase in the operating penalty costs associated with the resulting higher turbine back pressure. The actual functional relationships are discussed in Sec. 6.1 and 6.3.1 and will not be described here in detail.

The results of this check show that savings in overall system costs are achieved by sizing the wet-dry system for a high inlet hot water temperature. This improvement is limited by the maximum turbine back pressure of 5 in. Hg. (17,000 N/m^2). Higher inlet water temperatures would require the use of so-called high back pressure turbines. These proposed designs can accomodate back pressures of up to 15 in. Hg. (51,000 N/m^2) thus allowing a major reduction in the number of necessary modules. Inefficiency penalties are substantial, but in the case of a dry cooling system [16] proved to be the best alternative. For the wet-dry system (Table 6-4) costs were significantly increased.

6.2.2 Wet-Dry Module Design

Table 6-2 shows the results of the wet-dry optimization. The performance of this module design was calculated under a wide range of operating conditions by the computer analogy listed in Appendix I and the results summarized for both high and low back-pressure turbines in Table 6-3.

An estimate of the possible savings which could be produced by relaxing some of the initial design criteria follows. These figures are meant to point out possible directions for future investigation, not as definite savings.

With this in mind, the effect of increased water loading per channel was investigated. By re-shaping the water channel it may be possible to double or triple the water flow over a given plate surface area. Further assuming that this could be done with little or no in-

TABLE 6-2

DESIGN PARAMETERS OF WET-DRY MODULE

Configuration	crossflow (Fig. 6-2)
Surface Heat Transfer Coefficient	5.8 BTU/hr-ft^2-F (28 kcal/h-m^2-C)
Wet-to-Dry Surface Area Ratio	0.05
Packing Height	30 ft (9.1 m)
Packing Width	20 ft (6.1 m)
Spacing of Packing Plates	1.5 in (3.8 cm)
Packing Plate Material	galvanized steel
Plate thickness	0.025 in (0.64 mm)
Number of plates per module	620
Water Channels per plate	80
Air flow per module	1.5 x 10^6 ft^3/min (710 m^3/s)
Water flow per module	6000 gal/min (380 ℓ/s)
Pressure Drop across Packing Section	0.5 in H_2O (125 N/m^2)
Air Velocity in Packing Section	10.8 ft/sec (3.3 m/s)
Fan Horsepower	186 hp (140 kw)
Number of modules in System:	
Low Back-Pressure Design	59
High Back-Pressure Design	27

FIGURE 6-2 CROSSFLOW PACKING PLATE

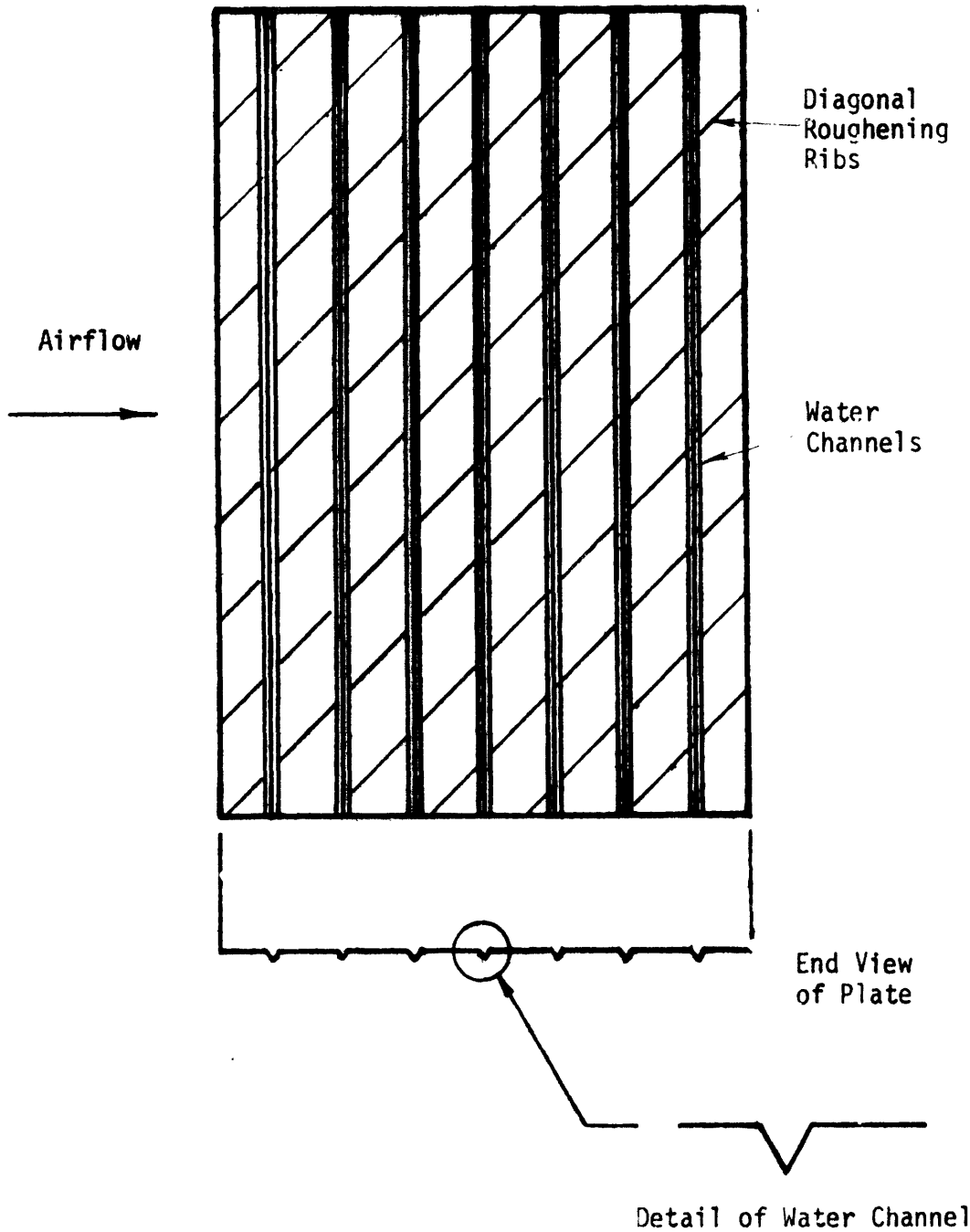

TABLE 6 -3 SUMMARY OF WET-DRY SYSTEMS PERFORMANCE

Ambient Air Temperature		Low Back-Pressure Design				High Back-Pressure Design			
		Inlet Hot Water Temperature		Capacity Penalty	System Water Consumption	Inlet Hot Water Temperature		Capacity Penalty	System Water Consumption
F	(C)	F	(C)	kwe	gal/hr (ℓ/s)	F	(C)	kwe	gal/hr (x105) (ℓ/s)
100	(38)	129	(54)	58,500	3.18×10^5 (23)	170	(77)	132,000	3.28 (24)
90	(32)	123	(51)	36,500	2.77×10^5 (20)	166	(74)	116,000	3.04 (22)
80	(27)	118	(48)	23,500	2.49×10^5 (18)	162	(72)	110,000	2.82 (21)
70	(21)	111	(44)	12,500	2.10×10^5 (15)	158	(70)	103,000	2.59 (19)
60	(16)	105	(41)	6,500	1.79×10^5 (13)	154	(68)	96,000	2.37 (17)
50	(10)	98	(37)	2,000	1.48×10^5 (11)	149	(65)	90,000	2.12 (16)
40	(4)	92	(33)	0	1.21×10^5 (8.9)	144	(62)	86,000	1.87 (14)
30	(-1)	84	(29)	-1,500	0.94×10^5 (6.9)	140	(60)	83,000	1.68 (12)
20	(-7)	80	(27)	-2,000	0.84×10^5 (6.2)	135	(57)	80,000	1.48 (11)

Yearly total water consumption for Middletown, U.S.A.

Low Back - Pressure Design - 1.39×10^9 gal (3.67×10^8 ℓ)

High Back - Pressure Design - 1.90×10^9 gal (5.01×10^8 ℓ)

crease in the wet-to-dry surface area ratio would produce an increase in the total module design heat transfer rate of 22% for 2X water loading and 32% for 3X water loading. This occurs due to the reduced water side effectiveness thus raising the log mean temperature difference [12].

In cost figures, if similar performance to the original module is assumed, capital cost reductions of 8% and 11% and total evaluated system cost reductions of 5% and 6% will be realized for the doubled and tripled water loading designs, respectively.

Continuing the process, should the plate height and spacing restrictions now be relaxed, the plates lengthened from 30 ft. to 45 ft. (9 to 14 m), plate spacing decreased to 1.25 in (3.2 cm), and normal water loading restored, the module design heat transfer will rise an estimated 20%. This translates into an estimated decrease of 7% in capital cost and 4% in total evaluated cost for the entire system. In this particular design, however, the lengthened plates also increase water consumption for a given amount of total heat transfer. Initial calculations show that this could be a 20% increase in system yearly water consumption. Further study into this type of optimization will be necessary for the final design process.

6.3 Cost Estimation

This step-by-step calculation presents only the values for the low back pressure design. The final figures for the high back pressure design are listed in Table 6-4.

6.3.1 Penalty Costs

Following the procedure described in Sec. 6.1.2,

Capacity Penalty Cost

$$P_1 = (K)(\Delta KW_{max}) \tag{6-1}$$

ΔKW_{max} = ΔKW @100F = 58,500 kwe

K = \$150/kwe

$P_1 = \$8.78 \times 10^6$

Replacement Energy Cost due to Turbine Back Pressure Variation

$$P_2 = Cap(1/afcr) \int_0^{8760} (R)\ [\Delta KW(T)]dt \tag{6-2}$$

Cap = 0.75

afcr = 0.15

$R = \$8.5 \times 10^{-3}$/kw-hr

$\int_0^{8760} \Delta KW(T)dt = 5.19 \times 10^7$ kw-hr

$P_2 = \$2.21 \times 10^6$

The integral $\int_0^{8760} \Delta KW(T)dt$ has been evaluated from Table 6-2 and climatic data for Boston, Mass. (Table G-3). This data is comparable to the composite climate of Middletown, U.S.A.

Cost for Operating Circulating Water Pumps

This cost has been set equal to that of the mechanical draft wet tower of Ref. [16],

$$P_3 = \$3.83 \times 10^6$$

This is felt to be accurate due to the similar water flow rate and pumping head requirements of the two designs.

Cost of Makeup Water and Water Treatment for the Cooling System

Due to the 40% lower water consumption of the wet-dry design (see Fig. 4.8), water consumption costs should be likewise reduced. Thus:

$$P_4 = \$0.07 \times 10^6$$

Cost for Operating the Terminal Heat Sink (fan power)

$$P_5 = (K)(HP_t)_{max} + Cap\left(\frac{1}{afcr}\right)\int_0^{8760}(R)\,[HP_t(T)]dt \qquad (6-4)$$

Assuming that all the module fans run constantly throughout the operating year,

$$(HP_t)_{max} = HP_t(T) = 11.8 \times 10^3 \text{ hp}$$

Thus:

$$P_5 = \$1.23 \times 10^6 + \$4.06 \times 10^6$$

$$P_5 = \$5.29 \times 10^6$$

Cost of Operating and Maintaining the Cooling System

This cost is based (as described in Sec. 6.1.2) on the amount of rotating machinery in the tower system. Assuming this is roughly proportional to the number of modules in the cooling system

and using the cost of $\$1.21 \times 10^6$ for a wet tower system with 23 modules, and $\$2.61 \times 10^6$ for a dry system with 94 modules, then for a wet-dry system of 59 modules:

$$P_6 = \$1.92 \times 10^6$$

Adding up all of these capitalized penalties gives a total penalty cost of $\$22.1 \times 10^6$. Individual penalties assessed to each system (wet, dry and wet-dry) have been tabulated for comparison in Table 6-3.

6.3.2 Capital Costs

The capital costs of the wet-dry tower system are very dependent on the system design parameters. However, all tower systems will have costs that will be relatively fixed for any given size system (water pumps, piping, electrical work, condensers), costs that will be proportional to the number of tower modules (fans, structure, basins) and costs that will be unique to each design (packing, fin-tube units, etc.).

Using the capital cost breakdown of Ref. [16] for mechanical draft wet and dry systems and the wet-dry module design of Sec. 6.2, the first two groups of these costs have been evaluated for the wet-dry systems. As the major difference between a wet and a wet-dry module is in the packing section, this cost for a wet-dry tower system will be based on the material requirement.

Using \$0.143 per ft^2 of 0.025 in. (0.06cm) thick galvanized sheet (a June 1976 U.S Steel quote adjusted for inflation) and the

total cooling system requirement of 21.9 x $10^6 ft^2$ of packing material gives a material cost of \$3.11 x 10^6. One rule of thumb for estimating fabrication costs is to set them roughly equal to material costs for a final cost of\$6.21 x 10^6 for packing plates alone. Adding this to the fixed and proportional costs gives a capital cost of \$26.6 x 10^6 for the low-back pressure wet-dry system.

A more complete breakdown of the capital cost estimation for the wet, dry and wet-dry design is presented in Table 6 -4.

TABLE 6-4

SUMMARY OF COST COMPARISONS

(millions of dollars)
(Year of printing 1973)

Category	Dry Tower (WASH-1360)	Wet Tower (WASH-1360)	Wet/Dry Towers High Back Pressure Design	Wet/Dry Towers Low Back Pressure Design
Capital Costs				
Circulating Water Structure	0.550	.710	.710	.710
Circulating Water Pumps	0.670	1.030	0.471	1.030
Concrete Pipe	1.920	1.100	1.100	1.100
Terminal Heat Sink Basins and Foundations	10.880 0.550	2.940 1.180	5.308 0.540	11.600 1.180
Condensers, Installed	4.780	4.950	4.780	4.950
Electrical Work	1.050	0.925	0.925	0.925
Indirect Charges (+25%)	5.100	3.209	3.459	5.38
Total Capital Investment	25.500	16.044	17.293	26.875

TABLE 6-4 Part 2

Category	Dry Tower (WASH-1360)	Wet Tower (WASH-1360)	Wet/Dry Towers High Back Pressure Design	Wet/Dry Towers Low Back Pressure Design
Operating Penalty Costs				
Capacity Penalty Due to highest turbine Back Pressure	17.78	3.53	19.8	8.78
Capitalized				
Energy Replacement Penalty Due to turbine back pressure variations	28.32	2.46	29.1	2.21
Capitalized Annual Cost for Operating Cooling Water Pumps	1.94	3.83	1.75	3.83
Capitalized Cost for Operating Terminal Heat Sink	6.80	2.04	2.42	5.29
Capitalized Annual Cost for Water Makeup and Treatment	-	0.18	0.07	0.07
Capitalized Annual Maintenance Cost	2.61	1.21	1.23	1.92
Total Penalty Costs	57.45	13.25	54.37	22.10
Total Evaluated Cost	82.95	29.29	71.66	48.70

6.4 Results

Referring to Table 6-4, it is now possible to get an estimate of the relative cost of the wet-dry alternative. The high back pressure design has an initial capital cost competitive with the mechanical draft wet tower of the WASH-1360 report. The price for this initial saving is paid, however, in the higher operating penalty costs which approach those of the mechanical draft dry tower. The low back pressure design wet-dry system has a higher initial cost due to the higher number of tower modules, but incurs penalty losses more on the order of the wet tower system, far below those of a dry tower system. On an overall basis, the wet-dry system has higher costs than a wet system, but again consumes only 40% as much water over the course of an operating year.

Using the results of Sec. 6.3 and Ref. [16] it is possible to roughly estimate the costs of the performance models described in Chapter 4. Although these models are not of exactly the same configuration, their behavior will be similar enough under varying operating conditions to permit sizing of each component for a combination tower system.

If the assumption is made of no economies of scale in tower construction (a good assumption for large multi-module systems), the capital costs of each type of cooling system may be compared as follows:

System (See Chap. 4)	Cost/kwe (generated)	Relative Water Consumption
Wet System	29.3	1.0 (basis)
WET + DRY @ 40°	53.2	0.18
WET + DRY @ 60°	60.0	0.06
DRY	83.0	0.00
WET/DRY + DRY @ 40°	63.9	0.08
WET/DRY + DRY @ 60°	68.3	0.03
WET/DRY (low back pressure)	48.7	0.38

Comparable designs for reduced water consumption, WET + DRY @ 60° and WET/DRY @ 40°, show the WET/DRY combination system costing about 7% more than a WET and DRY combination system.

These figures are open to some criticizm, which will appear here first. Material and fabrication costs have been rather arbitrarily assigned and may be much different in reality. For example, present day packing costs for a wet-dry tower have been estimated at about \$0.20 per ft^2 of air-side surface area (\$2.16/m^2). A check with dry cooling tower vendors has produced an estimate of \$0.30 to \$0.40 per ft^2 (\$3.24 to \$4.32/m^2) of air-side surface area. These figures do not demonstrate the major surface cost advantage that the wet-dry concept initially promised. Contact with an architect-engineering firm (United Engineers and Constructors, Inc., Philadelphia, PA) has suggested that doubling the packing plate raw material cost to account for fabrication and assembly may be too conservative. Using a suggested multiplier of 1.5 will give a reduction of $\$1.7 \times 10^{-6}$ (6%) in the initial capital investment for a wet-dry system.

The treatment of lost capacity when figuring system penalty costs can also be argued. A fixed capital charge for the worst possible loading condition (high temperature, peak power load) may not accurately reflect the true cost of meeting this load. Pumped storage, long distance transmission or specific peaking facilities are possible solutions to the peak load problem that depend on each power company's resources. The availability and cost of this peaking capacity could significantly influence a particular company's choice of system. This if further discussed in Section 6.5.

It may also be possible to operate the wet-dry concept towers in a peaking mode by deluging the packing. This could provide the additional cooling capacity at a minimal increase in cost and cumulative water consumption.

With the above points in mind, these approximate costs are presented with the belief that further analysis and optimization can only reduce them.

6.5 Discussion of Lost Capacity Penalty

The penalty charged to each type of cooling system for the highest operating turbine back pressure will be discussed here. This penalty (designated P1 in section 6.2) compares the capacity of a base generating system operating at 1.5" Hg absolute (5080 N/m^2a) turbine back pressure with the heat rate of an identical plant operating at the maximum yearly temperature, rejecting heat with the tower design being evaluated. The difference in the two generating capacities is called the maximum lost capacity and is charged to the tower at a rate representing the cost of replacing this capacity by gas turbine generators.

This charge as a percentage of the total penalty and evaluated costs varies with each type of tower system, wet tower (11% penalty, 12% total), dry tower (30%, 22%) wet-dry (40%, 18%).

Using the figures of Sect. 4.3 and Ref. [16], the following effects can be noted for a 50% reduction in the capacity charge rate:

Sensitivity of Tower Costs to Maximum Capacity

Penalty Rate (Base charge = $150/kwe)

Reduced Charge $75/kwe

Tower	$ Savings (millions)	% Penalty Cost Reduction	% Total Cost Reduction
DRY	8.89	15%	11%
WET	1.77	8%	6%
WET/DRY	4.39	20%	9%

The cost of this replacement capacity is a noteable factor in the case of the dry and wet-dry towers, and this price may easily vary from

system to system. Since this maximum temperature is encountered for only brief periods in the summer it is very likely that the system may have extra capacity elsewhere within its grid that is provided for scheduled maintenance and for peak periods such as this. The possibilities of pumped storage and inter-company sharing of power also come to mind. Each of these alternatives would differ in cost from gas turbine capacity and the penalty assessed to an individual plants' cooling tower system would vary with the available alternatives.

The applicability of the peak ambient temperature to this analysis can also be questioned. For Middletown (Boston, MA), the hypothetical site of this generating plant, the maximum temperature over the year was taken as 99 F (37C). Using the climatic data of Appendix G, it can be seen that the dry bulb temperature exceeds 90F (32C) for only 0.5% of the years. If the lost capacity is calculated for this temperature range:

Loss of Capacity for 1000 MWe Fossil Fuel Plants

Tower Type	Dry Bulb Temperatures 99F	89F	% Change in Lost Capacity	% Change in Total Cost
DRY	118,560	97,410	22%	5%
WET	23,500	17,870	31%	4%
WET/DRY	58,500	36,500	40%	7%

The last column indicates that the wet-dry tower is being more heavily penalized for the last few degrees in maximum ambient temperature. Another way of looking at this is to say that 7% of the total wet-dry cooling system cost is due to conditions found only 0.5% of the time.

This severe high temperature penalty could be avoided by providing a companion wet tower to the wet-dry system for occasional use as the weather demands. Due to the short duration of this peak period, a very attractive proposal is to provide a few of the wet-dry cells with moveable baffles that would defeat the water channeling plates and force the cells to run wet for the necessary length of time. This method would not significantly increase the yearly water consumption total although the instantaneous water consumption would be higher when running in he deluge mode.

The maximum lost capacity penalty charged to each cooling tower type thus seems to be biased toward the wet cooling tower system which experiences very little loss of capacity at high ambient temperatures.

These factors should be taken under consideration when sizing and pricing a new cooling tower system.

REFERENCES

1. Curcio, J.L., et al., Advanced Dry Cooling Tower Concept, Energy Lab Report No. MIT-EL75-023, Heat Transfer Laboratory Report No. 82267-95, Department of Mechanical Engineering, MIT, Sept. 30, 1975.

2. Yadigaroglu, G. and Pastor, E.J., "An Investigation of the Accuracy of the Merkel Equation for Evaporative Cooling Tower Calculations", AIAA Paper No. 74-756, ASME Paper No. 74-T-59, 1974.

3. Kreith, F.,Principles of Heat Transfer, Second Edition, McGraw-Hill, Inc., 1971.

4. Wark, K, Thermodynamics, Second Edition, McGraw-Hill, Inc. 1971.

5. ASHRAE Handbook of Fundamentals, 1972.

6. Zimmerman, O., and Lavine, I., Psychrometric Tables and Charts, Second Edition, Industrial Reserach Service, Inc., 1964.

7. American Institute of Physics, Temperature, Its Measurement and Control in Science and Industry, Reinhold Publishing Corp. 1941.

8. Kinzie, P.A., Thermocouple Temperature Measurement, John Wiley & Sons, 1973.

9. Holman, J.P., Experimental Methods For Engineers, McGraw-Hill Book Co., 1971.

10. Smithsonian Meteorological Tables, Sixth Revised Edition, 1966.

11. Sabersky, R.H., Acosta, A.J., and Hauptmann, E.G., Fluid Flow, Second Edition, The Macmillan Co., 1971.

12. Rohsenow, W.M. and Choi, H.Y., Heat, Mass and Momentum Transfer, Prentice-Hall, Inc., 1961.

13. Heller, Lazlo, "Wet/Dry Hybrid Condensing System", Dry and Wet/Dry Cooling Towers for Power Plants, ASME Winter Annual Meeting, Heat Transfer Division, Nov.1973.

14. "Decennial Census of United States Climate - Summary of Hourly Observations", U.S. Dept. of Commerce, Weather Bureau, 1963.

15. Kays, W.M. and London. A.L. Compact Heat Exchangers, Second Edition Edition, MeGraw-Hill, 1964.

References (Cont.)

16. Heat Sink Design and Cost Study for Fossil and Nuclear Power Plants, WASH-1360, USAEC Division of Reactor Research and Development, Washington, D.C., Dec. 1974.

APPENDIX A: RESULTS OF THERMOCOUPLE CALIBRATION TESTS

The following table reports the output differences in microvolts between each thermocouple and a standard when both are placed in the same constant temperature bath. The first test was made using a standard couple which was connected through the switches, but not the plugs and other hardware used with the other thermocouples. The second run, made four days later, used thermocouple #28 as a reference, which was four microvolts higher than the previous standard at the time of the test. The position numbers refer to Figure A-1. For more details of thermocouple installation see Figure 2-2. One microvolt corresponds to about .05°F.

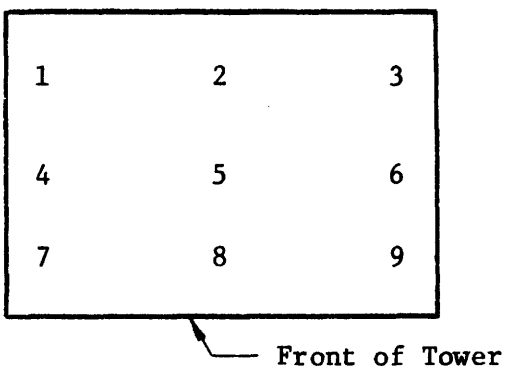

Figure A-1. Tower Cross Section showing the nine positions for Thermocouple Installation.

TABLE A-1: THERMOCOUPLE CALIBRATION RESULTS

T.C. #	Location	Run #1 12/11/75 Temp. ≅ 176°F External Std.	Run #2 12/15/75 Temp. ≅ 176°F Standard: T.C. #28	Run #3 12/17/75 Temp. ≅ 104°F External Std.
	Distribution Pipes			
1	1	+3	-2	0
2	2	+4	-1	0
3	3	+3	-5	+1
4	4	+4	-3	0
5	5	+4	-3	0
6	6	0	-2	0
7	7	0	-1	+1
8	8	-1	-2	+1
9	9	0	-1	0
	Air at Top of Plates			
10	1	+3	0	+1
11	2	+5	0	+4
12	3	+3	0	+3
13	4	+2	-3	+2
14	5	+1	-3	+1
15	6	+2	-2	0
16	7	+2	-3	0
17	8	+1	-3	+1
18	9	+1	-3	+1
	Water at Top of Plates			
19	1	+3	0	0
20	2	+4	0	+3

Table A-1 continued

T.C. #	Location	Run #1 12/11/75 Temp. = 176°F External Std.	Run #2 12/15/75 Temp. ≅ 176°F Standard: T.C. #28	Run #3 12/17/75 Temp. ≅ 104°F External Std.
	Water at Top of plates			
21	3	+3	+1	+4
22	4	+1	-4	+2
23	5	+2	-1	+1
24	6	+1	-2	+1
25	7	+3	-1	+1
26	8	+1	-2	+1
27	9	+1	-3	+1
	Air at Bottom of Plates			
28	1	+3	-	+1
29	2	+1	0	-1
30	3	+1	+1	+1
31	4	+3	-3	-1
32	5	0	-1	-1
33	6	+1	-4	0
34	7	+2	+1	+2
35	8	+4	-3	0
36	9	+3	-1	-2
	Water at Bottom of Plates			
37	1	0	-1	0
38	2	+2	-2	0
39	3	+1	0	+1
40	4	+4	-1	-2
41	5	+1	+1	-2
42	6	0	-3	-1

Table A-1 continued

T.C. #	Location	Run #1 12/11/75 Temp. ≅ 176°F External Std.	Run #2 12/15/75 Temp. ≅ 176°F Standard:T.C. #28	Run #3 12/17/75 Temp. ≅ 104°F External Std.
	Water at Bottom of Plates			
43	7	+4	-2	+2
44	8	+4	-1	+1
45	9	0	-3	0
	Collection Channels			
46	3	-2	-2	-1
47	6	+1	-1	0
48	9	+2	0	0
	Top Rake			
49	1,4,7	-2	-1	+1
50	2,5,8	-1	-1	+1
51	3,6,9	-1	-1	+1
	Bottom Rake			
52	1,4,7	-2	-1	+1
53	2,5,8	-1	no data	no data
54	3,6,9	0	-2	+1

APPENDIX B: SAMPLE CALCULATIONS

B.1 Error Analysis for the Heat Balance

From Chapter 2 the discrepancy in the heat balance is given by:

$$\delta\dot{Q} = \dot{m}_{air} \left(h_{air_{in}} + w_{in}\, h_{vapor_{in}} - h_{air_{out}} - w_{out}\, h_{vapor_{out}}\right)$$

$$+ \dot{m}_{water}\, c_{p_{water}} \left(T_{water_{in}} - T_o\right) -$$

$$c_{p_{water}} \left(\dot{m}_{water} - \dot{m}_{air}\, (w_{out} - w_{in})\right) \left(T_{water_{out}} - T_o\right) \qquad \text{(B-1)}$$

The uncertainty in $\delta\dot{Q}$ is given by:

$$u_{\delta\dot{Q}} = \left[\left(\frac{\partial\delta\dot{Q}}{\partial x_1}\, u_1\right)^2 + \left(\frac{\partial\delta\dot{Q}}{\partial x_2}\, u_3\right)^2 + \ldots + \left(\frac{\partial\delta\dot{Q}}{\partial x_n}\, u_n\right)^2\right]^{1/2} \qquad \text{(B-2)}$$

where $x_1, x_2, \ldots, x_n$ are the following ten variables:

$\dot{m}_{air}$, $h_{vapor_{in}}$, $h_{vapor_{out}}$, $h_{air_{in}}$, $h_{air_{out}}$, w_{in}, w_{out}, $\dot{m}_{water}$, $T_{water_{in}}$, $T_{water_{out}}$. $u_1, u_2, \ldots, u_n$ are the respective uncertainties of these variables. The calculation will be shown for a typical set of conditions:

$\dot{m}_{air}$ = 150 lb_m/min

$\dot{m}_{water}$ = 170 lb_m/min

Air Temperature in = 90°F

Dew Point Temperature in = 50°

Air Temperature Out = 100°F

Dew Point Temperature Out = 55°F

$T_{water_{in}}$ = 120°F

$T_{water_{out}}$ = 116.4°F

The following values may be obtained from air property tables using the air temperatures and the dew point temperatures.

$h_{air_{in}}$ = 13.938 BTU/lb

$h_{air_{out}}$ = 16,341 BTU/lb

$h_{vapor_{in}}$ = 1100.5 BTU/lb

$h_{vapor_{out}}$ = 1104.8 BTU/lb

w_{in} = .007655 lbm/lbm

w_{out} = .009225 lbm/lbm

The following uncertainties are determined directly by the instrument limitations:

$u_{\dot{m}_{air}}$ = 8 lbm/min

$u_{\dot{m}_{water}}$ = 1.7 lbm/min

$u_{\text{Air Temp. in}}$ = .1°F

$u_{\text{Dew Point in}}$ = .3°F

$u_{\text{Air Temp. out}}$ = .1°F

$u_{\text{Dew Point out}} = .3°F$

$u_{T_{\text{water}_{in}}} = .1°F$

$u_{T_{\text{water}_{out}}} = .1°F$

The uncertainties in the enthalpies and absolute humidities are determined by linear interpolation using the air property tables:

$u_{h_{\text{air}_{in}}} = .024$ BTU/Lbm

$u_{h_{\text{air}_{out}}} = .024$ BTU/Lbm

$u_{h_{\text{vapor}_{in}}} = .045$ BTU/Lbm

$u_{h_{\text{vapor}_{out}}} = .045$ BTU/Lbm

$u_{w_{in}} = .000087$ Lbm/Lbm

$u_{w_{out}} = .000102$ Lbm/Lbm

The partial differential are given in Table 11.

Substituting the appropriate values into equation B-2 results in an uncertainty:

$$u_{\delta\dot{Q}} = 45.87 \text{ BTU/min}$$

For the operating conditions given, 625.6 BTU/min is calculated using equation 2-4. The uncertainty therefore results in a 7.3% error.

TABLE B-1 PARTIAL DIFFERENTIALS FOR ERROR ANALYSIS

$$\frac{\partial \delta \dot{Q}}{\partial \dot{m}_{air}} = (h_{air_{in}} + w_{in}\, h_{vapor} - h_{air_{out}} - w_{out}\, h_{vapor_{out}})$$

$$+ (w_{out} - w_{in})\,(T_{water_{out}} - T_o)\, c_{p_{water}} = -4.038$$

$$\frac{\partial \delta \dot{Q}}{\partial h_{vapor_{in}}} = w_{in}\, \dot{m}_{air} = 1.148$$

$$\frac{\partial \delta \dot{Q}}{\partial h_{vapor_{out}}} = -w_{out}\, \dot{m}_{air} = -1.384$$

$$\frac{\partial \delta \dot{Q}}{\partial h_{air_{in}}} = \dot{m}_{air} = 150$$

$$\frac{\partial \delta \dot{Q}}{\partial h_{air_{out}}} = -\dot{m}_{air} = -150$$

$$\frac{\partial \delta \dot{Q}}{\partial w_{in}} = \dot{m}_{air} h_{vapor_{in}} - \dot{m}_{air}(T_{water_{out}} - T_o)\, c_{p_{water}} = 152415$$

$$\frac{\partial \delta \dot{Q}}{\partial w_{out}} = \dot{m}_{air}\, h_{vapor_{out}} + \dot{m}_{air}(T_{water_{out}} - T_o)\, c_{p_{water}} = -153060.$$

$$\frac{\partial \delta \dot{Q}}{\partial \dot{m}_{water}} = c_p\,(T_{water_{in}} - T_{water_{out}}) = 3.6$$

$$\frac{\partial \delta \dot{Q}}{\partial T_{water}} = \dot{m}_{water}\, c_{p_{water}} = 170$$

$$\frac{\partial \delta \dot{Q}}{\partial T_{water_{out}}} = -c_p(\dot{m}_{water} - \dot{m}_{air}(w_{out} - w_{in})) = -169.76$$

B.2 Energy balance for Experimental Data

The heat transfer to the air is given by:

$$\dot{Q}_{air} = \dot{m}_{air}(h_{air_{out}} + w_{out}\, h_{vapor_{out}} - h_{air_{in}} - w_{in}\, h_{vapor_{in}}) \qquad \text{(B-3)}$$

The heat transfer from the water is given by:

$$\dot{Q}_{water} = \dot{m}_{water}\, c_{p_{water}} (T_{water_{in}} - T_o) -$$

$$c_{p_{water}} (\dot{m}_{water} - \dot{m}_{air}\, (w_{out} - w_{in}))(T_{water_{out}} - T_o) \qquad \text{(B-4)}$$

As an example the data from the first experimental run will be used.

$\dot{m}_{air}$ = 143.4 lbm/min

Air Temperature in = 88 .4°F

Air Temperature out = 97.9°F

Dew Point Temperature in = 32.8°F

Dew Point Temperature out = 41.5°F

w_{in} = .003912 lbm/lbm

w_{out} = .005528 lbm/lbm

$h_{air_{in}}$ = 13.5526 BTU/lbm

$h_{air_{out}}$ = 15.8360 BTU/lbm

$h_{vapor_{in}}$ = 1099.76 BTU/lbm

$h_{vapor_{out}}$ = 1103.86 BTU/lbm

Substituting these values into equation B-3 and B-4.

$$\dot{Q}_{air} = 585.5 \text{ BTU/min}$$

$$\dot{Q}_{water} = 670.62$$

$$\dot{Q}_{average} = 628.1$$

$$\text{percent error} = \frac{\dot{Q}_{water} - \dot{Q}_{air}}{\dot{Q}_{average}} (100) = 13.5\%$$

APPENDIX C

RAW DATA

Table C-1 contains the raw inputs to the model tower and the computer analogy. The measured response of the model is also compared with the computer prediction. The first 5 runs were done with the unpainted packing plates and the last 4 (after 5/5) used the painted plates (see Section 2.4 and App.E).

Table C-1

Date of Run	3/19		3/22		3/23 AM	
	Data	Computer	Data	Computer	Data	Computer
Air Flow Rate (lbm/min)		136		110		110
Inlet Water Flow Rate (lbm/min)		152		152		192
Inlet Air Temperature (F)		87.8		84.2		86.6
Inlet Air Humidity (lbm/lbm)		.005065		.002212		.002373
Inlet Water Temperature (F)		131.5		120.9		124.7
Outlet Air Temperature (F)	99.9	101.7	94.5	95.9	97.4	98.9
Outlet Air Humidity (lbm/lbm)	.00870	.00920	.00521	.00541	.00619	.00598
Outlet Water Temperature (F)	125.5	126.0	116.3	116.5	120.9	120.9
Air Temperature Change (F)	12.1	13.9	10.3	11.7	10.8	12.25
Water Temperature Change (F)	6.0	5.5	4.6	4.4	3.8	3.8
Air Humidity Change (lbm/lbm)	.00364	.00414	.00300	.00320	.00382	.00361
Air Side of Energy Balance (Btu/min)	738	-	638	-	750	-
Water Side of Energy Balance (Btu/min)	938	-	727	-	767	-
Average Heat Transfer Rate (Btu/min)	839	875	677	700	759	766
Percent Error in Energy Balance	24	-	13	-	2	-
Evaporative Heat Transfer (Btu/min)	405	460	336	358	427	403
Percent Evaporative Heat Transfer	48	53	50	51	56	53

Table C-1 con't

Date of Run	3/23 PM		3/25		5/6	
	Data	Computer	Data	Computer	Data	Computer
Air Flow Rate (lbm/min)		110		109		105
Inlet Water Flow Rate (lbm/min)		190		126		170
Inlet Air Temperature (F)		91.7		89.8		90.8
Inlet Air Humidity (lbm/lbm)		.002613		.005400		.009363
Inlet Water Temperature (F)		135.0		134.3		133.1
Outlet Air Temperature (F)	103.0	105.2	102.6	103.7	101.1	104.3
Outlet Air Humidity (lbm/lbm)	.00703	.00736	.00961	.00978	.01200	.01200
Outlet Water Temperature (F)	129.9	130.3	127.4	127.5	129.9	129.4
Air Temperature Change (F)	11.3	14.1	12.8	13.9	10.2	13.5
Water Temperature Change (F)	5.1	4.8	6.9	6.8	3.2	3.7
Air Humidity Change (lbm/lbm)	.00441	.00475	.00421	.00438	.00263	.00263
Air Side of Energy Balance (Btu/min)	853	-	844	-	518	-
Water Side of Energy Balance (Btu/min)	1017	-	909	-	571	-
Average Heat Transfer Rate (Btu/min)	935	955	877	899	544	654
Percent Error in Energy Balance	18	-	7	-	10	-
Evaporative Heat Transfer (Btu/min)	490	527	463	482	279	278
Percent Evaporative Heat Transfer	52	55	55	54	51	43

Table C-1 con't

Date of Run	5/11		5/25		6/24	
	Data	Computer	Data	Computer	Data	Computer
Air Flow Rate (lbm/min)		111		111		91
Inlet Water Flow Rate (lbm/min)		171		95		164
Inlet Air Temperature (F)		89.2		85.5		95.9
Inlet Air Humidity (lbm/lbm)		.007512		.006241		.01946
Inlet Water Temperature(F)		142.3		138.3		124.3
Outlet Air Temperature (F)	101.3	106.0	96.9	101.6	104.8	105.2
Outlet Air Humidity (lbm/lbm)	.01146	.01085	.00909	.00899	.02156	.02131
Outlet Water Temperature (F)	138.5	137.5	130.5	130.5	122.3	122.0
Air Temperature Change (F)	12.1	16.8	11.4	16.3	8,9	9,3
Water Temperature Change (F)	3.8	4.8	7.8	7,8	2,0	2,3
Air Humidity Change (lbm/lbm)	.00395	.00334	.00285	.00275	.00210	.00185
Air Side of Energy Balance (Btu/min)	812	-	653	-	413	-
Water Side of Energy Balance (Btu/min)	697	-	749	-	346	-
Average Heat Transfer Rate (Btu/min)	755	866	701	771	379	399
Percent Error in Energy Balance	15	-	14	-	17	-
Evaporative Heat Transfer (Btu/min)	440	372	316	305	195	171
Percent Evaporative Heat Transfer	58	43	45	40	51	43

APPENDIX D

DESIGN FACTORS OF COMPARISON TOWERS

To provide some basis for the comparison of the advanced wet/dry packing section to the types of heat transfer surfaces now used by power generating companies, three types of towers have been modeled which meet the same standards of heat rejection and water temperature drop at a design inlet air temperature.

These three towers are: 1) Completely non-evaporative (DRY) where the water to be cooled is circulated through a closed system of finned tubes and the heat transferred by forced convection. 2) Evaporative (WET) where the hot water is distribued over a film-type packing to maximize the air-to-water surface area. Approximately 85% of the heat transfer in this tower is due to evaporation with the remaining heat transfer coming from convection at the water surface. 3) Wet/dry (WET/DRY) with the V-trough type packing now being tested at M.I.T. This design seeks to minimize the air-water contact area thus cutting evaporation while still allowing convective heat transfer by the fin effect of the unwetted plate surface.

The inlet conditions for each of the models was then varied from 10°F (-12°C) to 120°F (49°C) and their performance calculated by means of the compter program. This program is essentially the same as listed in [1] with a few additions determined by experimentation and design considerations.

No effort has been made to optimize any one model, rather the goal was to give each an equal advantage (or handicap) in order to make

a fair comparison. Thus the results can be extended, at least qualitatively, to give an indication of more efficient designs.

The following discussion will review the design parameters and summarize the final tower configuations.

Inlet Water Temperature; 130°F (54°C), corresponding to a turbine back pressure of 3.5 in Hg absolute (8.9 cm Hg).

Water Temperature Drop: 20°F (11°C) at the design point.

Design Point: inlet air at 90°F (32°C) dry-bulb and 40% R.H. giving an ITD of 40°F (22°C) and an approach temperature of 20°F (11°C) to the dry-bulb and 39°F (22°C) to the wet-bulb.

Packing Configuration: DRY tower, no exact fin arrangement was assumed in this case as the values for the surface heat transfer coefficient and the fin efficiency were arbitrarily fixed in this analysis (see Table D-1). For this reason, while the total surface area of the DRY model isaccurate for a counterflow design, the surface area per plan area value is subjective and therefore not included in the summary table. WET/DRY tower, this was chosen to be as close to the heat transfer model tested at M.I.T. Each packing plate is made of galvanized sheet steel 0.0233 in (.059 cm) thick. The V-troughs are one inch (2.5 cm) on a side and are bent to an angle of 60° at the bottom of the V. The wet-to-dry surface area ratio was set at 5%, close to the experimentally measured value. The plates were spaced 1.5 in (3.8 cm) center-to-center and no evaporation was assumed in

the distribution and collection processes. WET tower, this was modeled as a film-type packing with all heat transfer done at the water surface. The packing plates were considered to be flat and evenly coated with water. Plate spacing was increased to 4 in. (10 cm) and the plate angle to the vertical was changed from 10° to 45°.

Heat and Mass Transfer Coefficients: DRY tower, the surface convective heat transfer coefficient and fin efficiency were set at 8 BTU/hr-ft^2°F (39 kcal/h-m^2°C) and 0.8, respectively. These figures did not change with operating conditions. WET/DRY tower, the dry surface convective heat transfer coefficient was also set at 8 BTU/hr-ft^2°F (39 kcal/h-m^2°F) the reasoning begin that augmentation of the surface could produce a higher convective coefficient than was measured on the simple experimental packing plates. The water surface convective heat transfer coefficient was calculated from the Dittus-Boelter (see Section 2.1) equation and modified on the basis of experimental evidence [3-2]. The average value was approximately 5.3 BTU/hr-ft^2°F (26 kcal/h-m^2°C). The mass transfer coefficient was calculated by the Chilton-Colburn analogy and had an average value of 370 ft/hr (113m/h) (Section 2.1). WET tower, the coefficients for this model were calculated as above and had average values of 4.4 BTU/hr-ft^2°F (21 kcal/h-m^2°C) and 300 ft/hr (90 m/h) for the respective heat and mass transfer coefficients.

Water Flow per Unit Area - DRY tower, not relevant due to the fixed values of heat transfer surface area per unit plan area. WET/DRY tower, approximately 4 gpm/plan ft^2 (2.7ℓ/s/plan m^2). This value was within the range of the model tower tests. WET tower, approximately 6 gpm/plan ft^2 (4.1ℓ/s/plan m^2).

Air Flow Ratios - DRY tower, to give a temperature effectiveness of 0.7 where effectiveness is defined as:

$$\varepsilon = \frac{T_{C2}-T_{C1}}{T_{h1}-T_{c1}}$$

This produced a mass flow ratio of $\dot{M}_{air}/\dot{M}_{water} = 3.0$, WET/DRY tower, to give an air temperature rise approximately equal to that of the DRY model, $\dot{M}_{air}/\dot{M}_{water} = 1.5$. This was fairly close to the mass flow ratios used with the experimental model tower. WET tower, the mass flow ratio was set here at $\dot{M}_{air}/\dot{M}_{water} = 1$, a widely used value.

The following table summarized the three computer models used in the performance comparisons. Wherever possible parameters have been non-dimensionalized or related to heat load so that the results could be extended for any desired heat rejection rate.

Table D-1

Summary of Design Parameters of Tower Models

Tower type	DRY	WET/DRY	WET
Total Surface Area			
ft^2/1000 Btu/hr	9.8	7.1	0.4
m^2/1000 kcal/h	3.6	2.6	0.2
Mass Flow Rate of Air @ Design Point*			
lb_m/1000 Btu	150	75	47
kg/1000 kcal	270	135	85
Mass Flow Rate of Water @ Design Point*			
lb_m/1000 Btu	6.0	5.7	5.6
kg/1000 kcal	1.5	1.4	1.4
Specific Heat Ratio			
$\dot{M}_{air}Cp_{air}/\dot{M}_{water}Cp_{water}$	0.72	0.38	0.24
Average Fin Efficiency	0.8	0.7	-
Average Dry Plate Surface Heat Transfer Coefficient			
Btu/hr-ft^2-F	8.0	8.0	-
kcal/h-m^2-C	39.	39.	-
Average Wet Surface Heat Transfer Coefficient			
Btu/hr-ft^2-F	-	5.3	4.4
kcal/h-m^2-C	-	26.	21.
Average Water Surface Mass Transfer Coefficient			
ft/hr	-	370	300
m/h	-	113	91

*Design Point, all Towers

Inlet Air 90 F (32 C) Dry Bulb, 40% R.H.

Inlet Water 130 F (54 C)

ΔT_{water} 20 F (11 C)

APPENDIX E

CORROSION AND PAINTING OF PACKING PLATES

After several data runs had been completed with the model tower a white, crusty deposit was noticed in the bottom of the V-troughs. Visual observations showed that when water was present in the bottom of the troughs it tended to climb up the deposit layer in the same way water would soak up into a blotter.

The "blotter effect" increased the wet-to-dry surface area ratio and raised the portion of heat transfered by evaporation. Attempts to scrub away the scaling were only temporarily successful as the deposits returned very quickly.

Close examination of the packing plates revealed that the protective galvanizing had been worn away in some places and the reaction of the steel plate with the city water was contributing to the scaling.

To prevent this corrosion and to help keep the wet-to-dry surface area ratio low, one packing plate was coated with an acrylic spray paint as a test. Several combinations of primer and topcoat were compared and the one which seemed most resistant to deposit buildup was used. The plates were cleaned by scrubbing down the water side with citric acid and steel wool, then "aged" by rubbing down with acetic acid. The primer was standard for galvanized material, two coats of zinc chromate primer. This was followed by two spray coats of Crylon^{R} flat back.

The surface was fairly smooth to the touch and was not wetted by the water in the troughs. This tendency appeared to decrease after several hours of running but little or no deposit buildup was observed.

Micrometer measurements showed that the thickness of the paint layer was approximately .001 in (2.5×10^{-3} mm). Assuming the paint to have a thermal conductivity equal to that of hard rubber, 6.09 BTU/hr-ft^2°F (0.13 kcal/h-m°C), calculations showed a change in the surface convective heat transfer coefficient from 3.50 to 3.49 BTU/hr-ft^2°F (17.09 to 17.04 kcal/h-m^2°C), an insignificant change.

Only the side of the plates wetted by the water streams was painted as the dry side showed no corrosion or wear.

After approximately 48 running hours since painting very little deposition can be seen. What there is wipes off easily and does not seem to affect the wet-to-dry surface area ratio.

APPENDIX F

FLOW VISUALIZATION

The flow visualization test apparatus used in the inital design of the V-trough packing plates was used again to provide qualitative information on the relationship of vertical angle to the water channeling characteristics.

The angle presently used in the model tower is 10° from the vertical. After the plate surface had been cleaned and painted the water flowing down the plates was observed to wander at the top and in some cases did not settle in the bottom of the trough until well down the plate. These tendencies diminshed somewhat as total running time increased, but it was felt that observations of the channeling properties of a painted packing plate should be performed.

Using a small test plate whose surface had been treated similarly to those in the model tower, qualitative observations were taken for plate angles from 10° to 45° from the vertical.

At 45° water spread over the top portion of the plate channeled itself immediately into the bottom of the troughs and stayed channeled down the plate with no wandering. The water channel was approximately 0.125 in wide (0.32 cm) for the apparatus flowrate.

At 10° the water channeled itself poorly by comparison, in some cases jumping from one trough to another and in most troughs requiring several inches before becoming channeled in the trough bottoms. Once channeled the stream tended to stay that way, although several troughs

did exhibit a sort of meandering flow up and down the sides of the V-trough. The water surface, once channeled, was about .063 inches (0.159 cm), or about half that at 45°.

The compromise angle was felt to be about 30° from the vertical. At this angle the water was channeled much better than at 10° or 20° and the water surface was narrower than at either 45° or 40°.

The resulting recommendation is based on simple, qualitative observations and is meant to provide a starting point for further work. The flow visualization apparatus will have to be modified to allow more realistic flow rates and distribution if quantitative data are desired.

APPENDIX G

CLIMATIC DATA

Climatic Data from four representative cities were summarized from Reference [14]. The summaries show the number of hours each month that the ambient dry-bulb temperature was within each of a range of temperature spans. These spans are:

111 - 110 F	48 - 43 C
109 - 100 F	43 - 38 C
99 - 90 F	37 - 32 C
89 - 80 F	32 - 27 C
79 - 70 F	26 - 21 C
69 - 60 F	21 - 16 C
59 - 50 F	15 - 10 C
49 - 40 F	9 - 4 C
39 - 30 F	4 - 1 C
29 - 20 F	-2 - -7 C
19 - 10 F	-7 --12 C
9 - 0 F	-13 --18 C
-1 - -10 F	-18 --23 C
-11 - -20 F	-24 --29 C

Also included for each month is the total number of hours in the month and the average relative humidity.

Table G-1

Albequerque, N.M.

Jan.	7440 hrs	50% RH
69/60	45	
59/50	722	
49/40	2475	
39/30	2938	
29/20	1364	
19/10	178	
9/0	18	

Feb.	6792 hrs	30% RH
69/60	298	
59/50	1013	
49/40	2089	
39/30	2206	
29/20	924	
19/10	230	
9/0	22	

Mar.	7440 hrs	30% RH
79/70	120	
69/60	097	
59/50	1812	
49/40	2395	
39/30	1709	
29/20	484	
19/10	13	

Apr.	6792 hrs	30% RH
89/80	99	
79/70	918	
69/60	1758	
59/50	2201	
49/40	1716	
39/30	498	
29/20	10	

May	7440 hrs	30 % RH
99/90	75	
89/80	849	
79/70	1821	
69/60	2335	
59/50	1752	
49/40	561	
39/30	47	

June	7200 hrs	15% RH
109/100	6	
99/90	968	
89/80	1933	
79/70	2295	
69/60	1660	
59/50	328	
49/40	10	

Table G-1 (Continued)

July	7440 hrs	30 % RH
109/100	27	
99/90	1089	
89/80	2135	
79/70	2692	
69/60	1483	
59/50	14	

Aug	7440 hrs	40% RH
99/90	622	
89/80	2027	
79/70	2792	
69/60	2971	
59/50	29	

Sept	7200 hrs	30 % RH
99/90	188	
89/80	1527	
79/70	2223	
69/60	2409	
59/50	835	
49/40	28	

Oct	7440 hrs	25% RH
89/80	165	
79/70	1132	
69/60	2063	
59/50	2428	
49/40	1469	
39/30	183	

Nov	7200 hrs	30 % RH
79/70	24	
69/60	505	
59/50	1586	
49/40	2533	
39/30	1848	
29/20	630	
19/10	74	

Dec	7440 hrs	50% %H
79/70	2	
69/60	65	
59/50	658	
49/40	1874	
39/30	2974	
29/20	1789	
19/10	273	
9/0	7	

Table G-2

Los Angeles, Calif.

Jan	7440 hrs	75% RH
89/80	22	
79/70	196	
69/60	1234	
59/50	4212	
49/40	172	
39/30	49	

Feb	2792 hrs	70% RH
89/80	36	
79/70	218	
69/60	1510	
59/50	3987	
49/40	1132	
39/30	9	

Mar	7440 hrs	75% RH
89/80	40	
79/70	300	
69/60	1953	
59/50	4371	
49/40	765	
39/30	11	

Apr	7200 hrs	80% RH
89/80	58	
79/70	368	
69/60	2570	
59/50	4025	
49/40	189	

May	7440 hrs	70% RH
99/90	6	
89/80	49	
79/70	540	
69/60	4090	
59/50	269	
49/40	8	

June	7200 hrs	75% RH
99/90	13	
89/80	35	
79/70	1286	
69/60	5094	
59/50	772	

Table G-2 (Continued)

July	7440 hrs	75%
99/90	7	
89/80	287	
79/70	2617	
69/60	4283	
59/50	246	

Aug	7440 hrs	80% RH
99/90	6	
89/80	236	
79/70	2695	
69/60	4469	
59/50	34	

Sept	7200 hrs	75% RH
109/100	6	
99/90	36	
89/80	302	
79/70	2252	
69/60	4276	
59/50	338	

Oct	7440 hrs	80% RH
109/100	4	
99/90	39	
89/80	170	
79/70	1119	
69/60	4369	
59/50	1734	
49/40	5	

Nov	7200 hrs	75% RH
99/90	9	
89/80	142	
79/70	622	
69/60	2774	
59/50	3267	
49/40	386	

Dec	7440 hrs
99/90	2
89/80	70
79/70	351
69/60	1848
59/50	3992
49/40	1143
39/30	34

TABLE G-3

Boston, Mass.

Jan.	7440 hrs	50% RH
69/60	6	
59/50	253	
49/40	825	
39/30	3055	
29/20	2180	
19/10	906	
9/0	168	
-1/-10	47	

Feb	6792 hrs	50% RH
69/60	20	
59/50	261	
49/40	1144	
39/30	3092	
29/20	1561	
19/10	554	
9/0	119	
-1/-10	41	

Mar	7440 hrs	50% RH
70/70	1	
69/60	73	
59/50	391	
49/40	2168	
39/30	3521	
29/20	1115	
19/10	171	

Apr	7200 hrs	50% RH
89/80	26	
79/70	133	
69/60	633	
59/50	1990	
49/40	2579	
39/30	808	
29/20	29	
19/10	2	

May	7440 hrs	50 RH
99/90	11	
89/80	192	
79/70	729	
69/60	1925	
59/50	3270	
49/40	1312	
39/30	12	

June	7200 hrs	60% RH
109/100	1	
99/90	107	
89/80	737	
79/70	1909	
69/60	2895	
59/50	1500	
49/40	51	

Table G-3 Continued

July	7440 hrs	60% RH
99/90	209	
89/80	1367	
79/70	3363	
69/60	2410	
59/50	91	

Aug	7440 hrs	65% RH
109/100	1	
99/90	142	
89/80	997	
79/70	2931	
69/60	3149	
59/50	220	

Sept	7200 hrs	70% RH
109/100	1	
99/90	26	
89/80	357	
79/70	1703	
69/60	2949	
59/50	1947	
49/40	216	
39/30	2	

Oct	7440 hrs	60% RH
89/80	44	
79/70	289	
69/60	1658	
59/50	3344	
49/40	1848	
39/30	263	

Nov	7200 hrs	50% RH
79/70	32	
69/60	479	
59/50	1740	
49/40	2912	
39/30	1726	
29/20	286	
19/10	25	

Dec	7440 hrs	50% RH
69/60	44	
59/50	461	
49/40	1799	
39/30	2745	
29/20	1676	
19/10	596	
9/10	111	
0	8	

TABLE G- 4

New York, N.Y.

Jan	7440 hrs	50% RH
59/50	95	
49/40	1511	
39/30	3491	
29/20	1835	
19/10	485	
9/0	23	

Feb	6792 hrs	50% RH
69/60	13	
59/50	206	
49/40	1871	
39/30	3212	
29/20	1096	
19/10	337	
9/0	57	

Mar	7440 hrs	50% RH
79/70	3	
69/60	74	
59/50	560	
49/40	2345	
39/30	3097	
29/20	740	
19/10	21	

Apr	7200 hrs	50% RH
89/80	24	
79/70	164	
69/60	757	
59/50	2713	
49/40	3064	
39/30	463	
29/20	16	

May	7440 hrs	50% RH
99/90	3	
89/80	78	
79/70	772	
69/60	2669	
59/50	3244	
49/40	671	
39/30	3	

June	7200 hrs	50% RH
99/90	88	
89/80	614	
79/70	2464	
69/60	3358	
59/50	676	

Table G-4 (continued)

July	7440 hrs	60% RH
109/100	3	
99/90	132	
89/80	1405	
79/70	4524	
69/60	1354	
59/50	22	

Aug	7440 hrs	70% RH
99/90	85	
89/80	1223	
79/70	4296	
69/60	1881	
59/50	55	

Sept	7200 hrs	70% RH
99/90	19	
89/80	317	
79/70	2532	
69/60	3297	
59/50	969	
49/40	66	

Oct	7440 hrs	50% RH
89/80	33	
79/70	547	
69/60	2491	
59/50	3043	
49/40	1229	
39/30	97	

Nov	7200 hrs	50% RH
79/70	5	
69/60	402	
59/50	2428	
49/40	2840	
39/30	1350	
29/20	167	
19/10	8	

Dec	
69/60	14
59/50	659
49/40	2143
39/30	2999
29/20	1330
19/10	376
9/0	19

APPENDIX H. COUNTERFLOW COMPUTER LISTING

```
      REAL K,KP,L,MA,MUA,MUL,MV,NG,NPL,NU,ML,MLIN,MLOUT
      DIMENSION RT(200),RML(200)
    2 NAMELIST(MA,MLIN,P,TLIN,TIN,WIN,B,L,NPL,SP,THETA,TP,KP,
     *RATIO,NG,PACKW)
      J=0
    7 READ(8&2)
      J=J+1
      IF(MA.LT.0.)GO TO 80
      WRITE(6,100)J
  100 FORMAT(I3)
      TO=TLIN
      TO=32.
      MA=MA*60.
      MLIN=MLIN*60.
      P=P*70.727
      TLIN=TLIN+459.67
      TIN=TIN+459.67
      B=B/12.
      TO=TO+459.67
      L=L/12.
      SP=SP/12.
      THETA=THETA*.01745
      PACKW=PACKW/12.
      TP=TP/12.
      DZ=L/25.
      CA=.241
      CL=1.
      PR=.72
      RV=85.83333
      RA=53.35
      IF(RATIO.EQ.0.)BL=0.
      IF(RATIO.GT.0.)BL=B/(.5/RATIO+1.)
```

APPENDIX H. COUNTERFLOW COMPUTER LISTING

```
      IF(RATIO.EQ.1.)BL=2.*B
      BD=B-2.*BL
      D=BD/NG
      HFGO=-.5942*TO+1370.16
      DH=2.*PACKW*SP/(SP+B)
      MLOUT=.98*MLIN
      IF(RATIO.EQ.0.) MLOUT=MLIN
      TLOUT=TIIN-30.
      I=2
      RT(1)=0.
      RT(2)=0.
      RML(1)=0.
      RML(2)=0.
    1 I=I+1
      IF(I.GT.100)GO TO 40
      ML=MLOUT
      TL=TLOUT
      T=TIN
      W=WIN
      Z=0.
      QCL=0.
      QEL=0.
      QDP=0.
      Q=0.
      MV=W*MA
    5 ROA=P/((W*RV+RA)*T)
      IF(Z.GT.(L-.001))GOTO555
      ROV=W*ROA
      IF(TL-500.)3,3,4
    3 ROL=62.4
      GO TO 6
    4 ROL=62.4-.00024792*(TL-500.)**1.8
    6 PA=ROA*RA*T
```

```
      PV=P-PA
      HFG=-.5942*TL+1370.16
      PVSAT=((.0006369*TL+2.0883)*1.E24*TL**-5.387*EXP(-12386./TL))*144
     *.
      ROVSAT=PVSAT/(RV*TL)
      ROMIX=(ROA+ROV*W)/(1.+W)
      K=.0008946*SQRT(T)/(1.+205.2/T)
      MUA=7.420E-7*SQRT(T)/(1.+205.2/T)
      MUL=(EXP(-(TL-492.)/49.5)+.2)*1.E-3
      IF(TL.GT.613.5)MUL=MUL-.5936E-6*(TL-613.5)
      VA=(MA+MV)/(ROMIX*PACKW*SP*NPL)/3600.
      IF(RATIO.EQ.1.)VL=ROL*32.2*COS(THETA)*(3.*ML*MUL/ROL**2/BL/32.2/3
     *600./COS(THETA)/NPL)**(2./3.)/2./MUL
      IF(RATIO.GT.0..AND.RATIO.LT.1.)VL=ML/NPL/NG/ROL/.433/(BL/NG)**2/3
     *600.
      IF(RATIO.EQ.0.)VL=0.
      V=VA+VL
      CV=(19.86-597./SQRT(T)+7500./T)/18.
      CMIX=(CA+CV*W)/(1.+W)
      RE=V*DH*ROMIX/MUA
      H=.0230*K/DH*PR**.6*RE**.8
      H=H*1.5
      DV=.000146*((T+TL)/2.)**2.5/(((T+TL)/2.)+441.)*14.696*144./P
      HD=H/ROMIX/CMIX*(ROMIX*CMIX*DV/K)**(2./3.)
      REDP=VA*DH*ROMIX/MUA
      HDP=.0230*K/DH*PR**.6*REDP**.8
      HDP=8.
      IF(RATIO.GT.0..AND.RATIO.LT.1.)NU=TANH(SQRT(2.*DZ*(D/2.)**2*
     *HDP/KP/DZ/TP))/SQRT(2.*DZ*(D/2.)**2*HDP/KP/DZ/TP)
      IF(RATIO.EQ.0.0)NU=0.8
      IF(RATIO.EQ.1.)NU=0.
      IF(RATIO.EQ.0.0)NU=0.8
      DML=+HD*(ROVSAT-ROV)*BL*DZ*NPL
```

```
      DQCL=H*(TL-T)*BL*DZ*NPL
      DQEL=+(HFG+CL*(TL-TO))*DML
      DQDP=(NU*HDP*(TL-T)*BD*2.*DZ+HDP*(TL-T)*BL*2.*DZ)*NPL
      IF(RATIO.EQ.1.)DQDP=0.
      DQ=DQCL+DQEL+DQDP
      DTL=+((DQ+(ML*CL*(TL-TO)))/(+((ML+DML)*CL)))-TL+TO
      DMV=+DML
      DW=(MV+DMV)/MA-W
      DT=(-DQ-MA*CA*(T-TO)-W*MA*(CV*(T-TO)+HFGO)+(W+DW)*MA*HFGO)/(-MA*C
     *A-(W+DW)*MA*CV)-T+TO
      ML=ML+DML
      QCL=QCL+DQCL
      QEL=QEL+DQEL
      QDP=QDP+DQDP
      Q=Q+DQ
      TL=TL+DTL
      MV=MV+DMV
      W=W+DW
      T=T+DT
      Z=Z+DZ
      GOTO5
  555 DELTL=TLOUT-TL
      DELT=T-TIN
      PML=(ML-MLOUT)/ML*100.
      PT(I)=TL
      PML(I)=ML
      TOLT=TLIN-TL
      IF(ABS(TOLT).LE..001)GO TO 30
      IF(AINT(RT(I)*1.E3).EQ.AINT(RT(I-2)*1.E3).AND.ABS(TOLT).LE..002)
     *GO TO 30
      TLOUT=TLOUT+.50*TOLT
      GO TO 1
   30 TOLM=MLIN-ML
```

```
      IF(ABS(TOLM).LE..01)GO TO 40
      IF(AINT(RML(I)*10.).EQ.AINT(RML(I-2)*10.).AND.ABS(TOLM).LE..02)
     *GO TO 40
      MLOUT=MLOUT+.5*TOLM
      GO TO 1
   40 L=L*12.
      B=B*12.
      PACKW=PACKW*12.
      SP=SP*12.
      THETA=THETA/.01745
      TP=TP*12.
      TO=TO-459.67
      MA=MA/60.
      P=P/70.727
      TIN=TIN-459.67
      T=T-459.67
      MLIN=MLIN/60.
      TLIN=TLIN-459.67
      MLOUT=MLOUT/60.
      ML=ML/60.
      TLOUT=TLOUT-459.67
      TL=TL-459.67
      WRITE(5,45) J
      Q=(TLIN-TLOUT)*MLOUT+MA*(W-WIN)*(TLIN-32.)
      QEL=(MLIN-MLOUT)*(-.5942*(TLIN+460.)+1370.16-
     *  (.241)*(TLIN-T))
      PQEL=QEL/Q*100.
      PUT HDP,H,HD,NU    ,VL
      WRITE(5,50)RATIO,L,B,PACKW,NPL,NG,SP,THETA
      WRITE(5,60)TP,KP,TO,MA,P,TIN,T,WIN,W,ML,MLOUT
      WRITE(5,70)TL,TLOUT,DELTL,PML,DELT,Q,QEL,PQEL
   45 FORMAT(//1H1,40X,I3/)
   50 FORMAT(41X,'TOWER GEOMETRY'//43X,'WET-DRY SURFACE ',
```

```
     *'RATIO=',F5.3//43X,'PACKING HEIGHT=',F6.2,' IN.'//43X,'TOTAL ',
     *'HEAT TRANSFER SURFACE WIDTH=',F7.2,' IN.'//43X,'PACKING ',
     *'WIDTH=',F7.2,' IN.'//43X,'NUMBER OF PLATES=',F5.0//43X,'NUMBER',
     *' OF CHANNELS PER PLATE=',F5.0//43X,'PLATE SPACING=',F5.2
     *,' IN.'//43X,'PLATE ANGLE FROM VERTICAL=',F4.1,' DEGREES'/)
  60 FORMAT(43X,'PLATE THICKNESS=',F5.3,' IN.'//43X,'PLATE CONDUCTIVITY
     *=',F7.3,' BTU/HR FT F'//41X,'REFFRENCE TEMPERATURE=',F7.2,
     *' F'////64X,'INLET',17X,'OUTLET'//41X,'AIR FLOW RATE',6X,F8.2
     *,' LBM/MIN'//41X,'AIR PRESSURE',9X,F5.2,' IN. HG'//41X,
     *'AIR TEMPERATURE',5X,2(F7.2,' F',13X)//41X,'HUMIDITY',13X,2(F8.6,
     *' LBM/LBM',7X)//41X,'WATER FLOW RATE',4X,2(F9.3,' LBM/MIN',6X)/)
  70 FORMAT(41X,'WATER TEMPERATURE',3X,2(F7.2,' F',14X)////41X,'WATER '
     *,'TEMPERATURE CHANGE=',F7.2,' F'//41X,'PERCENT WATER LOSS=',
     *F6.3,' %'//41X,'AIR TEMPERATURE CHANGE=',
     *F7.2,' F'//41X,'TOTAL HEAT TRANSFER=',F11.2,' BTU/MIN'//
     *41X,'EVAPORATIVE HEAT TRANSFER=',F11.2,' BTU/MIN'//41X,
     *'PERCENT EVAPORATIVE HEAT TRANSFER=',F4.1,' %')
      GO TO 7
  80 WRITE(5,85)
  85 FORMAT(1H1)
     CONTINUE
     STOP
     END
```

TABLE H-1 LIST OF COMPUTER PROGRAM VARIABLES

B	Total Surface Area of a Plate Per Foot of Height	ft.
BD	Total Width of Dry Portion of a Plate	ft.
BL	Total Width of Wet Portion of a Plate	ft.
CA	Specific Heat at Constant Pressure for Air	BTU/lbm °R
CL	Specific Heat at Constant Pressure for Liquid Water	BTU/lbm °R
CMIX	Specific Heat at Constant Pressure for Air and Water Mixture	BTU/lbm °R
CV	Specific Heat at Constant Pressure for Water Vapor	BTU/lbm °R
D	Distance Between Water Channels in the Packing	ft.
DELT	Air Temperature Change	°F
DELTL	Water Temperature Change	°F
DH	Hydraulic Diameter of the Space Between Packing Plates	ft.
DML	Change in Water Flow Rate	lbm/hr.
DMV	Change in Vapor Flow Rate	lbm/hr.
DQ	Change in Heat Transfer Rate	BTU/hr.
DQCL	Change in Convective Heat Transfer from Water Surface	BTU/hr.
DQDP	Change in Convective Heat Transfer from Dry Surface	BTU/hr.
DQEL	Change in Evaporative Heat Transfer	BTU/hr.
DT	Change in Air-Vapor Temperature	°R
DTL	Change in Water Temperature	°R
DV	Diffusion Coefficient for Water Vapor in Air	$ft^2/hr.$
DW	Change in Absolute Humidity	lbm/lbm

DZ	Change in Distance Through the Packing	ft.
H	Convective Heat Transfer Coefficient from Liquid Water to Air	BTU/hr.ft^2°R
HD	Mass Transfer Coefficient for Water in Air	ft/hr.
HDP	Convective Heat Transfer Coefficient from Dry Surface to Air	BTU/hr.ft^2°R
HFG	Heat of Vaporization for Water	BTU/lbm
HFGO	Heat of Vaporization for Water at TO	BTU/lbm
I	Counter for Number of Iterations	
J	Counter for Number of Load Cases	
K	Thermal Conductivity of Air (used for Air-Vapor Mixture)	BTU/hr.ft°R
KP	Thermal Conductivity of the Plates	BTU/hr.ft°R
L	Total Height of Packing	ft.
MA	Mass Flow Rate of Air	lbm/hr.
ML	Mass Flow Rate of Water	lbm/hr.
MLIN	Mass Flow Rate of Water at Inlet	lbm/hr.
MLOUT	Mass Flow Rate of Water at Outlet	lbm/hr.
MUA	Absolute Viscosity of Air (Used for Air-Vapor Mixture)	lbm/ft.sec.
MV	Mass Flow Rate of Vapor	lbm/hr.
NG	Number of Channels on Each Packing Plate	
NPL	Number of Plates in the Packing	
NU	Fin Efficiency Between the Channels	
P	Total Pressure of the Air-Vapor Mixture	lbf/ft^2
PA	Partial Pressure of the Air	lbf/ft^2

PACKW	Actual Width of Packing	ft.
PQEL	Percent Evaporative Heat Transfer	
PR	Prandtl Number for Air (used for Air-Water Mixture)	
PML	Percent Water Loss	
PV	Partial Pressure of Water Vapor	lbf/ft^2
PVSAT	Partial Pressure of Water Vapor at Saturation	lbf/ft^2
Q	Total Heat Transfer Rate	BTU/hr.
QCL	Convective Heat Transfer from Water Surface	BTU/hr.
QDP	Convective Heat Transfer from Dry Surface	BTU/hr.
QEL	Evaporative Heat Transfer	BTU/hr.
RA	Gas Constant for Air	ft. lbf/lbm°R
RATIO	Fraction of Packing Surface Which is Wet	
RE	Reynold's Number for Air Over Water with Counter Flow	
REDP	Reynold's Number for Air Over Dry Surface	
RML	Array which Records the Values of ML After Each Iteration	
ROA	Density of Air	lbm/ft^3
ROL	Density of Water	lbm/ft^3
ROMIX	Density of Air-Vapor Mixture	lbm/ft^3
ROV	Density of Water Vapor	lbm/ft^3
ROVSAT	Density of Water Vapor at Saturation	lbm/ft^3
RT	Array which Records the Values of TL After Each Iteration	
RV	Gas Constant for Water Vapor	ft./lbf/lbm°R
SP	Spacing Between Packing Plates	ft.
T	Temperature of Air-Vapor Mixture	°R

THETA	Angle Between the Plates and Vertical	radians
TIN	Temperature of Air at Inlet	°R
TL	Temperature of Water	°R
TLIN	Temperature of Water at Inlet	°R
TLOUT	Temperature of Water at Outlet	°R
TO	Reference Temperature	°R
TOLM	Parameter Used to Check Convergence of TL	
TOLT	Parameter Used to Check Convergence of ML	
TP	Thickness of the Plates	ft.
V	Velocity of Air Relative to Water	ft/sec.
VA	Air Velocity	ft/sec.
VL	Water Velocity	ft/sec.
W	Absolute Humidity of the Air	lbm/lbm
WIN	Absolute Humidity of the Air at Inlet	lbm/lbm
Z	Distance from Air Inlet	ft.

TABLE H-2: LIST OF PROGRAM INPUT PARAMETERS

B	Total Surface Area of Plate Per Foot of Height	in.
KP	Thermal Conductivity of Plates	BTU/hr.ft°R
L	Total Height of Packing	in.
MA	Mass Flow Rate of Air	lbm/min.
MLIN	Mass Flow Rate of Water at Inlet	lbm/min.
NG	Number of Channels on Each Packing Plate	
NPL	Number of Plates in the Packing	
P	Total Pressure of the Air-Vapor Mixture	in.hg
PACKW	Actual Width of Packing	in.
RATIO	Fraction of Packing Surface Which is Wet	
SP	Spacing Between Packing Plates	in.
THETA	Angle Between the Plates and Vertical	degrees
TIN	Temperature of Air at Inlet	°F
TLIN	Temperature Water at Inlet	°F
TP	Thickness of the Plates	in.
WIN	Absolute Humidity of Air at Inlet	lbm/lbm

APPENDIX I. CROSSFLOW COMPUTER LISTING

```
      INTEGER AIRHUM,AIRTEM,AIRFLO
      REAL OUTAIR(50),OUTHUM(50),OUTLIQ(50),OUTFLO(50),NU
      REAL K,KP,L,NG,NPL,MLIN,MLOUT,DATA(41,41,5),MA,NOMIX
      LOGICAL LMIX,SCAN
      DATA YESMIX/'  '/,NOMIX/'UN'/
    2 NAMELIST(MA,MLIN,P,TLIN,TIN,WIN,B,L,NPL,SP,THETA,
     C TP,KP,RATIO,NG,PACKW,LMIX,SCAN)
      JJJ=0
    7 LMIX=.FALSE.
      SCAN=.FALSE.
      JJJ=JJJ+1
      READ(8&2)
      IF(MA.LT.0.) GOTO444
      IXX=25.
       IXX=20
      XX=IXX
      LIQTEM=1
      AIRTEM=2
      LIQFLO=3
      AIRFLO=4
      AIRHUM=5
      AFABLK=L*NPL*SP/144./XX
      TO=TLIN+459.67
      DO 11 I=1,IXX
      DATA(1,I,LIQTEM)=TLIN+459.67
      DATA(I,1,AIRTEM)=TIN+459.67
      DATA(1,I,LIQFLO)=MLIN*60./XX
      DATA(I,1,AIRFLO)=MA*60./XX
      DATA(I,1,AIRHUM)=WIN
   11 CONTINUE
      IF(RATIO.EQ.0.)ABLIQ=0.
      IF(RATIO.GT.0.) ABLIQ=B/(.5/RATIO+1.)*L*NPL/XX**2.
```

```
C /144.
 IF(RATIO.EQ.1.) ABLIQ=2.*B*L*NPL/144./XX**2.
 ABDRY=L*NPL*D/XX**2./144. -2.*ABLIQ
 DH=2.*AFABLK/L/NPL*12.*XX*PACKW/B
 D=ABDRY/L*XX/NG*XX*12./NPL
 DO 33 J=1,IXX
 DO 22 I=1,IXX
 II=I+1
 JJ=J+1
 CALL BLOCK(DATA(I,J,AIRTEM),DATA(I,J,LIQTEM),
C  DATA(I,J,AIRHUM),DATA(I,J,LIQFLO),DATA( I,JJ,AIRTEM),
C  DATA(II, J,LIQTEM),DATA( I,JJ,AIRHUM),DATA
C  (II, J,LIQFLO),IXX,AFABLK,DH,ABLIQ,ABDRY,P,DATA
C  (1,1,4),D,TC,KP,TP,RATIO,NU,HDP,H,HD)
22  CONTINUE
    IF(LMIX)CALL MIX(DATA,IXX,J+1,DATA(1,1,4),XWAV,XTAV)
    IF(.NOT.LMIX)GOTO33
    DO 34 IROW=1,IXX
    DATA(IROW,J+1,AIRHUM)=XWAV
34  DATA(IROW,J+1,AIRTEM)=XTAV
33  CONTINUE
    DO 18 I=1,IXX
    OUTAIR(I)=DATA(I,IXX+1,AIRTEM)-459.67
    OUTHUM(I)=DATA(I,IXX+1,AIRHUM)
18  CONTINUE
    DO 19 I=1,IXX
    OUTLIQ(I)=DATA(IXX+1,I,LIQTEM)-459.67
    OUTFLO(I)=DATA(IXX+1,I,LIQFLO)/60.
19  CONTINUE
24  FORMAT(/1X,I5,F10.4,F10.4)
    FL=0.
    ATL=0.
    DO 31 I=1,IXX
```

```
      ATL=ATL+DATA(IXX+1,I,LIQTEM)
      FL=FL+DATA(IXX+1,I,LIQFLO)
   31 CONTINUE
      MLOUT=FL/60.
      TLOUT=ATL/XX-459.67
      J=IXX+1
      CALL MIX(DATA,IXX,J,DATA(1,1,4),WOUT,TAV)
      TOUT=TAV-459.67
      QTOT=(TLIN-TLOUT)*MLOUT+MA*(WOUT-WIN)*(TLIN-32.)
      QEL=(MLIN-MLOUT)*(-.5942*(TLIN+460.)+1370.16
     C  -(.241)*(TLIN-TOUT))
      QRAT=QEL/QTOT*100.
      DELT=TOUT-TIN
      DELTL=TLOUT-TLIN
      FML=(MLIN-MLOUT)/MLIN*100.
      TO=TO-459.67
      OUTMIX=NOMIX
      IF(LMIX)OUTMIX=YESMIX
      WRITE(5,45)JJJ,OUTMIX
      PUT JJJ,H,HDP,HD,NU
   45 FORMAT(1H1     ,40X,I3,4X,'CROSSFLOW CONFIGURATION, AIRFLOW ',
     C  A2,'MIXED'/)
      WRITE(5,50)RATIO,L,B,PACKW,NPL,NG,SP,THETA
      WRITE(5,60)TP,KP,TO,MA,P,TIN,TOUT,WIN,WOUT,MLIN,MLOUT
      WRITE(5,70)TLIN,TLOUT,DELTL,FML,DELT,QTOT,QEL,QRAT
   50 FORMAT(41X,'TOWER GEOMETRY'//43X,'WET-DRY SURFACE ',
     *'RATIO=',F5.3//43X,'PACKING HEIGHT=',F6.2,' IN.'//43X,'TOTAL ',
     *'HEAT TRANSFER SURFACE WIDTH=',F7.2,' IN.'//43X,'PACKING ',
     *'WIDTH=',F7.2,' IN.'//43X,'NUMBER OF PLATES=',F7.0//43X,'NUMBER',
     *' OF CHANNELS PER PLATE=',F5.0//43X,'PLATE SPACING=',F5.2
     *,' IN.'//43X,'PLATE ANGLE FROM VERTICAL=',F4.1,' DEGREES'/)
   60 FORMAT(43X,'PLATE THICKNESS=',F5.3,' IN.'//43X,'PLATE CONDUCTIVITY
     *=',F7.3,' BTU/HR FT F'//41X,'REFERENCE TEMPERATURE=',F7.2,
```

```
     *' F'////64X,'INLET',17X,'OUTLET'//41X,'AIR FLOW RATE',6X,E9.3
     *,' LBM/MIN'//41X,'AIR PRESSURE',9X,F5.2,' IN. HG'//41X,
     *'AIR TEMPERATURE',5X,2(F7.2,' F',13X)//41X,'HUMIDITY',13X,2(F8.6,
     *' LBM/LBM',7X)//41X,'WATER FLOW RATE',4X,2(E9.3,' LBM/MIN',6X)/)
  70 FORMAT(41X,'WATER TEMPERATURE',3X,2(F7.2,' F',14X)////41X,'WATER '
     *,'TEMPERATURE CHANGE=',F7.2,' F'//41X,'PERCENT WATER LOSS=',
     *F6.3,' %'//41X,'AIR TEMPERATURE CHANGE=',
     *F7.2,' F'//41X,'TOTAL HEAT TRANSFER=',E11.3,' BTU/MIN'//
     *41X,'EVAPORATIVE HEAT TRANSFER=',E11.3,' BTU/MIN'//41X,
     *'PERCENT EVAPORATIVE HEAT TRANSFER=',F4.1,' %')
      IF(.NOT.SCAN)GOTO7
      WRITE(5,878)
      DO 879 I=1,IXX
  879 WRITE(5,877)I,OUTLIQ(I),OUTFLO(I),OUTAIR(I),OUTHUM(I),I
  878 FORMAT(1H1,5X,'WATER OUTLET CONDITIONS-',6X,'AIR OUTLET CONDIT',
     C  'IONS'/6X,'IN DIRECTION OF AIRFLOW',7X,'TOP TO BOTTOM'/7X,
     C  'TEMP.',7X,'FLOW RATE',10X,'TEMP.',6X,'SPEC. HUMIDITY'/7X,
     C  'DEG. F',5X,'LBM/MIN',12X,'DEG. F',5X,'LBM/LBM'/)
  877 FORMAT(1X,I3,2X,F7.1,5X,F7.1,11X,F7.1,5X,F8.5,4X,I3)
      GOTO7
  444 STOP
      END
PROGRAM  *MAIN* HAS     NO ERRORS
```

APPENDIX I. CROSSFLOW COMPUTER LISTING

```
      SUBROUTINE BLOCK(TIN,TLIN,WIN,MLIN,TOUT,TLOUT,
     C WOUT,MIOUT,IXX,AFABLK,DH,ABLIQ,ABDRY,PP,MA,D,
     C  TO,KP,TP,RATIO,NU,HDP,H,HD)
      REAL K,KP,L,MA,MUA,MUL,MV,NU,MLIN,MLOUT
      CA=.241
      CL=1.
      ER=.72
      RV=85.8333
      P=PP*70.727
      RA=53.35
      HFGO=-.5942*TO+1370.16
      MV=WIN*MA
      ROA=P/((WIN*RV+RA)*TIN)
      ROV=WIN*ROA
      IF(TLIN-500.)3,3,4
    3 ROL=62.4
      GOTO6
    4 ROL=62.4-.00024792*(TLIN-500.)**1.8
    6 PA=ROA*RA*TIN
      PV=P-PA
      HFG=-.5942*TLIN+1370.16
      PVSAT=((.0006369*TLIN+2.0883)*1.E24*TLIN**-
     C  5.387*EXP(-12386./TLIN))*144.
      ROVSAT=PVSAT/RV/TLIN
      ROMIX=(ROA+ROV*WIN)/(1.+WIN)
      K=.0008246*SQRT(TIN)/(1.+205.2/TIN)
      MUA=7.42E-7*SQRT(TIN)/(1.+205.2/TIN)
      MUL=(EXP(-(TLIN-492.)/49.5)+.2)*1.E-3
      IF(TLIN.GT.613.5)MUL=MUL-.5936E-6*(TLIN-613.5)
      VA=(MA+MV)/ROMIX/AFABLK/3600.
      CV=(19.86-597./SQRT(TIN)+7500./TIN)/18.
      CMIX=(CA+CV*WIN)/(1.+WIN)
      RE=VA*DH*ROMIX/MUA
```

```
      H=5.78
      DV=.000146*((TIN+TLIN)/2.)**2.5/(((TIN+TLIN)/
     C  2.)+441.)*14.696*144./P
      HD=H/ROMIX/CMIX*(ROMIX*CMIX*DV/K)**(2./3.)
      HDP=5.78
C
C      H AND HDP CALCULATED BY HAND FROM JE-CHIN CORRELATION
C
      IF(RATIO.GE.0.)NU=TANH(SQRT(2.*(D/2.)**2.*HDP/
     C  KP/TP*12.))/SQRT(2.*(D/2.)**2.*HDP/KP/TP*12.)
      IF(RATIO.EQ.1.)NU=0.
      IF(RATIO.EQ.0.)NU=.8
      DML=HD*(ROVSAT-ROV)*ABLIQ
      DQCL=H*(TLIN-TIN)*ABLIQ
      DQEL=(HFG+CL*(TLIN-TO))*DML
      DQDP=(NU*HDP*(TLIN-TIN)*ABDRY*2.)+HDP*(TLIN-TIN)
     C  *ABLIQ*2.
      IF(RATIO.EQ.1.)DQDP=0.
      DQ=DQCL+DQEL+DQDP
      DTL=+((DQ+((MLIN-DML)*CL*(TLIN-TO)))/(+(MLIN*CL)))-TLIN+TO
      DMV=DML
      DW=(MV+DMV)/MA-WIN
      DT=(-DQ-MA*CA*(TIN-TO)-WIN*MA*(CV*(TIN-TO)+HFGO)
     C  +(WIN+DW)*MA*HFGO)/(-MA*CA-(WIN+DW)*MA*CV)
     C  -TIN+TO
      MLOUT=MLIN-DML
      TLOUT=TLIN-DTL
      WOUT=WIN+DW
      TOUT=TIN+DT
      RETURN
      END
PROGRAM  BLOCK  HAS     NO ERRORS
```

APPENDIX I. CROSSFLOW COMPUTER LISTING

```
      SUBROUTINE MIX(DATA,IXX,J,AIRFLO,WOUT,TOUT)
      INTEGER AIRHUM,AIRTEM
      REAL DATA(41,41,5)
      AIRTEM=2
      AIRHUM=5
      HAIR=0.
      WAIR=0.
      DO 1 I=1,IXX
      HAIR=HAIR+((.241)+(.45)*DATA(I,J,AIRHUM))*AIRFLO*
     C  DATA(I,J,AIRTEM)
    1 WAIR=WAIR+DATA(I,J,AIRHUM)
      XX=IXX
      WOUT=WAIR/XX
      TOUT=HAIR/XX/AIRFLO/(.241+.45*WOUT)
      RETURN
      END
PROGRAM  MIX    HAS    NO ERRORS
```

TABLE I-1 LIST OF VARIABLES - CROSSFLOW PROGRAM UNITS

VARIABLE	DESCRIPTION	UNITS
ABDRY	Convective heat transfer surface area per grid section	ft^2
ABLIQ	Water free surface area per grid section	ft^2
AFABLK	Airflow area per grid section	ft^2
AIRFLO	Dummy index for DATA array	
AIRHUM	Dummy index for DATA array	
AIRTEM	Dummy index for DATA array	
ATL	Intermediate variable for averaging exit water temperature	F
B	Total plate width	in
BLOCK	Subroutine which calculates heat and mass transfer for a grid section	
D	Distance between water channels in the packing plates	ft
DATA	Array holding air and water inlet conditions for each grid section	
DELT	Average air temperature change across the tower	F
DELTL	Average water temperature change across the tower	F
DH	Hydraulic diameter of airflow channel	ft
FL	Sum of exit water flow rates	lb_m/hr
FML	Ratio of water evaporation rate to inlet flow rate	%
H	Convective heat transfer coefficient from free water surface	$BTU/hr\text{-}ft^2\text{°}F$
HD	Mass transfer coefficient from free water surface	ft/hr
HDP	Convective heat transfer coefficient from dry surface of packing plate	$BTU/hr\text{-}ft^2\text{°}F$
I,II	Dummy counting variables	
IROW	Dummy variable	
IXX	Number of rows and columns of grid	
J,JJJ	Dummy counting variables	

VARIABLE	DESCRIPTION	UNITS
KP	Thermal conductivity of packing plate	BTU/hr-ft°F
L	Height of packing plate	in
LIQFLO	Dummy index for DATA array	
LIQTEM	Dummy index for DATA array	
LMIX	Logical switch for unmixed or well-mixed flow conditions	
MA	Inlet air mass flow rate	lb_m/min
MIX	Subroutine for mixing air flows across tower	
MLIN	Water mass flow rate into tower	lb_m/min
MLOUT	Water mass flow rate out of tower	lb_m/min
NG	Number of water channels per plate	
NOMIX	Character string for printout title	
NPL	Number of packing plates in tower	
NU	Fin efficiency	
OUTAIR	Scan of air outlet temperatures	F
OUTFLO	Scan of water outlet flow rates	lb_m/min
OUTHUM	Scan of outlet air specific humidity	lb_m/lb_m
OUTLIQ	Scan of outlet water temperatures	F
OUTMIX	Character string for printout title	
P	Air pressure	in. Hg.
PACKW	Width of packing section	in.
QEL	Evaporative heat transfer rate	BTU/min
QRAT	Ratio of Evaporative to total heat transfer rate	%
QTOT	Total heat transfer rate	BTU/min
RATIO	Wet-to-dry surface area ratio	
SCAN	Logical switch for exit scan output	
SP	Packing plate spacing	in
TAV	Average column air temperatures from MIX	R
THETA	Packing plate angle from vertical	°
TIN	Inlet air temperature	F
TLIN	Inlet water temperature	F

VARIABLE	DESCRIPTION	UNITS
TLOUT	Average Outlet water temperature	F
TO	Reference Temperature	R
TOUT	Average outlet water temperature	F
TP	Packing plate thickness	in.
WIN	Inlet air specific humidity	lb_m/lb_m
WOUT	Outlet air specific humidity	lb_m/lb_m
XTAV	Average column air temperature from MIX	R
XWAV	Average column air specific humidity from MIX	lb_m/lb_m
XX	Number of rows and columns in grid	
YESMIX	Character string for title printout	

SUBROUTINE BLOCK

VARIABLE	DESCRIPTION	UNITS
ABDRY	Convective heat transfer surface area per grid section	ft^2
ABLIQ	Water free surface area per grid section	ft^2
AFABLK	Air flow area in grid section	ft^2
CA	Heat capacity of air	$BTU/lb_m°F$
CL	Heat capacity of liquid water	$BTU/lb_m°F$
CMIX	Heat capacity of air-water vapor mixture	$BTU/lb_m°F$
CV	Heat capacity of water vapor	$BTU/lb_m°F$
D	Distance between water channels in packing plate	ft
DH	Hydraulic diameter of air flow channel	ft
DML	Evaporation rate of water in grid section	lb_m/hr
DMV	Rate of change of water vapor mass flow across grid section (= DML)	lb_m/hr
DQ	Total heat transfer rate from grid	BTU/hr
DQCL	Heat transfer rate due to convection from water free surface	BTU/hr
DQDP	Heat transfer rate due to convection from dry plate surface	BTU/hr
DQEL	Heat transfer rate due to mass transfer from water free surface	BTU/hr
DT	Change in air temperature across grid section	F
DTL	Change in water temperature across grid section	F
DV	Diffusivity of water vapor in air	ft^2/hr

VARIABLE	DESCRIPTION	UNITS
DW	Change in specific humidity across grid section	lb_m/lb_m
H	Convective heat transfer coefficient for water free surface	$BTU/hr\text{-}ft^2°F$
HD	Mass transfer coefficient for water free surface	ft/hr
HDP	Convective heat transfer coefficient for dry surface of packing plate	$BTU/hr\text{-}ft^2°F$
HFG	Latent heat of vaporization of liquid water	BTU/lb_m
HFGO	Latent heat of vaporization of liquid water at TO	BTU/lb_m
IXX	Number of rows and columns of grid	
K	Thermal conductivity of air	BTU/hr-ft°F
KP	Thermal conductivity of packing plate	BTU/hr-ft°F
MA	Air mass flow rate through grid section	lbm/hr
MLIN	Water mass flow rate into grid section	lbm/hr
MLOUT	Water mass flow rate out of grid section	lbm/hr
MV	Water vapor mass flow rate into grid section	lbm/hr
NU	Fin efficiency	
P	Atmospheric pressure	in.Hg.
PA	Partial pressure of dry air	lb_f/ft^2
PP	Atmospheric pressure	in. Hg.
PR	Prandtl number of air	
PV	Partial pressure of water vapor	lb_f/ft^2
PVSAT	Partial pressure of water vapor at saturation conditions	lb_f/ft^2
RA	Gas constant for air	$ft\text{-}lb_g/lb_m\text{-}R$
RATIO	Ratio of wet-to-dry surface area	
RE	Reynolds number	
ROA	Density of air	lbm/ft^3
ROL	Density of liquid air	lbm/ft^3
ROMIX	Density of air-water vapor mixture	lbm/ft^3
ROV	Density of water vapor	lbm/ft^3
ROVSAT	Density of water vapor at saturation conditions	lbm/ft^3
RV	Gas constant for water vapor	$ft\text{-}lb_f/lb_m\text{-}R$

VARIABLE	DESCRIPTION	UNITS
TIN	Temperature of air entering grid section	R
TLIN	Temperature of water entering grid section	R
TLOUT	Temperautre of water exiting grid section	R
To	Reference temperature	R
TOUT	Temperature of air leaving grid section	R
TP	Thickness of packing plate	in
VA	Velocity of air through grid section	ft/sec
WIN	Specific humidity of air entering grid section	lbm/lbm
WOUT	Specific humidity of air leaving grid section	lbm/lbm

Subroutine MIX

VARIABLE	DESCRIPTION	UNITS
AIRFLO	Mass flow rate of air through grid section	lbm/hr
AIRHUM	Dummy index for DATA matrix	
AIRTEM	Dummy index for DATA matrix	
DATA	Array holding air and water inlet conditions for each grid section	
HAIR	Summing variable for air enthalpy averaging	BTU/lbm
I	Counting variable	
IXX	Number of rows and columns in grid	
J	Counting variable	
TOUT	Average air temperature of well-mixed flow	R
WAIR	Summing variable for specific humidity average	lbm/lbm
WOUT	Average specific humidity of well-mixed flow	lbm/lbm
XX	Number of rows and columns in grid	

APPENDIX J

DETERMINATION OF THE DRY PLATE SURFACE HEAT TRANSFER COEFFICIENTS

The dry surface heat transfer coefficient for the model tower packing plates was experimentally determined by monitoring the temperature response of a single plate when subjected to a step change in air temperature.

Chilled air was used to cool the metal packing plates 15 to 20°F below ambient laboratory conditions. When the plate reached a uniform temperature the model tower exhaust fan was started, drawing the warmer laboratory air over the plates. Plate surface and local air temperatures were recorded at 10 second intervals until plate temperature matched air temperature. A set of typical data is shown in Table J-1.

Reference [15] contains an analysis for this type of experimental data. Given air flowrate intake temperature, time-temperature behavior of the plates and air stream, and tower physical properties, the average dry surface heat transfer coefficient may be calculated. The steps involved in this calculation are outlined below with the values in parentheses being a sample calculation with the data of Table J-1.

A more detailed explanation of the assumptions and dimensionless parameters can be found in Reference [15].

TABLE J-1

Temperature Response of Glavanized Packing Plate

Time	Air Temperature°F	Time	Plate Temperature°F
0	56.8	10	57.3
20	64.4	30	60.4
40	67.9	50	63.0
60	69.8	70	65.2
80	71.1	90	67.1
100	72.0	110	68.6
120	72.7	130	69.9
140	73.3	150	71.0
160	73.7	170	71.9
180	73.8	190	72.5
200	74.0	210	73.0
220	74.0	230	73.4
240	74.2	250	73.7
260	74.4	270	74.0

Plate Properties

Length 28 inches

Width 43 inches

Spacing 1.5 inches

Thickness .0225 inches

Density 487 lb_m/ft^3

Heat Capacity 0.113 BTU/lb_m-F

Initial Temperature 56.8°F

Air Properties

Density 0.24 lbm/ft^3

Heat Capacity .08 BTU/lb_m-F

Velocity 476 ft/min

Temperature 74.4°F

Steps for Calculating h

1. Compute C_w from properties and air flow rate (C_w = 104.8)
2. Compute $\theta^*(t)$ ($\theta(t) = 3.4\ t$)
3. Compute NTU from properties allowing h as an unknown (NTU = 0.148 h)
4. Compute $\theta^* t - 1/C_w^*$ ($\theta^*(t) - 1/C_w^* \simeq \theta^*(t)/C_w^* = .0327\ t$
5. Select a value of $\theta^* - 1/C_w^*$ and compute the time at which that value occurs. (For $\theta^* - 1/C_w^* = 4$, t = 122 sec)
6. From experimental data find T_{plate} at time calculated in Step 5. (T_{plate} = 69.4).

7. Using this value of T_{plate} calculate ε^*_w ($\varepsilon^*_w = 0.716$)
8. From Fig. 3-14 (Ref [15]) use ε^*_w from Step 7 and θ^*-1/C_w^* from Step 4 to find NTU. (NTU = 0.48).
9. Use NTU values from Steps 4 and 8 to solve for h. ($h = 3.3$ BTU/hr-ft^2°F)